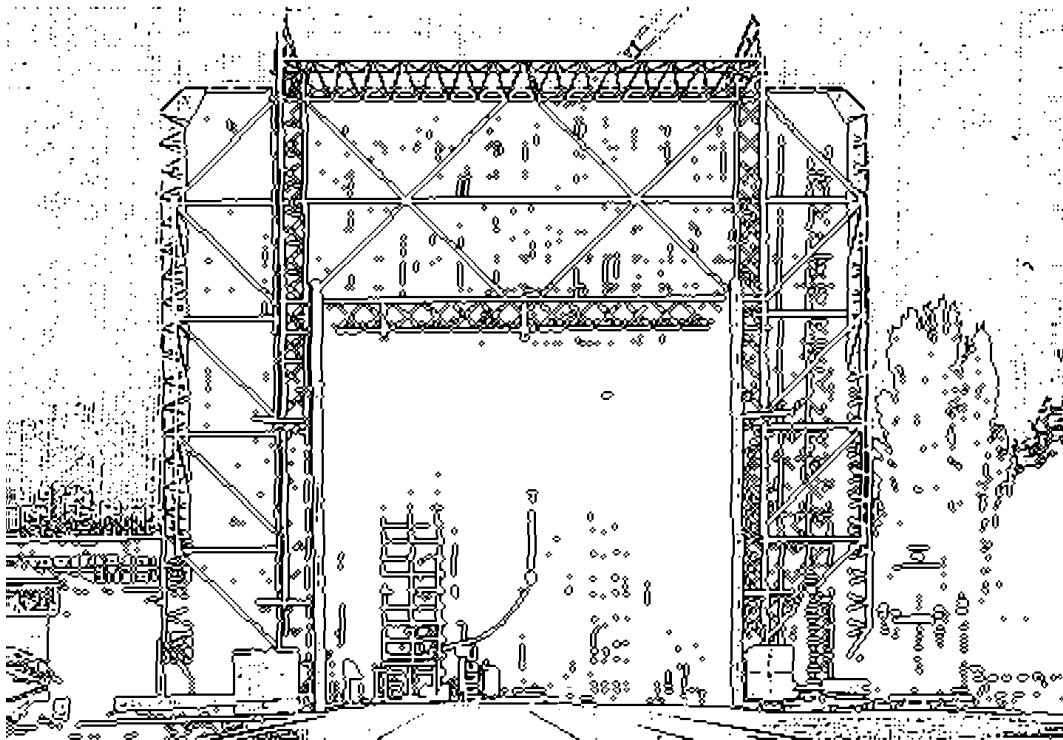


GRAZ UNIVERSITY OF TECHNOLOGY

DISSERTATION



INSTITUT FÜR HOCHSPANNUNGSTECHNIK
UND SYSTEMMANAGEMENT

***Real-time remote monitoring
of high voltage surge arresters***

Tarik Sadovic

***Dissertation
for the academic degree
“Doctor of Technical Science“***

***Permitted by the
Faculty of Electrical Engineering
of the
Graz University of Technology***

***Institute of
High Voltage Engineering
and System Management***

Submitted by:

- 1. Supervisor: O.Univ.-Prof. Dipl.-Ing. Dr.techn. Dr.h.c. Michael MUHR*
- 2. Expert: Ph. D. Electrical Engineering Prof. Maks BABUDER*

Boulogne-Billancourt, France, November 2009

TABLE OF CONTENT

Acknowledgments	5
Abstract	6
Abstraktum	7
List of figures	8
List of tables	11
List of equations	12
List of definitions	13
I. Introduction	14
II. Line Surge Arrester and Energy.....	17
II.1. Electrical stresses	17
II.1.1. Lightning overvoltages	17
II.1.2. Switching overvoltage	18
II.2. Line Lightning performance improvement method	18
II.3. Line Surge Arrester	19
II.3.1. Energy considerations.....	19
II.3.2. Different designs.....	20
II.3.3. Line arrester energy duty	21
II.3.4. Line surge arrester monitoring.....	24
II.3.5. Purpose of this work	25
III. New arrester monitoring system	26
III.1. Existing devices	26
III.1.1. Surge counter and total leakage current measurement device	26
III.1.2. Line arrester monitoring device	27
III.1.3. Research projects.....	28
III.2. Contribution to the arrester monitoring field	30
III.3. Presentation of the new monitoring system	31
III.3.1. Description of the systems hardware.....	32
III.3.2. Software operating the monitoring system.....	44
IV. Simulation.....	61
IV.1. Simulation scenarios	62
IV.1.1. Scenario number 1.....	62

IV.1.2. Scenario number 2.....	63
IV.1.3. Scenario number 3.....	64
IV.2. Simulation Results	65
IV.3. First conclusions	68
V. Testing and Installation.....	69
V.1. Laboratory Testing	69
V.1.1. Remote Laboratory Concept.....	69
V.1.2. Lightning first leader acquisition testing.....	72
V.1.3. Multicomponents acquisition testing.....	74
V.1.4. Accuracy of the measurement	75
V.1.5. Mobile communication testing.....	76
V.2. Real field installation	77
V.2.1. Tower selection	77
V.2.2. Installation equipment	78
V.2.3. Installation procedure	80
VI. Results and conclusion	81
VI.1. Field results.....	81
VI.2. Conclusion	87
VII. Future developments	89
VII.1. Arrester energy duty sharing	89
VII.2. GPS time synchronization	90
VII.3. Wireless communication along towers.....	92
VII.4. Existing equipment use and upgrade.....	95
VIII. Summary.....	96
IX. References	98
X. Annexes	107
X.1. Annex I – Arrester energy duty calculation	107
X.2. Annex II – Surge arrester operating duty tests.....	110
X.3. Annex III – Simulation study with emtp_rv	116
X.4. Annex IV - Monitoring system solar power requirements calculation.....	127
X.5. Annex V – Laboratory Testing	130
X.6. Annex VI – ECOMPACT 4 automatic control software source code	133
X.7. Annex VII – Monitoring system installation in real field.....	139

ACKNOWLEDGMENTS

The author of this thesis would like to express his gratitude to the following institutions and persons for their participation and support.

Institutions

- Technische Universität Graz, Austria
- Electricité de France, France
- Hrvatska elektroprivreda - Operator prijenosnog sustava, Croatia
- Elektrotehnički fakultet Sarajevo, Bosnia-Herzegovina

Persons

- Michael MUHR, TU Graz, Austria
- Stephan PACK, TU Graz, Austria
- Alain XEMARD, EDF, France
- Miroslav MESIC, HEP, Croatia
- Jadranko RADOVANOVIC and his team, HEP Split, Croatia

ABSTRACT

For the design, testing and selection of the high voltage surge arresters it is very important to know real stresses arrester will be exposed to in the service. The most important parameter in the assessment of the arrester stresses is the arrester energy duty. Arrester energy duty is mainly related to the stresses imposed by the lightning discharges and by the switching operations. Arrester correct operation, protection characteristics and the ageing are directly related to the arrester energy duty.

In order to determine arrester energy duty in service it is important to know frequency of the arrester operation and the shapes of the impulse currents discharged through the arresters. The main characteristic of the lightning caused arrester impulse current is high amplitude, short duration and multiplicity, while for the switching overvoltages arrester currents have low amplitude but longer duration.

The purpose of this thesis is to develop a real time remote arrester monitoring system, based on latest technologies in communication and data acquisition fields. This system, being remotely installed, will monitor permanently surge arrester current shapes in order to determine arrester real field stresses and also to monitor arrester condition. The main idea is to estimate arrester energy duty of the electrical stresses and make conclusions regarding arrester selection and software simulations.

The proposed content is to study the basics of line lightning performance, describe line surge arrester energy duty considerations and present existing arrester monitoring devices. Then the new monitoring system is introduced with the requirements it has to meet and solutions retained among different possibilities for the data acquisition, power supply and communication parts. Finally it is installed in real field, and results are presented.

Keywords:

Surge arrester, arrester monitoring, energy duty, electrical stress, lightning overvoltage, insulation coordination, line lightning performance.

ABSTRAKTUM

Bei der Ausführung, Prüfung und Auswahl von dem Überspannungsableiter eine von wichtigsten Informationen sind die Elektrische Beanspruchung während den Betriebsbedingungen. Präziser gesagt, der bedeutendste Parameter sind der Ableiter Energieaufgaben. Die Überspannungsableiter Energieaufgaben sind meistens verbunden mit den Belastungen verursacht durch den Blitzentladungen oder durch den Schaltvorgang. Die korrekte Überspannungsableiter Betriebsbedingungen, seine Schutzeigenschaften und Alterungs- Prozess sind direkt abhängig von seinen Energieaufgaben.

Um die Überspannungsableiter Energieaufgaben während dem Betrieb zu bestimmen, es ist wichtig die Häufigkeit von dem Überspannungsableiter Betriebsoperationen und die Form von dem Entladungsstrom durch den Ableiter zu kennen. Die Haupteigenschaften den durch den Blitzentladung entstehende Strom sind grosse Amplitude, kurze Laufzeit und Vielfachheit. Auf andere Seite, die Ströme die bei dem Schaltvorgang entstehen haben niedrigere Amplituden mit längerer Laufzeit.

Das Ziel dieser Doktorarbeit ist zu entwickeln ein Echtzeitmonitoringsystem (Real-Time Monitoring System) die auf der modernsten Kommunikation Technologien und Datenerfassung Systemen basiert ist. So ein ferngesteuertes System soll permanent die Form von dem Ableiter Ströme überwachen und damit ein Real-Life Kontrolle von den Feldanspannungen sicherstellen. Die Haupt Idee ist zu ermöglichen eine Abschätzung von dem Ableiter Beanspruchungen im Bezug auf elektrische Stresses and herleiten die Entscheidungen über Ableiter Auswahl and entsprechende Software Simulation.

Die vorgeschlagenen Aufgaben sind die Studie über den Grundlagen den Übertragungsleitung Blitzentladungen Hochleistung, Analyse von den Überspannungsableiter Betriebsaufgaben und eine Vorstellung von den existierende Ableiter Monitoring Systemen. Ein neue Monitoring System soll vorgestellt werden zusammen mit dem Aufgabe er soll ausführen und einen Auswahl von den begleitenden Datenerfassung Systemen, Stromversorgung und Kommunikation Komponenten. Schliesslich so ein System wird installiert in die realen Feldbedingungen und entsprechende Resultate werden präsentiert.

Stichwörter:

Überspannungsableiter, Ableiter Monitoring, Ableiter Energieaufgaben, Elektrische Beanspruchung, Blitzüberspannungen, Isolationskoordination.

LIST OF FIGURES

Figure 1 - Arrester gapless design (left) and with gap	20
Figure 2 - ABB EXCOUNT-II installed on line arrester	28
Figure 3 - Block diagram of the new monitoring system.....	31
Figure 4 - Installation on tower of the new monitoring system	32
Figure 5 - Top view of the monitoring system controller	33
Figure 6 - View of the acquisition card.....	34
Figure 7 - Monitoring system assembled	35
Figure 8 - Side view of the current transformer	38
Figure 9 - Monitoring system mobile communication.....	41
Figure 10 - Top view of mobile communication card (top) next to the wireless one (bottom).....	42
Figure 11 - Solar supply setup.....	43
Figure 12 - View of the client application running on the monitoring system	46
Figure 13 - Memory allocation for data acquisition.....	47
Figure 14 - Acquisition process on memory	49
Figure 15 - Trigger conditions verified in memory.....	49
Figure 16 - Nth sample check explained	50
Figure 17 - Trigger detection with the Nth sample loop	50
Figure 18 - Software function for trigger detection	51
Figure 19 - Acquisition data saving steps explained (1/3).....	52
Figure 20 - Acquisition data saving steps explained (2/3).....	54
Figure 21 - Memory saving buffer structure	54
Figure 22 - Acquisition data saving steps explained (3/3).....	55
Figure 23 - Event file structure.....	55
Figure 24 - Example of shape display by server application	57
Figure 25 - Time drift issues in the arrester monitoring field	58
Figure 26 - Monitoring system time synchronization with a NTP server	59
Figure 27 - EMTP_RV Simulation preview.....	61
Figure 28 - EMTP_RV simulation preview of Scenario 1	62
Figure 29 - EMTP_RV simulation preview of Scenario 2.....	63
Figure 30 - EMTP_RV simulation preview of Scenario 3.....	64
Figure 31 - Currents flowing through bottom and middle arresters in Scenario 1.....	65

Figure 32 - Currents flowing through bottom and middle arresters in Scenario 2.....	66
Figure 33 - Currents flowing through bottom and middle arresters in Scenario 3.....	67
Figure 34 - Application developed for automatic control of Haefely ECOMPACT 4	70
Figure 35 - Monitoring System Laboratory Testing Setup	71
Figure 36 - View of the server application with successful trigger arrivals.....	73
Figure 37 - Generated shape for multicomponents acquisition testing	75
Figure 38 - Mobile communication testing	76
Figure 39 - Real field transient current measurement (1/5)	81
Figure 40 - Real field transient current measurement (2/5)	82
Figure 41 - Real field transient current measurement (3/5)	82
Figure 42 - Real field transient current measurement (4/5)	83
Figure 43 - Real field transient current measurement (5/5)	83
Figure 44 - Application developed for arrester energy duty calculation.....	86
Figure 45 - Proposed configuration for the study of arrester energy duty sharing	89
Figure 46 - Time drift issues with monitoring systems installed for different utilities.....	90
Figure 47 - Monitoring system time synchronization over GPS.....	91
Figure 48 - Fiber optics along a transmission line	93
Figure 49 - Application of wireless communication next to fiber optics.....	93
Figure 50 - Application of wireless communication along whole line	94
Figure 51 - Arresters voltage discharge curve example	109
Figure 52 - Switching surge operating duty test: Conditioning	112
Figure 53 - Switching surge operating duty test: High current impulse conditioning	113
Figure 54 - Switching surge operating duty test: Application of impulses	114
Figure 55 - Lightning stroke model (left) and sub-circuit modelisation (right).....	116
Figure 56 - Line model.....	117
Figure 57 - Tower model.....	118
Figure 58 - Tower sub-circuit.....	119
Figure 59 - Insulator model	120
Figure 60 - Tower footing soil ionization model	121
Figure 61 - Arrester model	123
Figure 62 - Tower model equipped with arresters on bottom and middle phase	124
Figure 63 - Line source model	124
Figure 64 - EMTP_RV full scale simulation preview (part 1/3).....	125
Figure 65 - EMTP_RV full scale simulation preview (part 2/3).....	126
Figure 66 - EMTP_RV full scale simulation preview (part 3/3).....	126

Figure 67 - Laboratory setup for the ECOMPACT 4 generated shape acquisition	130
Figure 68 - Oscilloscope view of the generated shape in laboratory	131
Figure 69 - Current shape acquired by the monitoring system and transmitted to server.....	131
Figure 70 - Multicomponents acquisition test setup	132
Figure 71 - Difficult access area to towers.....	139
Figure 72 - Interior view of the EMC enclosure	140
Figure 73 - Current transformer installation over the ground lead conductor.....	140
Figure 74 - Enclosure view	141
Figure 75 - Solar panel view	141
Figure 76 - Monitoring system successful installation (1/2).....	142
Figure 77 - Monitoring system successful installation (2/2).....	142

LIST OF TABLES

Table 1 - IEC standard arrester classification	19
Table 2 - Basic comparison between gapless arrester and arrester with the gap	21
Table 3 - Surge counter Tyco SC13 main characteristics	26
Table 4 - ABB EXCOUNT-II main specifications	27
Table 5 – Monitoring system controller specifications	33
Table 6 - Acquisition card specifications	35
Table 7 - Analog input accuracy basics.....	37
Table 8 - Current transformer specifications.....	39
Table 9 - Current to voltage conversion	40
Table 10 - Analog to digital conversion	48
Table 11 – Example of parameters sent by server application.....	60
Table 12 - Absolute current peaks flowing through arresters for all scenarios.....	67
Table 13 - Absolute current amplitude variation as function of tower footing resistance	68
Table 14 - Impulse generator specifications.....	69
Table 15 - Arbitrary waveform generator specifications	74
Table 16 - Monitoring system installation towers data	78
Table 17 - Monitoring system results (Tower 38, Dates: 28 May 2009 – 23 June 2009).....	84
Table 18 - ABB EXCOUNT-II readings (Tower 38, Dates: 28 May 2009 – 23 June 2009)...	84
Table 19 - Relay protection operation (Dates: 28 May 2009 – 23 June 2009)	85
Table 20 – Voltage discharge curve data	109
Table 21 - Switching surge operating duty test based on IEC 60099-4 Standard.....	111
Table 22 - Input data for the simulated line	118
Table 23 - Current / Voltage characteristics of a 20 Ω tower footing resistance	122
Table 24 - Tower footing resistance measurement example	123
Table 25 - Current / Voltage characteristics of the simulated arrester	123
Table 26 - Typical monitoring system power consumption.....	127
Table 27 - Typical lifetime of an AGM battery	128

LIST OF EQUATIONS

Equation 1 - Number of steps acquisition card can differentiate	36
Equation 2 - Accuracy of the acquisition card	36
Equation 3 - Bytes to bits conversion.....	47
Equation 4 - Memory space required for data acquisition	47
Equation 5 - Energy duty of a surge arrester calculation	107
Equation 6 - Trapezoid rule applied to energy duty calculation at each time step.....	107
Equation 7 - Interpolation applied to voltage discharge curve.....	108
Equation 8 - Total energy duty calculation	108
Equation 9 - Air gap EMTP_RV model flashover criteria.....	120
Equation 10 - Tower footing soil ionization	121

LIST OF DEFINITIONS

AC: Alternating Current

AGM: Absorbed Glass Mat

A/D: Analog to Digital

BNC: Bayonet Neill-Concelman

CIGRE: Conseil International des Grands Réseaux Électriques

DC: Direct Current

EDGE: Enhanced Data Rates for GSM Evolution

EGLA: Externally Gapped Line Arrester

EGM: Electrogeometric Model

EMC: Electromagnetic Compatibility

EMI: Electromagnetic Interference

EMTP_RV: Electromagnetic Transients Program Restructured Version

GMT: Greenwich Mean Time

GPRS: General Packet Radio Service

GPS: Global Positioning System

IEC: International Electrotechnical Commission

IP: Internet Protocol

LAN: Local Area Network

LSA: Lightning Surge Arrester

NTP: Network Time Protocol

PCI: Peripheral Component Interconnect

RAM: Random-Access Memory

SIM: Subscriber Identity Module

ULV: Ultra Low Voltage

USB: Universal Serial Bus

WiFi: Wireless Fidelity

ZnO: Zinc Oxide

I. Introduction

Line surge arresters are devices used to improve transmission line lightning performance. Electrically, they are installed in parallel to the line insulators, with the main function to prevent line insulation flashover. This technology is today used worldwide as a standard solution for line lightning performance improvement of transmission and distribution lines.

Surge arrester Zinc Oxide (ZnO) disc volume, and therefore disc diameter determines the maximum energy capability of the arrester. It is very important to select arrester energy capability according to the expected energy stresses. If incorrectly chosen, or if facing a higher energy stress due to the incoming transient current, the arrester may fail to absorb the energy.

Nowadays some of the line surge arrester manufacturers try to promote higher energy duty surge arresters. This higher energy capability corresponds to higher metal oxide blocks size leading to heavier and more expensive arresters. Main argument remains the additional safety provided by this product since it is capable to absorb more dangerous electrical stresses, even the ones that are impossible to occur in reality based on software simulations.

Without the measurement of real electrical stresses a particular line is exposed to, and based only on recommendations from CIGRE regarding lightning parameters such as stroke median value of the current peak, front time and duration, a line surge arrester cannot be stated as correctly chosen or over dimensioned regarding its energy capability.

Arrester monitoring field is of primary importance as well. Next to the surveillance of the arrester condition, this monitoring offers a better understanding of the stresses arrester is exposed to in service.

An arrester monitoring system can measure different parameters such as the leakage current flowing through the surge arrester, the transient current, the temperature of the ZnO blocks.

This different data leads to conclusions regarding arrester condition, whenever it has to be removed from service or not, and arrester selection, whenever it has been correctly designed for a particular line. Also the measured parameters may validate or not the accuracy of simulation software results.

Existing monitoring devices offer a good overview of the arrester condition regarding its energy capability. However most of them are based on laboratory experiments or artificially triggered lightning, thus the link between the measured electrical stresses and the real ones is discussable.

Transient software is also widely used for the line lightning performance simulations. But its input data regarding lightning characteristics is based on recommendations and therefore this may lead to inaccurate electrical stresses estimations.

The new contribution of this thesis is the development of a complete arrester monitoring system. It is capable of measuring real field parameters related to the electrical stresses such as the shape of the transient current which is of primary importance in the correct selection of surge arrester regarding its energy capability.

Indeed this data enables the calculation of the energy discharged through the arrester and therefore this monitoring system as well the software operating it permit to make comments regarding the correct choice of the arrester for a particular line.

Also this acquired data regarding current shape is useful for the simulation software validation. With the different transient programs presenting various results for a particular line design, it is very important to compare the simulated shapes with the acquired ones, for a similar scenario.

The scientific output of this thesis is a better understanding of real electrical stresses a surge arrester is exposed to on a particular line, as well early conclusions regarding its correct selection and the accuracy of simulation software results. A major conclusion of a recent colloquium [33] regarding exclusively line surge arresters was that much more input parameters from the real field regarding electrical stresses are needed for the correct selection of arresters. Otherwise it is impossible to confirm whenever a line surge arrester is correctly designed, under dimensioned or over dimensioned for a particular line. This insufficiency leads to much confusion for the utilities when trying to purchase the correct arrester for their needs. Therefore the possibility to measure real field stresses offered by this new monitoring system is positively approved.

The scope of this work is to develop a new monitoring system that is capable of measuring the real electrical stresses a line surge arrester is exposed to. Thanks to its current transformer installed on the grounding lead conductor, and data acquisition card, the real current shape discharged through the arrester is measured. With this measurement, next to the number of operations, current peak and duration, energy duty of the arrester can be calculated as well for the first and subsequent strokes.

This new monitoring system operates at distance and in real time, thanks to the new possibilities in the communication and power supply fields. Being correctly designed thanks to the software simulations and successfully tested in laboratory, two monitoring systems are installed on a pilot line. Real stresses on the surge arrester due to real lightning activity are monitored, and first results are included in this thesis. Next to the calculations regarding arrester energy duty, comments are presented regarding arrester condition.

Based on this framework, main chapters of this thesis are presented below.

The main topics of this thesis are:

- Study of present recommendations regarding lightning characteristics and line surge arrester selection based on energy duty considerations.
- Presentation of existing monitoring devices for line surge arresters as well present research projects.

- Proposal of a new monitoring system with its advantages in the measurement of real stresses.
- Software simulations regarding the line surge arrester energy duty for a particular transmission line.
- Laboratory testing of the developed monitoring system in order to verify its operation.
- Installation in real field of two monitoring systems on a particular transmission line.
- Gathering of the real results due to real electrical stresses and conclusion about arrester condition.

Also several annexes are included at the end of this work.

- Annex I presents the calculation method of the arrester energy duty based on the measured currents flowing through it due to real stresses as well its voltage discharge curve, also called current–voltage characteristics.
- Annex II describes the operating duty test procedure an arrester has to pass successfully in a laboratory before commercialization. This test enables for the manufacturer to state the energy capability of its arrester.
- Annex III gives an extensive modelisation of each device used for the simulation studies, as well the justification of input parameters.
- Annex IV presents the calculation procedure in the determination of solar power supply requirements for the proposed monitoring system.
- Annex V is a set of illustrations demonstrating the laboratory testing of the monitoring system.
- Annex VI contains the complete source code of the application used for the remote control of the Haefely EMC ECOMPACT 4 impulse generator.
- Annex VII is a set of illustrations demonstrating the real field installation of the monitoring system.

II. Line Surge Arrester and Energy

An overhead line is exposed to different electrical stresses during its operation. Most important of them are the lightning overvoltages due to atmospheric discharges and the switching overvoltages due to line closing and line re - closing at substation. According to the worldwide experience more than 50 % of all line outages are related to the lightning.

Line lightning performance is the annual number of outages due to lightning per 100 km of line length. Improving it is of primary importance for the quality of energy supply.

II.1. ELECTRICAL STRESSES

II.1.1. Lightning overvoltages

Lightning stroke can hit tower top, shield wire, phase conductor or nearby object. Lightning overvoltage is generated which may produce line insulation flashover.

A direct hit to the tower or the shield wire may produce a backflashover. In the case that the lightning surge bypasses the shield wire and hits the phase conductor directly, this event is called a shielding failure.

A backflashover is a flashover from the tower to the phase conductor. The lightning surge with a defined current peak and front time hits the tower directly or the shield wire if present. In both cases, lightning current is discharged to the tower earthing which has a defined footing resistance. The amplitude of the voltage potential of the tower rises quickly. If the voltage potential difference between the tower and the phase conductor is higher than the insulation critical flashover level, a flashover occurs on the insulator. Therefore the backflashover is related to the tower footing resistance. The higher is this resistance value, the higher is the probability of backflashover.

Shielding failure results in two equal waves with half the lightning current amplitude flowing through the phase conductor to the towers on both ends. This transient current may produce a flashover from the phase conductor to the tower. This event is called shielding failure flashover. However with the Electrogeometric Model (EGM) [2], only lightning surges with smaller current peaks can produce a shielding failure on a typical shielded overhead line.

II.1.2. Switching overvoltage

A switching overvoltage is a so called slow front overvoltage compared to the lightning one. It has a longer duration as well. This type of overvoltage is of great importance for the transmission system voltages of 245 kV and higher [1].

II.2. LINE LIGHTNING PERFORMANCE IMPROVEMENT METHOD

Different solutions are possible in order to improve line lightning performance. Main of them are [3], [5]:

- Tower footing resistance improvement.
- Additional shield wire.
- Installation of guy wires, in order to divert locally part of the transient current away of the tower earthing.
- Installation of underbuilt ground wire that diverts part of the transient current to the neighboring towers.
- Insulation increase in order to improve its withstand level.
- Application of line surge arrester.

In practice, solutions such as underbuilt ground wire, guy wire and insulation increase are not applied due to technical or economical constraints. Remaining possibilities are detailed below.

Reducing tower footing resistance reduces the probability of the backflashover. In some cases tower footing resistance reduction is very difficult and very costly and in some cases impossible.

In the case that the line has no shield wire, installing one would prevent the high current lightning hit directly to the phase conductors. Adding an additional shield wire to the existing one can improve the shielding angle of the line thus allowing that only low current peak lightning surges may bypass it based on the EGM estimation. In addition, shield wires divert part of the lightning current to the neighboring towers reducing probability of the backflashover.

If none of the above two methods are feasible, from a technical or economical point of view, a third option to improve line lightning performance is the application of line surge arresters (LSA).

II.3. LINE SURGE ARRESTER

Line surge arresters are devices used to improve transmission line lightning performance. Electrically, they are installed in parallel to the line insulators, with the main function to prevent line insulation flashover. This technology is today used worldwide as a standard solution for line lightning performance improvement of distribution and transmission lines [40] - [56]. They are used on shielded and on unshielded lines. Hundreds of thousands of these devices are in service today with an excellent service experience. It is possible to have a complete control over line flashover rate by the use of line surge arresters. By their installation on all phase conductors and on all towers along the line it is possible to have zero outages, but today's practice is to optimize installation of these devices according to the target line performance. On the shielded lines, surge arresters are usually installed on the sections of the line exposed to lightning and on the towers with high footing resistance. Software simulation tools are used for the selection of an optimum installation configuration.

II.3.1. Energy considerations

Surge arrester Zinc Oxide (ZnO) disc volume, and therefore disc diameter determines the maximum energy capability of the arrester. It is very important to select arrester energy capability according to the expected energy stresses. If incorrectly chosen, or if facing a higher energy stress due to the incoming transient current, the arrester may fail to absorb the energy.

ZnO disc diameter defines the arrester energy capability. According to the IEC standard the following arrester classes are defined:

Arrester Class	Disc diameter (mm)
IEC Class I	40
IEC Class II	48
IEC Class III	63
IEC Class IV	76
IEC Class V	100

Table 1 - IEC standard arrester classification

II.3.2. Different designs

There are two line surge arrester designs:

- Gapless LSA
- LSA with a gap

Gapless line surge arrester has similar design to the station class arresters. Gapless LSA are normally equipped with disconnecting device, which disconnects arrester from the service in the case of the arrester failure.

Line surge arrester with a gap (EGLA - Externally Gapped Line Arrester) has an external series gap. ZnO part of this LSA has the same design as gapless LSA. Thanks to the external gap, this type of the arrester needs no disconnecter. In general, EGLA has less ZnO blocks than gapless LSA.

The majority of the LSA used today are gapless design. EGLA are used in a few countries only such as Japan and France.

Main differences between the two designs which are important to underline in the arrester monitoring field are presented in Table 2.

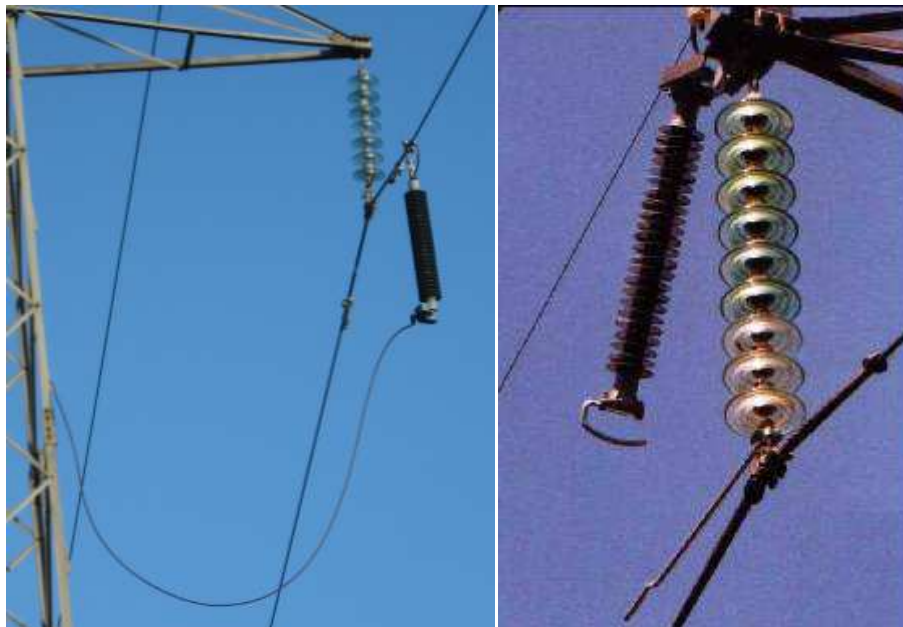


Figure 1 - Arrester gapless design (left) and with gap (right)

Design	Advantages	Disadvantages
Gapless arrester	<ul style="list-style-type: none"> - Easy to install - May be installed live - Better energy sharing - Controls switching surge overvoltages - Easy monitoring [both leakage and impulse current] 	<ul style="list-style-type: none"> - Frequent disconnecter operation - Permanently stressed by power frequency voltage - Stressed by all overvoltages
Arrester with the gap	<ul style="list-style-type: none"> - No need for disconnecter - No stress from power frequency voltage and switching overvoltages - Less ZnO blocks in ZnO part 	<ul style="list-style-type: none"> - Difficult to install - Gap distance change in service - Impossible live installation - No leakage current monitoring - No energy sharing

Table 2 - Basic comparison between gapless arrester and arrester with the gap

II.3.3. Line arrester energy duty

Determination of LSA energy duty is very important in the application of this technology for the line lightning performance improvement. LSA are stressed in service by temporary overvoltages, switching overvoltages and lightning overvoltages. These overvoltages determine arrester energy duty. Arrester energy capability determines LSA price. For example, IEC Class II LSA is about 30 % more expensive, and IEC Class III cost almost 50 % more than IEC Class I LSA. In addition to the higher prices higher class arresters have higher weight and cross section. Higher weight sometimes may limit application of this technology since some utilities don't like to put heavy devices on their line. It is also important to take into account that higher class arrester increase transportation, storage and installation cost. Line surge arrester energy duty calculation is presented in Annex I.

LSA rated / duty cycle voltage is generally determined by the system temporary overvoltages. Taking into account that LSA main function is to prevent flashover over line insulators there is no need to take the same rated voltage as for the arrester used for other system equipment protection. It is normally recommended to take a slightly higher rated voltage for LSA than for station arresters. When LSA rated voltage is correctly selected there is no important energy duty related to this type of the overvoltages. Thermal runaway of the surge arrester corresponds to the situation when power losses in the arrester exceeds the thermal dissipation capability of the housing and connections, leading to a cumulative increase in the temperature of the ZnO blocks culminating in failure.

Surge arrester thermal stability is best checked in the Operating duty test [Annex II]. In this test, after so-called conditioning and ZnO blocks preheating two rectangular impulses are applied [for the considered arrester - IEC Class II] injecting in the blocks energy, which

corresponds to this arrester class [about $5 \text{ kJ/kV}_{\text{rated}}$]. After application of the impulses the elevated rated voltage is applied for 10 seconds followed the application of the elevated continuous operating voltage for 30 minutes. Arrester has to demonstrate thermal stability in this test.

In the selection of the surge arrester characteristics it is very important to correctly match so-called 'Power frequency withstand voltage versus time characteristic of the arrester' with the expected temporary overvoltage characteristic of the system in which arrester will be installed. The power frequency withstand voltage versus time characteristic of the arrester shows the maximum time durations for which power frequency voltage may be applied to the arrester without causing damage or thermal instability.

When temporary overvoltage characteristics of the system [peak and duration] in which arrester will be installed are known, selecting slightly higher rated voltage for LSA will reduce arrester stresses related to this type of the overvoltages.

Surge arrester energy duty related to the switching overvoltages depends on the line length, type of the line closing [closing, single pole re- closing, three pole re-closing] and surge arrester protective level. There is a big difference in the selection of the surge arrester energy capability for the station arrester and for the LSA. In fact, station surge arrester normally discharges all energy related to the line switching overvoltages. LSA installed along line length [the whole length or on the line sections] share energy related to the slow front line switching overvoltages. So LSA energy capability can be lower than station class energy capability. LSA energy duty depends on the number of LSA installed on the different phases, LSA type [gapless or with gap], LSA location along line length, and system voltage.

Taking into account that LSA share switching surge energy, their energy capability can be lower than station arrester switching surge capability. For example, if station arrester has IEC Class III energy capability, very often IEC Class I switching surge energy capability will be sufficient. It is important to note that surge arrester switching surge test, defined in arrester Duty cycle test presented in Annex II, is related to the station arrester energy capability verification.

When LSA lightning surge energy duty is in question, it is very important to take into account the following information:

- Line design [shielded or unshielded]
- Lightning stroke distribution
- Lightning current shape through LSA
- Lightning stroke polarity
- Tower footing resistance
- Lightning stroke multiplicity

It is well known that LSA are differently stressed on the shielded and on the unshielded lines. Shield wires are collecting “higher energy strokes” and diverting fraction of the lightning stroke current. Lightning stroke current through LSA depends also on the number of shield wires. Lightning current shape through LSA is different for the shielded and for the unshielded line. Its duration is shorter for the shielded line.

Phase conductors on the unshielded line can be struck directly by “high energy” lightning strokes. Lightning current shape through LSA is similar to the shape of the lightning stroke hitting the line [longer duration than for shielded line] meaning that LSA on the unshielded lines are much more stressed than LSA on the shielded line.

In the determination of the LSA energy duty for the shielded lines tower footing resistance plays very important role, especially for the all phase conductors LSA installation. Higher is tower footing resistance higher is LSA energy. This has to be taken into account in the LSA selection.

In the software statistical simulation for the LSA energy duty determination it is very important to have stroke distribution which corresponds to the region in which line is installed. In CIGRE brochure [3] median of the stroke distribution is 31 kA. This value is obtained by the measurement on the tall towers in the regions with a very high lightning activity. Latest research based on the modern lightning location systems show that the median of the current is much lower [for example 14 kA in Austria, 16 kA in Slovenia]. Making software simulation with 31 kA will produce very high energy stresses which are not realistic.

The majority of the lightning strokes are negative polarity [more than 85 %]. The positive polarity strokes have higher current peaks and longer duration [higher than negative strokes energy], but they appear in few regions in the world [In Japan during winter, in the high mountains]. In the rest of the world the negative polarity stroke dominates and arrester energy duty determination has to be based on this polarity distribution.

Almost all lightning flashes consist of several components [first and a few subsequent ones]. Average number of components per flash is three, while some flashes may consist of eight or more components. The subsequent strokes are normally lower peak than the first component [in 95 % of cases] and they have shorter duration.

Usual time separation between subsequent flashes is about 100 ms, meaning that flash energy [related to the first and to the subsequent] has to be taken into account. This is because ZnO blocks have no time for cooling.

In the case of the shielded lines subsequent components hitting tower top or shield wire usually will not produce arrester operation [being lower amplitude]. So their energy input

to the LSA is not so important. But in the case of the shielding failure all subsequent strokes energy input have to be considered. The same is for unshielded line.

II.3.4. Line surge arrester monitoring

As per previous discussion arrester energy duty determination is of great importance. To determine arrester energy duty it is necessary to know LSA current shapes. LSA current peaks, obtained by some standard surge monitors can give some indications for the energy duty but this is not sufficient. LSA current shapes can be determined by the software simulation and by the measurement [real field or laboratory].

Software simulations for LSA current shape determination suffer from the correct simulation parameter selection. As indicated before wrong median current selection may lead to unrealistic energy duty. The same is for the surge tail selection, as well the number and distribution of the subsequent components. This means that software simulations are useful for the indication of the expected arrester energy duty, but this is not sufficient for the final LSA selection.

LSA current shape monitoring may be performed in a laboratory or in the real field. Laboratory measurements are performed during the LSA development and testing phase using surge shape that is different from the shapes LSA will receive in the field. In fact, all these lab measurements are performed in order to verify the arrester energy capability.

Real field measurements are performed in the special test sites or on the real lines. The special test sites have just section of the line [usually distribution line with a limited length]. Standard laboratory instruments [oscilloscopes or transient recorders], laboratory dividers and sensors are used for the arrester current shape measurement. Rocket triggered lightning is used to bring lightning stroke to the desired point of line. It is important to indicate that the triggered lightning is different than natural lightning.

There are a few projects performed on the real distribution lines with real lightning activity, but the main purpose of those tests is to verify the arrester disconnector operation. Arresters under the test are standard distribution arresters installed for the distribution transformer protection. Standard measurement equipment is used, with no real time data transfer.

One project, which includes high voltage LSA, is performed in Japan, with the purpose to check LSA energy capability for the positive stroke lightning current. In addition to the real lightning strokes hitting to the line, the majority of the stroke are rocket triggered. Standard laboratory recording equipment is used with no remote data transfer.

II.3.5. Purpose of this work

The main purpose of this work is to develop a real time, remote LSA current shape monitoring system installed permanently in the field. It was decided to install this system on a 123 kV line in Croatia. The considered line operates in a very heavy lightning environment [South of Croatia - estimated ground flash density is 7 strokes/km²/year]. This shielded single circuit line is 46 km long and has 144 towers. To improve line lightning performance 106 IEC class II gapless LSA, having rated voltage of 108 kV are installed. LSA are installed on the selected towers [bottom or bottom and middle conductor]. LSA installation configuration is determined using software simulation. After LSA installation line lightning performance is improved for 50 %.

III. New arrester monitoring system

Before introducing the proposed arrester monitoring system it is important to describe existing devices in order to underline differences and improvements to expect. Two monitoring systems are presented. First of all a surge counter and total leakage current measurement device is introduced. Then a line arrester monitoring system is described. Finally next to those commercially available devices, current most advanced research projects are presented.

III.1. EXISTING DEVICES

III.1.1. Surge counter and total leakage current measurement device

The SC13 is a surge counter and total leakage current measurement device from company Tyco [24]. A similar monitoring system is the 3EX5 050 from the company Siemens [25]. It is mainly used in substation for station surge arresters.

Main specifications of this device are given in the table below.

Meter	6 digit cyclometer at least 5 counts/second
Minimum count current	200 A 8/20 μ s
Maximum High Current Withstand	100 kA 4/10 microsecond wave
Nominal Residual Voltage at 100 kA with 4/10 microsecond wave	5 kV
Auxiliary contact rated 0,5 A 250 V for connection to remote signaling equipment	YES

Table 3 - Surge counter Tyco SC13 main characteristics

It gives two type of information:

- Total leakage current measurement
- Number of arrester operations

The Tyco SC13 can also be installed on a line surge arrester. Indeed it is an outdoor device that connects easily to the arrester base. However tower installation is not its primary application since the data it gives is accessible by direct reading only and not by a communication link.

Therefore the access to its information is difficult since it would require a technician to climb on tower or the usage of binoculars.

It has also an external output giving the instant value of the total leakage current and to which one a third party acquisition device can connect such as an oscilloscope.

III.1.2. Line arrester monitoring device

The ABB EXCOUNT-II is a line arrester monitoring device [26]. It measures the leakage current of the arrester as well the number of its operations, and has wireless communication ability.

This device is based on the measurement of the third harmonic of the leakage current with compensation [09]. Compensation means that this device is equipped with a field probe which monitors the harmonics content in the system voltage and eliminates them from the total leakage current measurement for greater accuracy. It is also solar powered. It contains two current transformers, one for the leakage current and one for the transient currents. A wireless handheld reader is used in order to retrieve the surge data and to synchronize the sensors internal timer with its own. Specifications of this device are given in the table below.

Surge Current amplitude classification (8/20 μ s)	10 - 99 A 100 - 999 A 1000 - 4999 A 5000 - 9999 A > 10000 A
Error in surge counting amplitude	< 20 %
Operation range	up to 60 m

Table 4 - ABB EXCOUNT-II main specifications

However peak values in a range are insufficient to calculate the arrester energy duty which requires the current shape.

Also each of the monitoring devices has own internal timer synchronized with the handheld reader during the data receiving phase. Therefore the time drift between two sensors is possible. This may lead to false conclusions such as the same lightning event recorded as two separate ones by two monitoring devices.

Finally in order to retrieve the data from the sensors installed on a line, a technician has to come close to the tower ground. This operation is difficult in some areas and cannot be considered remote or real time.

Nevertheless the information given by the ABB EXCOUNT-II is still useful for the basic line lightning performance understanding.

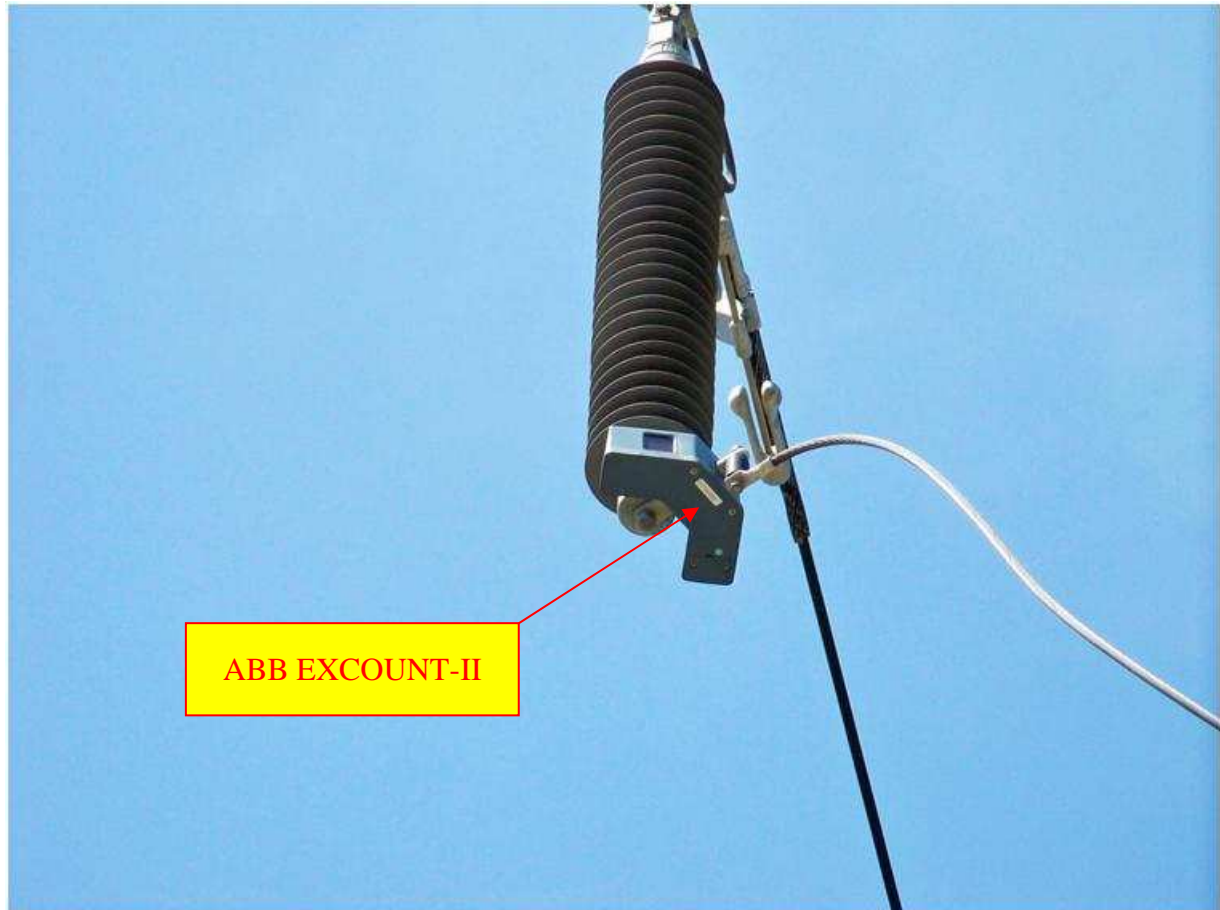


Figure 2 - ABB EXCOUNT-II installed on line arrester

III.1.3. Research projects

This chapter summarizes the most advanced research projects in the arrester monitoring field. Reference to each of them is presented as well.

First of all, a substation monitoring system has been developed in Germany to monitor station surge arresters [13]. System consists of measuring sensors, electronic unit and standard computer connected to the system by fiber optic link. Rogowski coil is used to monitor lightning currents, and measured signal is integrated to obtain arrester current peak. Surge arrester current peaks are then saved as a number of impulses belonging to the different current ranges. Surge arrester lightning current shapes are not monitored.

Next to it, a modern surge counter is used mainly in Germany for more than 10 years, which can indirectly indicate energy related with the arrester discharge current [14]. This device, called control spark gap, consists of two pairs of the electrodes, which are bypassed by a resistor. This resistor allows leakage current to flow in the arrester during normal operation, but when arrester discharges lightning current, voltage drop on the resistor will cause a sparkover of the gaps. The resistor is released and a full discharge current flows through the gaps, leaving visible marks on the copper electrodes. By the examination of the marks on the spark gaps it is possible to indirectly estimate arrester energy duty. The gaps removed from the service are compared with the gaps for which marks are produced in laboratory (with different current shapes). It is difficult to apply this system for the monitoring of line surge arresters. Indeed it is necessary to climb on the towers to remove the gaps, and there is no indication of the time of operation. This system is therefore not remote and real time.

A different project is monitoring surge arresters for a 154 kV transmission line that are installed on the instrumented tower [15], [16]. The instrumented tower is struck by natural and artificially triggered lightning. Lightning current to the tower top and in the earth wires are measured by the coaxial resistive shunts. The currents through tower legs and through line arresters are measured by the impulse current transformers. Overvoltage shapes on the insulators string are measured by the standard resistive voltage dividers. All signals are transferred to the measuring unit by the fiber optic links. Standard storage transient recorders are used for the voltage and current shape recording. It is necessary to come to the site to transfer measured shapes to computer for analysis. Therefore this system is not remote and real time as well.

Another project has for main purpose to measure lightning current shapes to the distribution surge arresters used for the distribution transformers protection [17]. Several utilities have participated in it. Distribution arresters used for the measurements are modified for this purpose. Coaxial shunts for current measurements and thin ZnO blocks for voltage measurements are installed inside arrester housing. Standard transient recorders with 7 bits analog to digital converters are used for the measurement. Data from the transient recorders are downloaded using a specially developed hardware and software. One result of the project is that 28 % of all currents through distribution surge arrester had bipolar shape.

Finally, the interaction of rocket-triggered lightning with two un-energized unshielded power distribution lines of about 800 m length was studied at the International Center for Lightning Research and Testing in Florida [18]. The tested distribution lines are equipped with six and four arrester stations. The total current flowing to earth through the multiple line groundings and the total phase-to-neutral current flowing through the line arresters and line terminations are measured using standard and commercially available digital oscilloscopes with 12 bits vertical resolution. The main purpose of this experiment is to check the lightning surge energy capability of the distribution arresters and the arresters disconnectors.

III.2. CONTRIBUTION TO THE ARRESTER MONITORING FIELD

The main contribution of this thesis is the development of a new arrester monitoring system. Its advantages are presented below.

First of all, the real current shape discharged through the arrester is measured. Next to the number of operations, current peak and duration, energy duty of the arrester can be calculated as well for the first and subsequent strokes. This is possible thanks to the introduced trigger acquisition algorithm.

Secondly, new monitoring system operates at distance and in real time, thanks to the new possibilities in the data acquisition, communication and power supply fields. This offers a wide scope of advantages such as quick and easy access to the results, as well the device diagnosis, software maintenance and upgrade.

Accurate timing of the monitoring system is possible thanks to the permanent connection to the mobile network. With this timing it is possible to compare recorded events with the data obtained by relay protection systems as well the lightning location systems.

In order to validate the working principle of the new monitoring system, a remote laboratory testing concept is introduced. It consists of equipment such as generators controllable at distance, adequate software developed for that purpose, and digital cameras for the remote viewing. This original testing simulates the monitoring system behavior in real field conditions but also demonstrates that it is effectively working, as this was the case during several conferences [31], [32], [33], [34], [35].

The measured results and energy duty calculations offer better understanding of the real stresses the arrester is exposed to in service. This information is of primary interest for simulation software validation and for the correct selection of the arrester.

Introduced monitoring system has been designed to be applied to any transmission and distribution line equipped with line surge arresters. It can be applied also to monitor station surge arresters installed in substation.

System is installed in real field on the pilot line for permanent operation. Two towers are monitored with arresters installed on middle and bottom phases. First results are already available.

Also future developments of the monitoring system are possible thanks to the technological breakthrough, since it is easily customizable. This covers topics such as computer networks along overhead lines and upgrade of existing equipment.

III.3. PRESENTATION OF THE NEW MONITORING SYSTEM

The new monitoring system is composed of the following parts:

- Industrial motherboard as controller
- Acquisition card
- Sensors such as current transformer
- Communication unit
- Power supply based on solar energy
- Interference and weather resistive enclosure
- Software

A block diagram is described in Figure 3. Each of the hardware parts are detailed below, as well the software operating it.

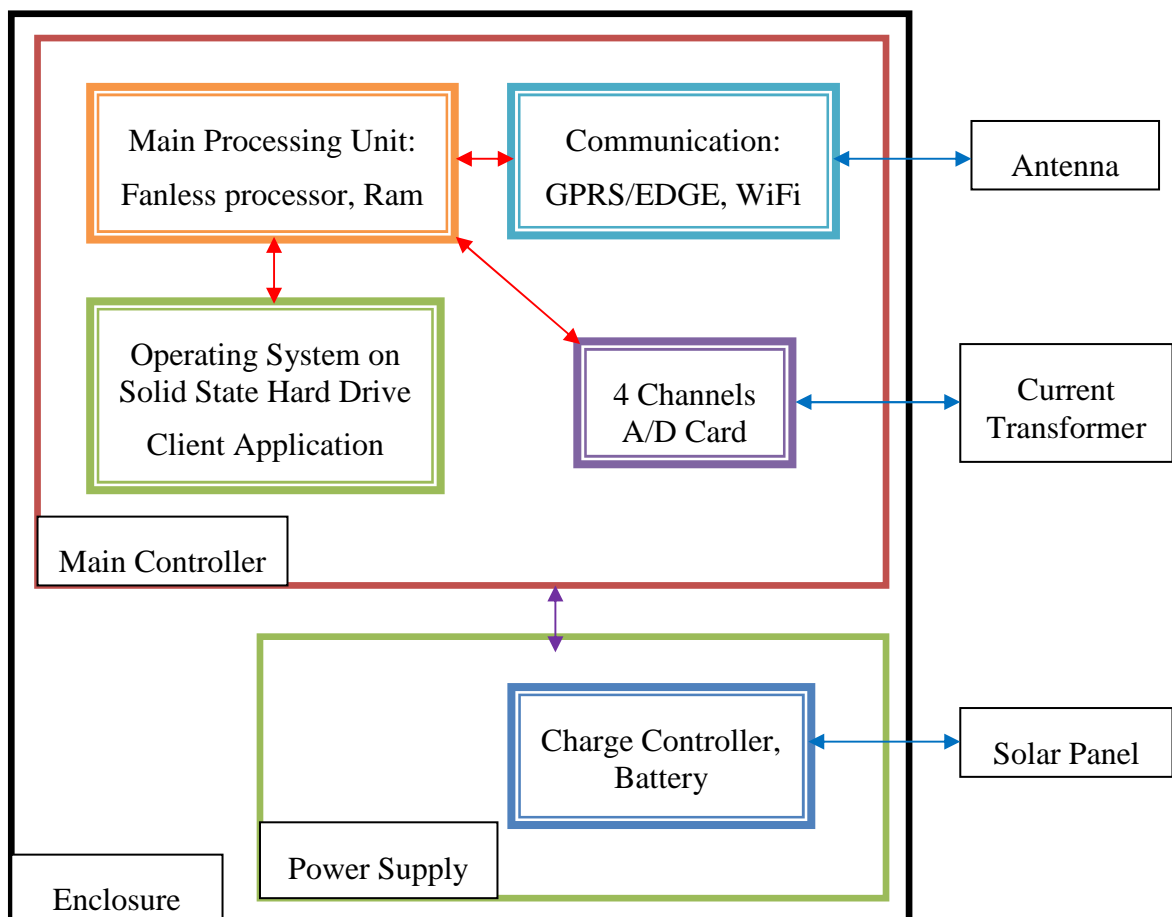


Figure 3 - Block diagram of the new monitoring system

System is designed to be installed on a high voltage tower. Illustration of this installation is shown in the figure below.

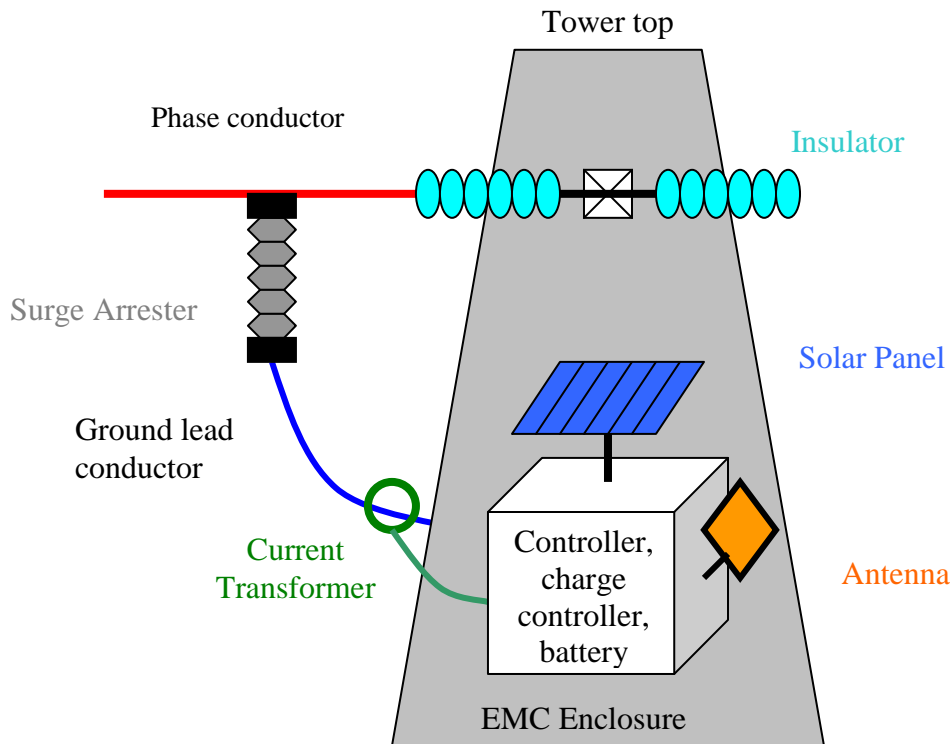


Figure 4 - Installation on tower of the new monitoring system

III.3.1. Description of the systems hardware

III.3.1.1. Controller

The monitoring system controller is an industrial motherboard. This main computing unit is in charge of coordinating the different tasks such as the acquisition of data and communication over a network. Indeed it gathers the acquired shapes, stores them into memory and the hard drive, connects to the server and transmit them.

It is composed of a fanless processor, memory and compact flash card behaving as a solid-state hard drive. Absence of fan avoids any risk of mechanical failure of the system. Indeed processor cooling is often mandatory for the correct operation but the cooler can sooner or later fail. Also with a low power processor and without a rotating fan the overall system consumption is reduced. Same advantages apply to the solid-state hard drive when compared to the mechanical one. Heat generation, power consumption and risk of failure due to vibrations such as heavy wind are reduced.

Chosen motherboard specifications are given in the table below.

Processor	VIA Eden 1,5 GHz ULV (fanless)
Memory	1 Gbyte DDR2 533 MHz
Interfaces	1 x LAN 4 x USB 2.0 1 x PCI
Power Supply	6 - 24 volts DC
Operating System	Microsoft Windows XP, Vista

Table 5 – Monitoring system controller specifications

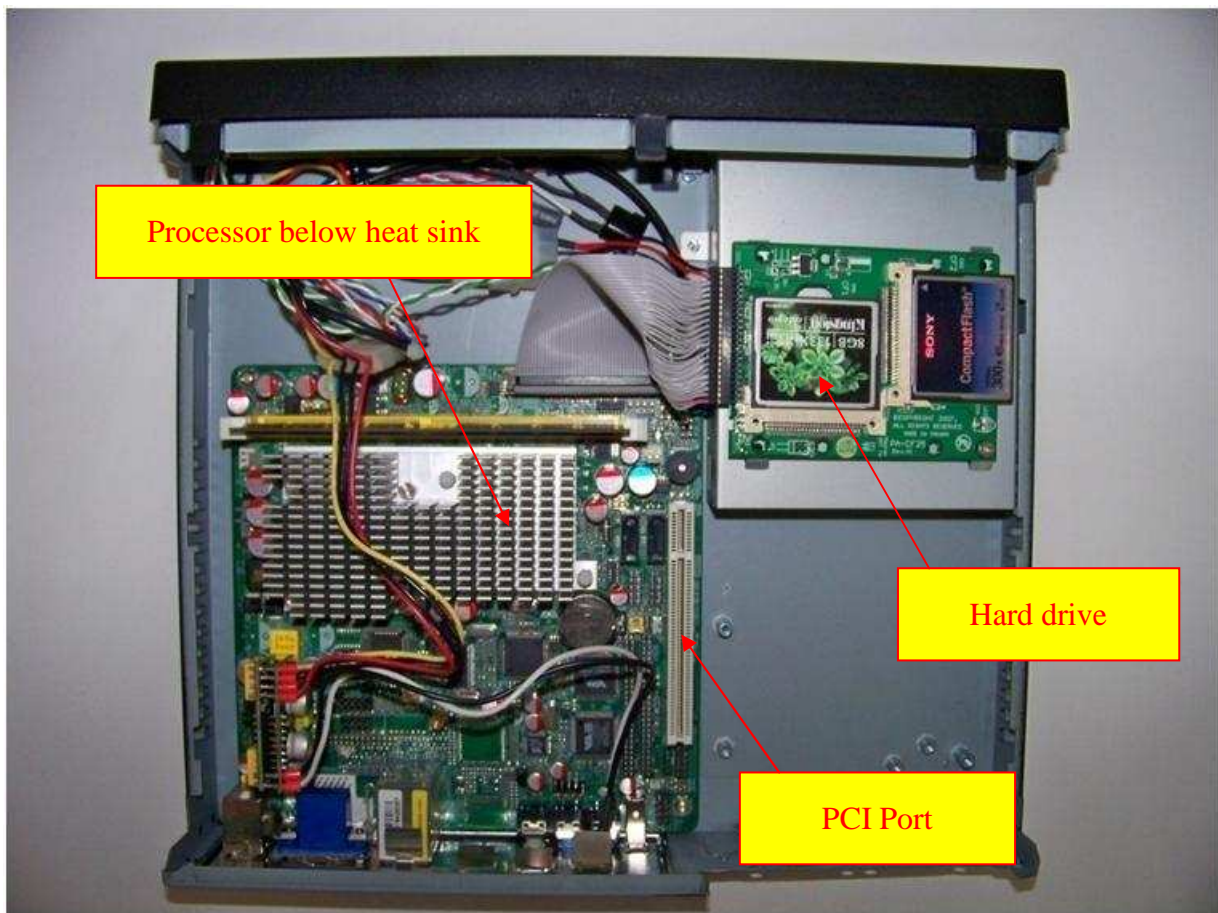


Figure 5 - Top view of the monitoring system controller

The PCI port enables the connection of the fast acquisition card to the controller. The presence of USB ports is important for the usage of mobile and wireless communication cards.

III.3.1.2. Acquisition card

III.3.1.2.1. Presentation

The acquisition card is connected to the PCI port of the controller. It acquires the sensors data continuously and sends them to the controller's memory.

Chosen model name is PCI-DAS4020/12 from company Measurement Computing [27].

Up to four input channels can be monitored with one card. Each of them can be configured independently. The acquisition speed of the card is 10 million samples per second and per channel, which corresponds to 10 data points taken in one microsecond. This is fair enough to acquire in detail the lightning transient current. Card input voltage range is ± 5 volts, with a maximum absolute of 15 volts. Any higher value may result in electrical damage for the system. Vertical resolution of the card is 12 bits. When compared to the acquisition speed, this parameter enables accurate results, as described in the next paragraph.

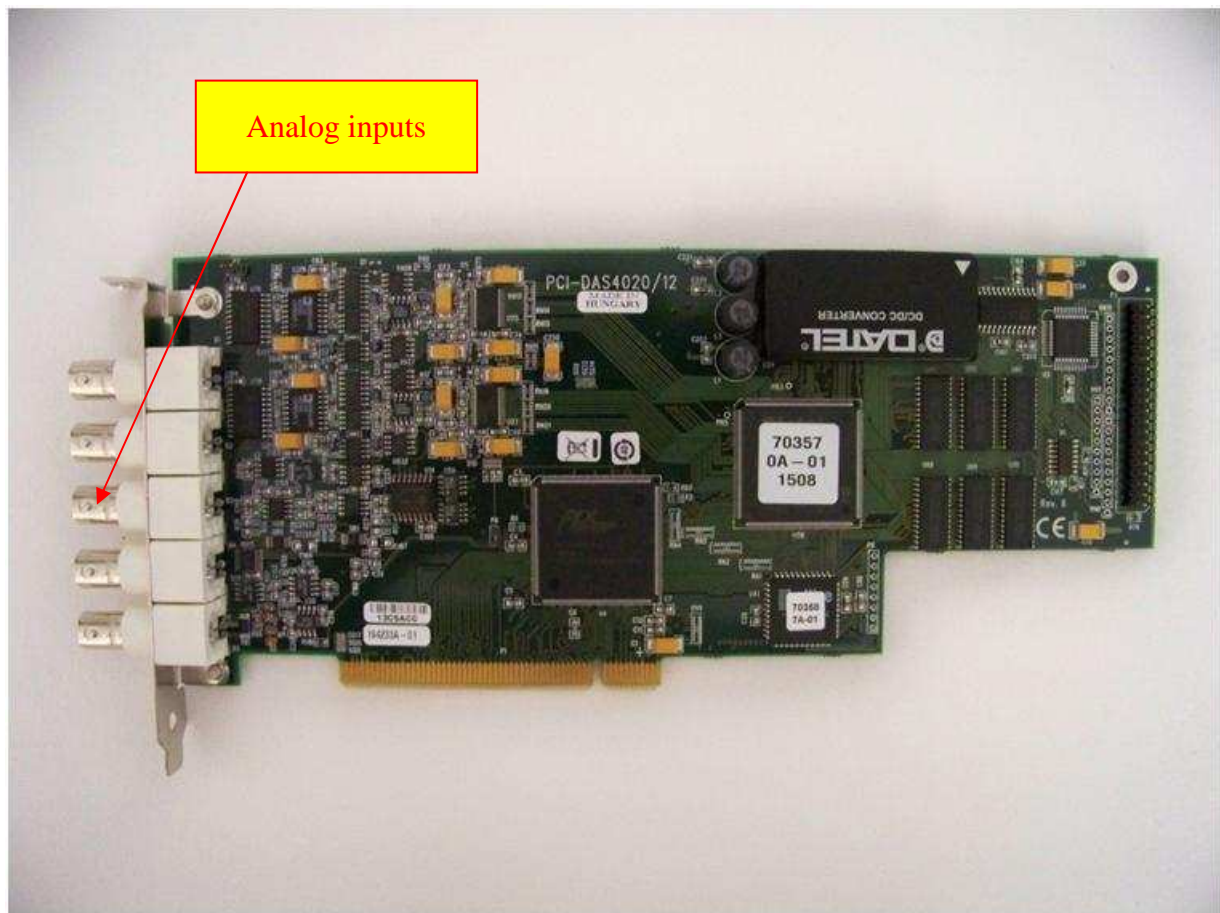


Figure 6 - View of the acquisition card

Detailed specifications of the acquisition card are given in the table below.

Number of acquisition channels	4
Acquisition speed (samples/s/channel)	10000000
Bandwidth	17 MHz
Input range (volts)	Software selectable: -/+ 1, -/+5
Vertical resolution (bits)	12
Number of digital inputs/outputs	24

Table 6 - Acquisition card specifications



Figure 7 - Monitoring system assembled

III.3.1.2.2. Vertical resolution, input range and accuracy

For a given input range, the resolution defines the number of steps the acquisition card can differentiate among that range. This number is calculated with the following formula:

$$N_s = N_b^{Res}$$

Where:

N_s is the number of steps the card can differentiate

N_b is equal to 2 – this is different values each bit can take, hence here 0 or 1.

Res is the resolution in bits

Equation 1 - Number of steps acquisition card can differentiate

Therefore with a resolution of 12 bits, the acquisition card can differentiate for an analog input:

$$N_s = 2^{12} = 4096 \text{ steps}$$

But this value has to be correlated to the analog input voltage range. The accuracy of the acquisition card, or the step between 2 data values, is given by the following formula:

$$Acc = \frac{R_g}{N_s}$$

Where:

Acc is the step between 2 data values

R_g is the analog input range

Equation 2 - Accuracy of the acquisition card

For an input range of –5 to +5 volts, the acquisition card has to differentiate values among a 10 volts range:

$$R_g = +5 - -5 = 10 \text{ V}$$

And with a resolution of 12 bits, this would give us an accuracy of:

$$Acc = \frac{10}{4096} \cong 2,44 \text{ mV}$$

This value means that each data point acquired by the card input will be a multiple of 2,44 mV due to the analog to digital processing. Also any smaller value will be digitized to the closest step. An example of real voltages values presented at the analog input and measured ones by the card is given in the table below.

Real voltage presented at analog input (mV)	Measurement shown by the card (mV)
1	0
1,5	2,44

Table 7 - Analog input accuracy basics

This is however a theoretical accuracy of the acquisition card. In practice this value is higher due to hardware limitations such as offset error and gain error [27].

III.3.1.2.3. Calibration of the acquisition card

Over time a well-known phenomena called voltage drift of the acquisition card happens, resulting in an accuracy loss of the A/D processing [27]. In order to get precise measurements again, it is important to calibrate the analog to digital converters with a voltage reference value.

In most cases acquisition card has to be calibrated every few months by connecting each analog input to a fixed value voltage source. This is however very difficult in this scenario since the monitoring system is installed on a high voltage tower inside an enclosure and no intervention shall happen during months.

The chosen acquisition card has a so called auto calibration mode. Thus there is no need to connect an external voltage source to its input. This is also an important advantage of this system since accurate measurements are possible over a long period of time without the need to intervene on it for a manual calibration.

III.3.1.3. Sensors

III.3.1.3.1. Presentation

The current transformer is installed on the grounding lead conductor. This is a cable that connects the bottom base of the arrester to the pylon. The same transient current flowing through the arrester flows through this conductor in order to divert it to the ground.

The proposed monitoring system can virtually accept any sensor at its input. For the presentation purpose a single current transformer is described below. Main reason of its choice is that this sensor is selected for the first monitoring system installation in real field, and has been approved during simulations and laboratory testing.

As shown in the simulation part below, no current with a peak higher than ± 20 kA can flow through the bottom and middle phase arresters, for the chosen line configuration and voltage level.

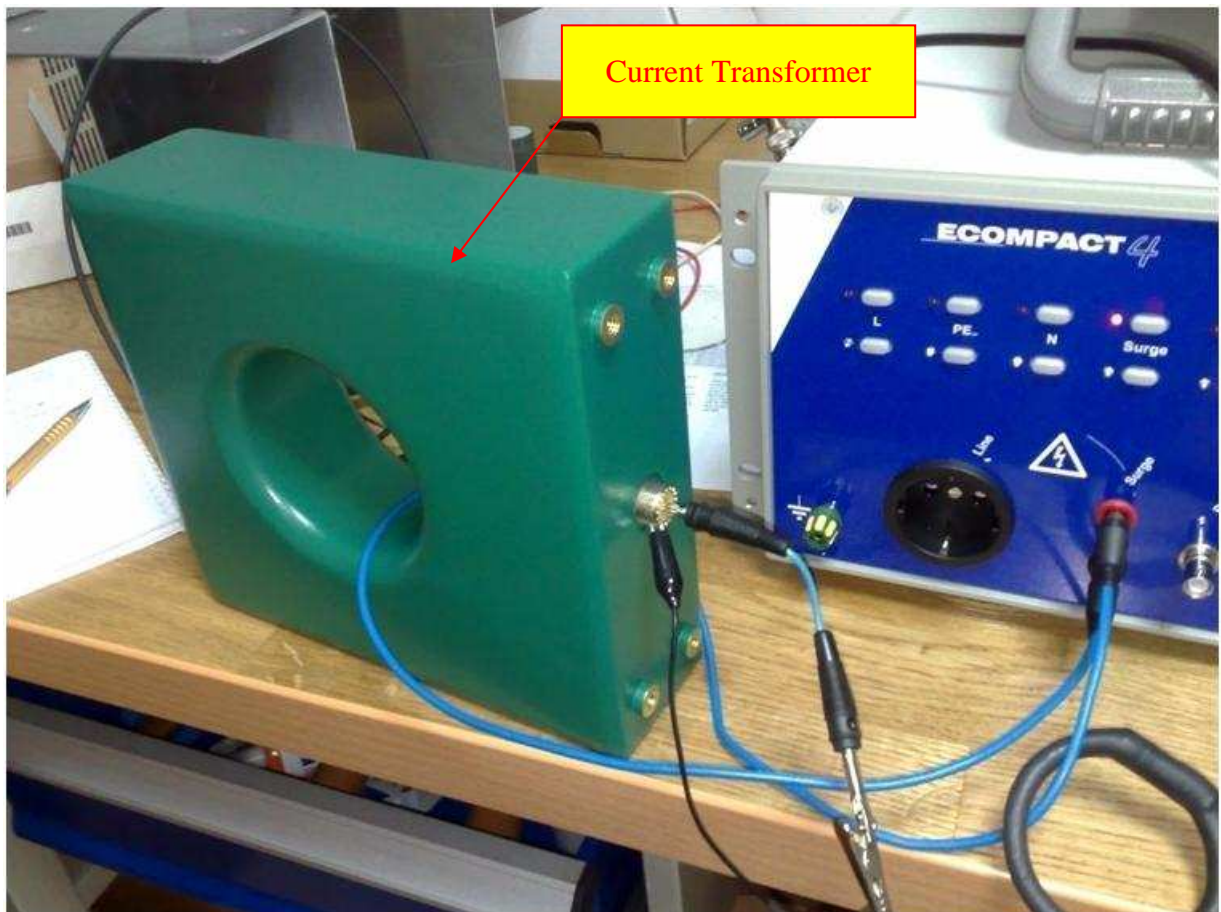


Figure 8 - Side view of the current transformer

The frequency of the current transformer is 4 MHz, which is important for the lightning transient acquisition.

The sensor has an output ratio of 0,025 V/A. This means that for a current of 20 kA, the voltage at its output is 500 volts. However since the acquisition card has an absolute maximum input of 15 volts, attenuators have to be used. Voltage dividers with a 100/1 ratio are installed at the entrance of each input channel.

The output of the sensor is connected to the attenuators with coaxial cable. A weather and electromagnetic interferences resistant tube is mounted on this cable to protect it.

The chosen current transformer is the model named 3025 from the company Pearson Electronics, Inc [28]. Specifications are given in the table below.

Input current (kA)	-/+ 20
Output ratio (V/A)	0,025
Useable rise time (nanoseconds)	100
High frequency 3dB cut-off (MHz)	4 (approximate)
Protection	Double EMI shield
Output connector	BNC

Table 8 - Current transformer specifications

It is important to note that 20 kA is the maximum input in the sense of linearity of the output and not as an absolute value which may damage the sensor if reached. Therefore any higher current will result in a higher output voltage at the transformer end, but the ratio of 0,025 V/A will be incorrect.

III.3.1.3.2. Acquisition accuracy at the current level

As described previously, the sensor of the monitoring system is selected in order to monitor currents from -20 kA to +20 kA. At the sensor's output these values correspond respectively to -500 volts and +500 volts. With the attenuation ratio of 100/1, this correspondence is related to -5 volts and +5 volts at the acquisition card input. Following table describes the correlation between current value at the sensor input and the voltage value at the acquisition level.

Current value measured (kA)	Sensor output value (V)	Acquisition card input (V)
-20	-500	-5
-10	-250	-2,5
0	0	0
10	250	2,5
20	500	5

Table 9 - Current to voltage conversion

The -5 and +5 volts range corresponds also to the analog input range. Therefore the previous accuracy calculation at the acquisition card level can be applied at the current level as well. Indeed the sensor has to monitor values from -20 kA to +20 kA, which correspond to a 40 kA range. And for this range, the acquisition card can differentiate 4096 steps because of the 12 bits resolution. With the acquisition formula in Equation 2 introduced previously, accuracy of the card at the current level is the following:

$$Acc2 = \frac{40000}{4096} \cong 10 A$$

This value means that theoretically the card can differentiate currents with a 10 A step. It also means that any smaller currents will be considered as a 10 A one, or will not be acquired at all (0 A).

III.3.1.4. Mobile Communication

The monitoring system communicates with the main server via the mobile network. Since the controller is installed on a high voltage tower in a rural area, the telecom base stations are the most convenient provider for this link. This is mainly due to the immediate availability of this network because the infrastructure is already in place. However it has a monthly fee per system to be paid to the telecom operator. And another drawback is that the reliability of this link is dependant of the mobile provider network.

Although the fiber optic cable installed next to the shield wire is also present on most of the high voltages lines, it is only possible to connect to it at a limited number of towers. Indeed around every three kilometers a junction box enables the connection of any device to the utility network. Main reason for this distance is the limited length of the bulk cable used during the installation on the shield wire. Since only every tenth or fifteenth pylon is communication ready and there is no guaranty that those towers are of interest for the lightning transient acquisition, the fiber optic communication is not an option. Also it would require some special authorizations from the utilities in order to connect this third party monitoring system directly to their network.

The wireless communication is also possible but for a price. It requires more time and money for the installation but offers a much more reliable and faster link. Also past the initial investment there is no more monthly fee to be paid to the telecom providers since the utility owns the network. Also the privacy of the data transmitted over this wireless link is total compared to mobile network. Finally the speed of wireless network in terms of bandwidth and response time is faster by a factor of 10 times. This type of communication is more detailed in the future development chapter.

Components required for this link on the monitoring system side is a computer card which behaves similar to the mobile phone. It has a SIM card inside which registers itself and connects the controller to the network. The chosen model is an USB card which supports different protocols such as GPRS and EDGE.

Next to the mobile communication, a wireless card is also present for backup purposes. Indeed in case of failure of the primary connection, this one allows a short range communication with a local user.

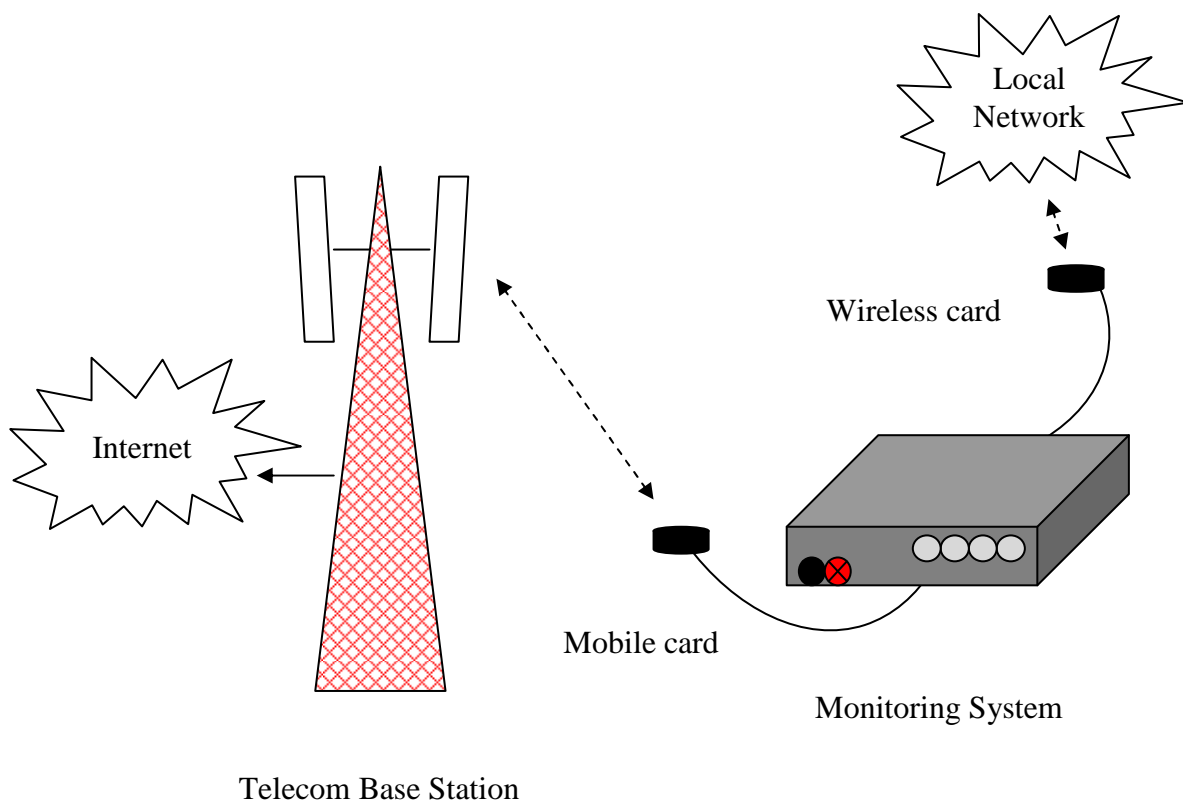


Figure 9 - Monitoring system mobile communication



Figure 10 - Top view of mobile communication card (top) next to the wireless one (bottom)

Also another important requirement for this communication card is the antenna. Indeed it must be removable. Since the controller with the mobile card is installed inside an enclosure, the antenna has to remain outdoors in order to establish a quality link with the base station. Therefore an outdoor model is used and fixed on the tower, with cable connecting it to the card.

This communication is important for the following points:

- Transmission of the acquired shapes from the monitoring system to the server
- Synchronization of the time of all controllers with a time server

And also some of minor points are:

- Remote update of the software inside the controller
- Diagnosis of errors if any, for the hardware and software

III.3.1.5. Power supply

Since the monitoring system is to be installed on a high voltage tower, solar power is the main power supply source.

Wind generator is also an option. However solar panels are preferred because of the price performance for this low power consumption system and the ease of installation on high voltage tower.

The solar power is composed of different elements:

- Solar panels
- Charge controller
- Battery

Each of them is chosen carefully depending of the power consumption of the system as well the solar region where the monitoring device is to be installed.

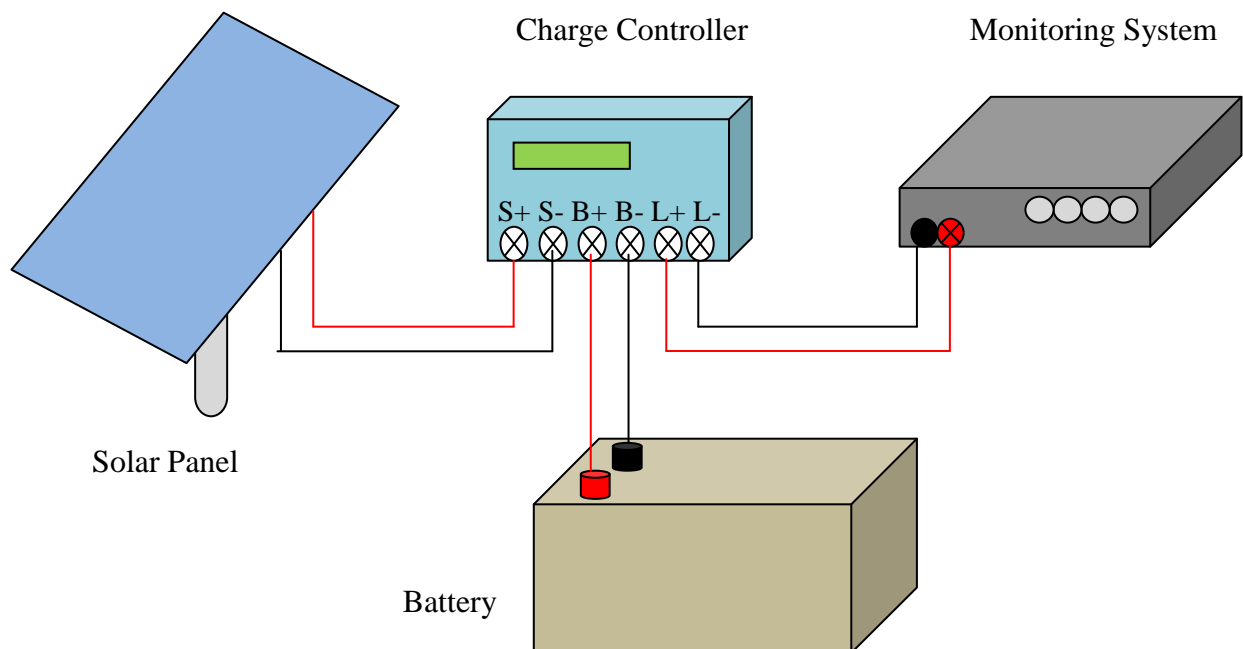


Figure 11 - Solar supply setup

Basic operation is described in Figure 11. The charge controller plays the major role since at daytime it supplies the system and the battery from the solar panel. At nighttime it supplies the system from the battery. Also the charge controller can prevent the monitoring system and the battery failure such as overcharge by disconnecting them.

Power requirements calculation is detailed in Annex IV. For the selected monitoring system, following solar equipment is chosen:

- Two solar panels with a nominal rated power of 130 watts each
- Charge controller with 20 A maximum current
- 12 V battery with a capacity of 200 Ah

III.3.1.6. Enclosure

Most parts of the monitoring system are placed inside an Electromagnetic Compatibility (EMC) enclosure. It protects them from interferences and weather conditions. The enclosure is designed to be mounted on high voltage tower.

Devices that are remaining outside the enclosure are the mobile antenna, the solar panel and the current transformers. Their cabling is protected with proper flexible tubes that are connected to the enclosure and grounded to it. Rest of the equipment is placed inside the enclosure.

III.3.2. Software operating the monitoring system

The software is composed of a client application that is installed on the controller, and the server program running on a distant computer. They are related to each other since they are communicating between them in order to exchange data over a network.

The client application is in charge of:

- Getting acquisition data
- Transferring the data to the server application
- Warn server of any error

The server application has to:

- Gather the data of all controllers
- Display the data shapes

Both of those programs are described below.

III.3.2.1. Client side software

Each monitoring system is running on an embedded version of Microsoft Windows XP operational system. This is mainly due to the fact that it has to be installed on a compact flash card behaving as a solid-state hard drive, which is fanless and low power consuming. Nevertheless the embedded version is similar in functionalities to the standard one.

Several applications are installed on the controller. First of all, a connection manager application is in charge of connecting it to the mobile network. It registers the communication card to the telecom provider, and maintains this link on all the time. Even in the case of disconnection from the mobile network this program reconnects automatically the monitoring system as soon as possible.

Then a remote client desktop software is installed in order to be able to manage the controller at distance. Indeed with this program it is possible to connect remotely to the monitoring system and execute tasks such as update of the software, file transfer and reboot if needed.

Finally, the main acquisition application is running on the monitoring system. This own developed program is detailed below.

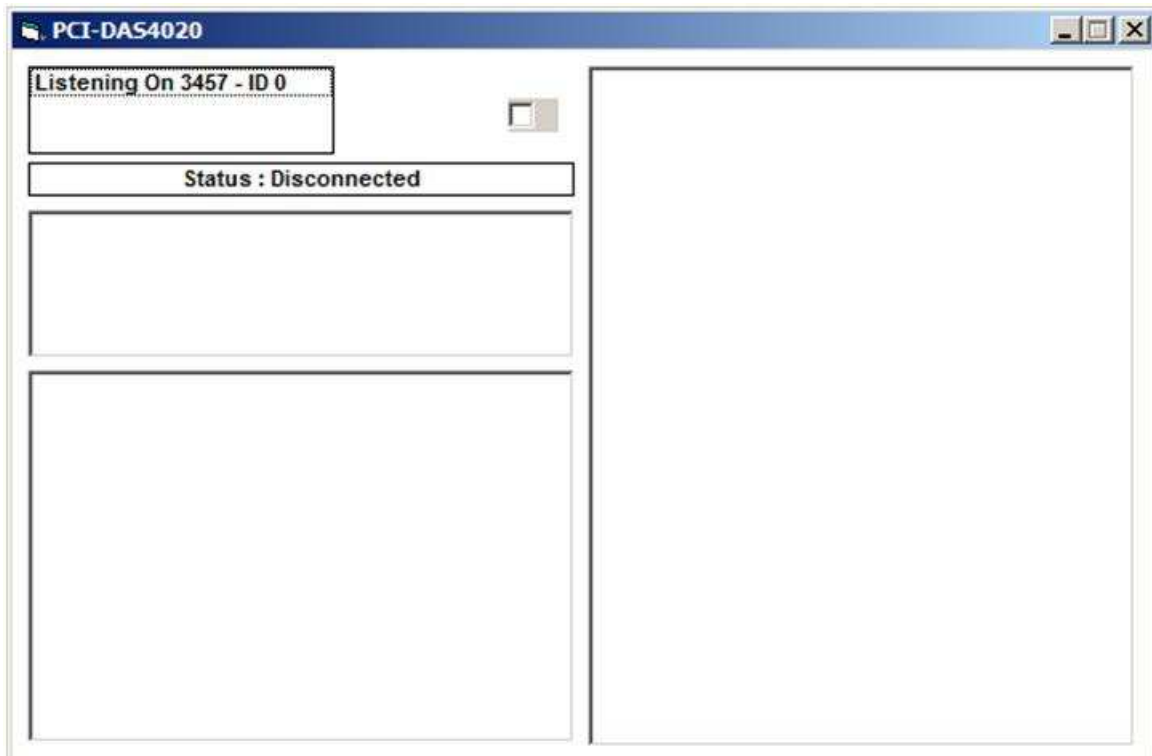


Figure 12 - View of the client application running on the monitoring system

Main functionality of this client software is to acquire the trigger event, such as lightning transient, based on user-defined criteria. Its functionality can be divided in three parts:

- Trigger event acquisition
- Data saving
- Shape transmission

Each of them is detailed below, as well some minor functions.

III.3.2.1.1. Trigger event acquisition

The acquisition card is not able to automatically acquire the right shape based on user-defined criteria and save it to its memory. Main reason is a hardware limitation and therefore the software needs to recognize the transient event. This is done with the following procedure.

First of all the acquisition card is acquiring data points continuously and stores them to the controller memory. Computer memory space of about 60 Mbytes is reserved for this operation, among the 1 Gbytes available for the motherboard. The acquisition speed is of 10 Msamples per second and per channel. Since vertical resolution of the card is 12 bits, this

means that each data point requires 16 bits of space to be saved. Indeed computer memory stores data as multiples of 8, thus 12 bits are stored as 16. Equation between byte and bits is the following:

$$1 \text{ byte} = 8 \text{ bits}$$

Equation 3 - Bytes to bits conversion

Therefore each data point saved requires 2 byte of computer memory, among the 60 Mbytes reserved.

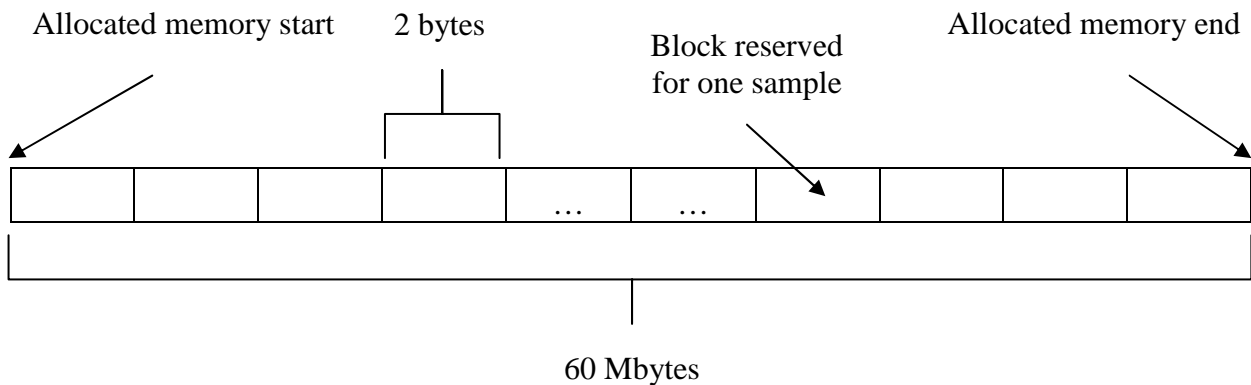


Figure 13 - Memory allocation for data acquisition

Thus a monitoring system acquiring samples will require the following amount of memory space each second:

$$Mem = Cn * As * Ms$$

Where:

Mem is the memory space required per second

Cn is the number of channels

As is the acquisition speed per channel per second

Ms is the memory space required for one sample in bytes

Equation 4 - Memory space required for data acquisition

For a 2 channels acquisition at 10 Msamples per channel and per second speed:

$$Mem = 2 * 10000000 * 2 = 40 \text{ Mbytes}$$

Therefore one second of acquisition requires 40 Mbytes among the 60 Mbytes available. This means that the allocated memory space can hold 1,5 seconds of acquisition data. Once this buffer is full, the operation starts again from the beginning, with new samples overwriting the old ones. Although this reserved space seems low, it is sufficient for lightning transients acquisition because even with multiples subsequent strokes one full event doesn't exceed one second [3]. Monitoring system is ready to acquire a second event even if it occurs immediately after the first one, as described below.

It is important to underline that the controller does not function with analog values, but digital ones. Indeed values such as 0,1 volts have no meaning in the acquisition field. Analog to digital conversion is described below. With a vertical resolution of 12 bits, the acquisition card is able to differentiate 4096 values as described in a previous paragraph. This number is correlated to the analog input range of the card, such as -5 to + 5 volts. In the digital world, this means that a -5 volts value acquired by the card corresponds to 0, and that +5 volts corresponds to 4096. A more comprehensive table of this analog to digital conversion is given below.

Analog value (V)	Digital value
-5	0
-2,5	1024
0	2048
2,5	3072
+4,99	4095

Table 10 - Analog to digital conversion

This means that the majority of data points taken by the acquisition card under normal operation will have a 2048 value, which corresponds to 0 volts measured. With the acquisition error of few millivolts, this value can fluctuate between 2044 and 2052. This also means that for example thresholds of -/+ 0,1 volts correspond to digital values of 2008 and 2098.

The acquisition operation is active all the time because no data must be lost and the trigger event may arrive at any time. In order to acquire the right transient, the application is analyzing the memory buffer with some criteria, while continuously filling it with new samples. At each time loop defined by a timer, a previous amount of samples up to the present instant T are inspected. The next loop will analyze the points from this previous instant T to the new one.

First acquisition pass

Data acquisition from card analog input to computer memory

2048	2047	2048	2046	2048			
------	------	------	------	-----	-----	------	--	--	--

Second acquisition pass -> overwrite of previous pass data

2047	2048	2048	2046	2048	2046	2048	2049
------	------	------	------	-----	-----	------	------	------	------

Figure 14 - Acquisition process on memory

Typical timer loop is executed every 500 ms. This means that at the beginning of a new loop, the client application will examine the newest 500 ms of acquired data into the memory. At the same time and independently of the timer loop, another function is filling continuously the computer memory with the latest acquisition data points. Since the reserved memory space can hold 1,5 seconds of acquisition, this also means that after 3 timer loops the old data is overwritten forever by the new one.

During one timer loop of 500 ms, the controller has to analyze latest 10 Msamples hold in a memory space of 20 Mbytes. Inspection criteria is the following: if the data sample is higher than a positive threshold value, or lower than a negative threshold value, then a trigger event has been detected. Indeed most of the time under normal operation, no current is flowing through the arrester except the leakage one. At the acquisition card level, passed the current transformer output and voltage dividers, this corresponds to data points with 0 volts value.

If any data point is higher than a positive threshold such as 0,1 volts, or lower than a negative threshold such as -0,1 volts, then this probably means that a current higher than the leakage one has flowed through the arrester. Therefore if the conditions of these threshold criteria are met, a trigger event has been detected.

Trigger criteria met

2048	2050	2072	2105	2114	...	2048	2046	2048	2049
------	------	------	------	------	-----	------	------	------	------

Figure 15 - Trigger conditions verified in memory

Threshold value selection is also an important task. Monitoring system is designed in the way that a peak current of 20 kA corresponds to 500 volts at the transformers output, and 5 volts at the acquisition card entrance thanks to the voltage dividers. Since the sensor and the attenuators are linear up to that level, this also means that for example for a transient current of 200 A, the monitoring system shall measure 0,05 volts.

However there are some limitations. With the chosen motherboard processor speed, it is impossible to analyze each sample among the 20 millions in one second, in order to see if it is higher or lower than defined threshold. And at the same time the controller has to fill the memory with new acquired samples. Therefore every Nth sample is analyzed among the 20 millions, with this number being calculated in laboratory during processor load testing. Typical value of N is 50. This fact leads to the question about the risk of monitoring system failing to detect a trigger event since not each consecutive sample point is analyzed. Answer is detailed below.

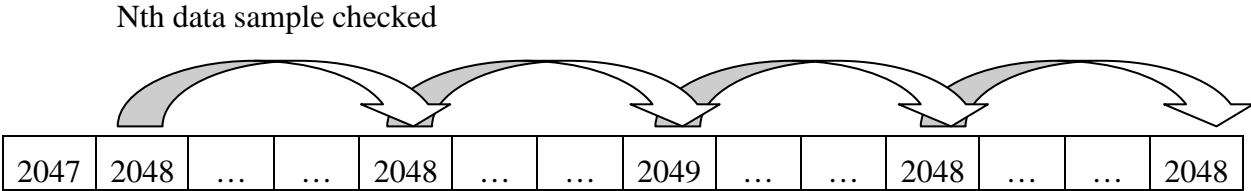


Figure 16 - Nth sample check explained

If a trigger event appears, with the chosen acquisition speed, not only one data point will meet the threshold criteria, but dozens of consecutive ones. Indeed at 10 Msamples per second and per channel, 100 data points are acquired in 10 μs for each channel. A fast lightning transient with very short rise time of 1 μs and a 4 μs tail time will still present a current shape of 7 μs. With the defined card speed, those 7 μs are digitalized as 70 samples in the memory. Therefore for this transient, at least 70 consecutive points might meet the threshold conditions. Thus even if every 50th sample is analyzed in the memory buffer, there is no chance to miss this trigger event.

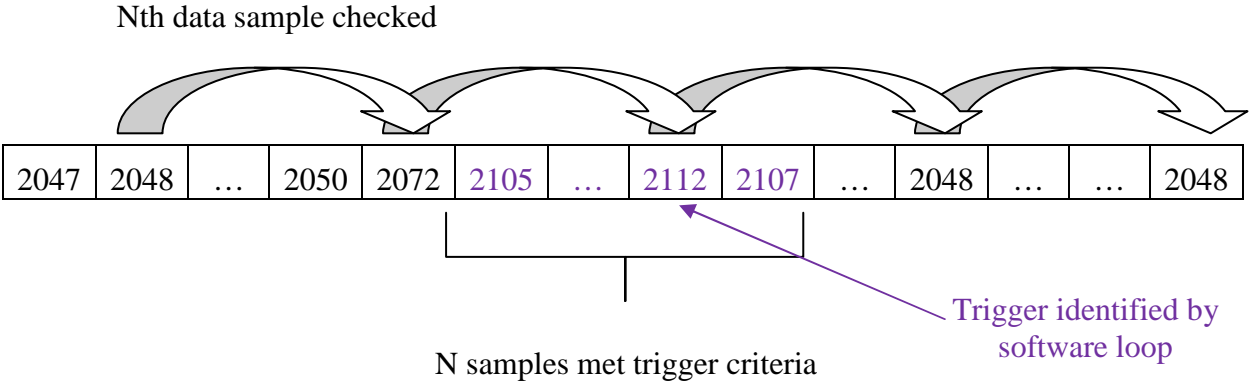


Figure 17 - Trigger detection with the Nth sample loop

Simplified own software function used for trigger detection is presented below.

Simplified trigger research function with:

- index -> memory position
- value(index) -> digital value contained at the memory position index
- MaxPoints -> number of samples
- N-> Nth sample data to be checked
- LowThreshold -> Digital value of low threshold
- HighThreshold -> Digital value of high threshold

Private function FindTrigger()

```
For index = 0 to MaxPoints step N
    If value(index) < LowThreshold then
        FindTrigger = index
    Elseif value(index) > HighThresold then
        FindTrigger = index
    End if
Next index

End function
```

Figure 18 - Software function for trigger detection

However it is also true that transient currents with very low amplitude that have less than 50 consecutive points meeting the threshold criteria may be missed. Nevertheless those events are not of primary interest in the energy duty monitoring due to their low contribution to it. And with the technological breakthrough with fanless processing speed improving continuously, the defined N value is smaller and smaller, making successful acquisition probability higher.

III.3.2.1.2. Data saving

Once a trigger event has been detected, it is important to extract all the data points of interest from the memory and save them, before they are overwritten after 1,5 seconds of new acquisition data, or 3 timer loops.

Data is saved by two ways, one based on computer memory and second one on hard drive disk file. Both are described below.

Memory saving

If a data point has met the threshold conditions during one timer loop, its position into the computer memory is saved by a programming variable, as well the accurate date and time of event. No further steps are taken during this first time loop analyzing 500 ms of acquisition data. Also during this loop if a criteria data point has been found then the Nth sample point threshold verification is stopped.

Previous timer loop

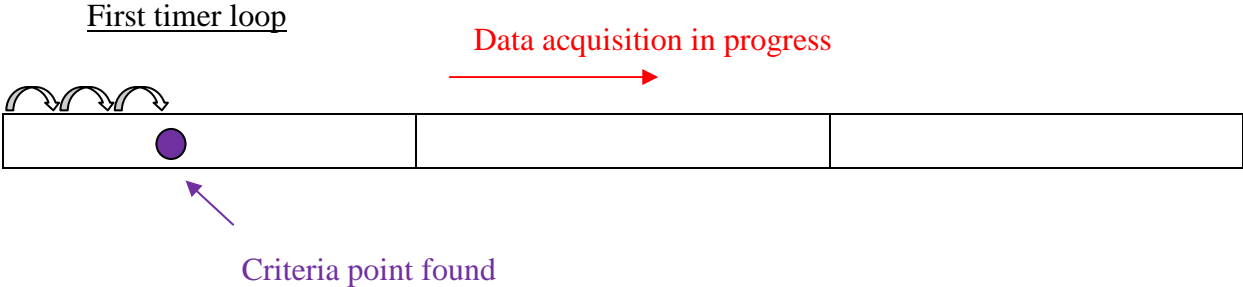
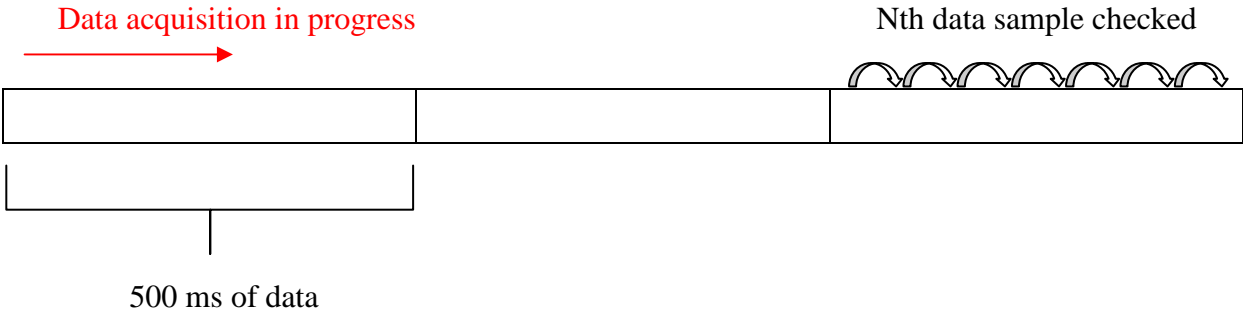


Figure 19 - Acquisition data saving steps explained (1/3)

Next time loop shall analyze the newest 500 ms of acquired data. However since the previous one has detected a criteria point, this loop doesn't consume the processor power on inspecting every new Nth sample. Instead of that, it creates a new memory space equal to the acquisition one (60 Mbytes) and copies the whole acquisition buffer to this one. This buffer corresponds to the memory saving for this complete event. Processor has the time to copy all the 30 Msamples because operations from memory to memory are fast and not as consuming as the threshold check function. Also since about 1 Gbytes of computer memory is available,

dozens of those memory saving buffers can be created before the need to start overwriting them. What is included inside one of them is described below.

First of all, a memory saving buffer contains the complete acquisition parameters that are saved in order to remember them. This is useful in case that they are changed in the meantime by server application. Also accurate date and time of the trigger event is contained, as well the position of the criteria data point inside this memory. This position inside this saving buffer is the same to the one inside the acquisition buffer since whole memory space has been duplicated. Finally the whole 60 Mbytes of data represent the 1,5 seconds of acquisition.

However the samples hold inside have to be explained, in order to not make confusion between data acquired during one pass and the new ones which started to overwrite them.

For sure after the first timer loop, and during the second one, the memory saving buffer has a defined structure and can be divided into 3 parts:

- First part: The 500 ms of data that were checked during the first loop contain the criteria sample, and for sure there is no risk that this part was overwritten by the new acquisition pass. This is because they were saved from the acquisition buffer before a third timer loop during which the new acquisition pass would start to overwrite them.
- Second part: Next 500 ms of data are also safe and represent the continuation of the ones of the first part.
- Third part: Last 500 ms of data is the most critical. Indeed during the memory saving of the second timer loop, the monitoring system just started at the same time to overwrite data contained inside this part of acquisition buffer. Therefore those 500 ms were not totally overwritten, but do contain at the same time some new data which are continuous to the 500 ms ones of the second part, as well some old data which are previous to the ones of the first part.

Based on the previous statements, the memory saving buffer is rearranged. First two parts are kept inside because for sure they contain the criteria point in the first half of it, and its position is known.

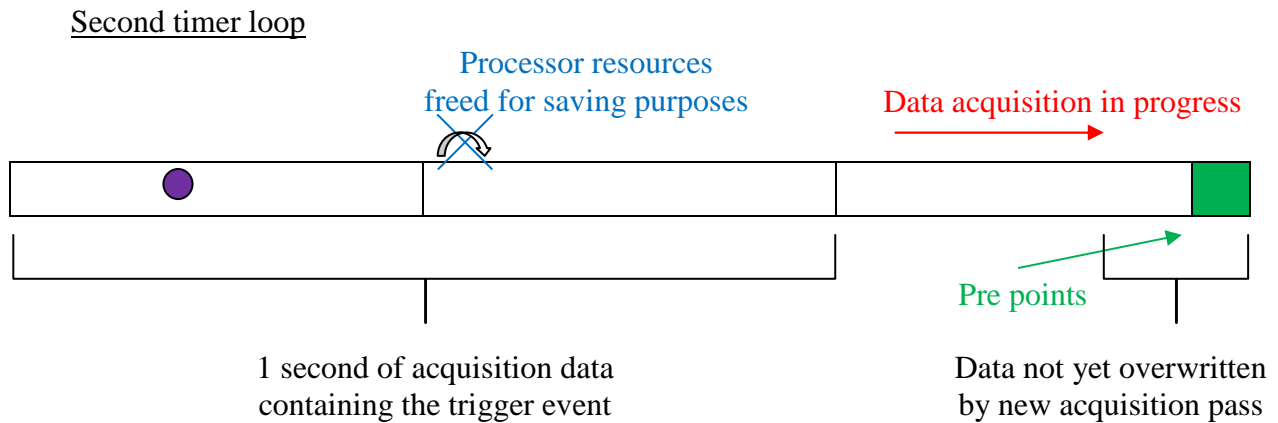


Figure 20 - Acquisition data saving steps explained (2/3)

Third part is not totally rejected however. Since it contains for sure at its end some data points which are previous to the criteria point, these samples are of primary interest. Indeed with the Nth sample based threshold inspection, if the first part contains the trigger event at its very beginning, then the last points of the third part may also contain the very first samples of the trigger event of just few μ s.

Therefore a small amount of points are saved from the third part end and are added at the beginning of the memory saving buffer. Typical value of these pre-points is 10 to 15 μ s, or 100 to 150 data points for the chosen acquisition speed, and corresponds to 2 to 3 times the N value. They are considered as part of acquisition data that might contain the early beginning of a transient shape, but that was missed by the Nth sample inspection.

Thus the final memory saving rearranged buffer contains one second and few μ s of acquisition data, with the known position of the criteria point that is hold in the first half of it. Also it is sure that if this trigger event is verified, it contains for sure the complete current shape of the lightning leader, as well the ones of the subsequent strokes if any, in the remaining hundreds of ms after the first one.

Memory saving buffer



Figure 21 - Memory saving buffer structure

It is important to note that this whole work of memory saving and rearrangement is accomplished during the present timer loop, such as the second one in this detailed case. This way the next timer loop or the third one is completely ready for new trigger searching with the Nth sample inspection. If the threshold criteria is met again all the above process reapplies

with the new second of acquisition data being saved in a new memory saving buffer. This guarantees that no trigger event is missed such as consecutive lightning strokes.

Third timer loop

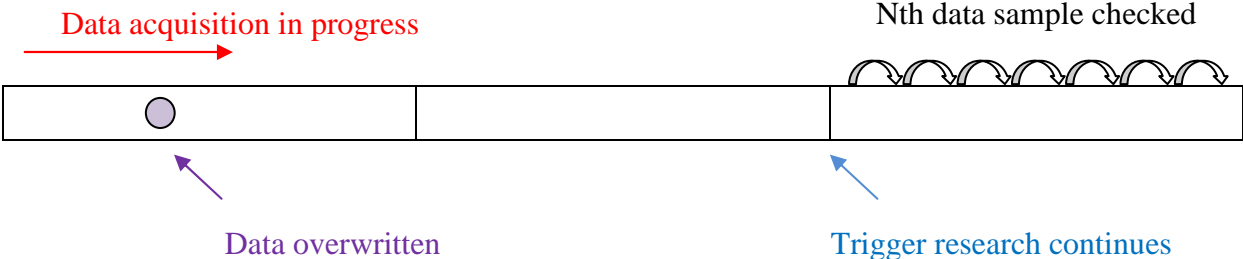


Figure 22 - Acquisition data saving steps explained (3/3)

File saving

During the second timer loop event with trigger detection, a small file is also created on the hard drive which may contain the most useful part of the transient: the lightning leader current shape. Based on the position of the criteria point, several points before and after it are considered. Pre-points are similar in number to the ones introduced previously, and the reason for this remains the same as the memory saving one. Post-points are also fixed to 1400 points per channel or 140 μ s of data which represents the possible duration of the lightning leader stroke when added to the pre-points. Therefore this file contains 150 μ s of data per channel, or 1500 data points.

Its saving is possible regarding processor load since the Nth sample inspection is stopped after the first criteria point is found. The name of this file contains the most important parameters such as the controller Internet Protocol address, date and time of event, trigger channel and criteria point measured digital value.

Event file creation

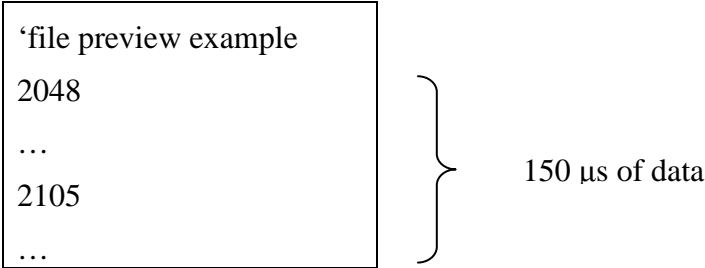


Figure 23 - Event file structure

The decision of the creation of this file on hard drive has several reasons. First of all its small size which shall contain the most essential part of data enables easier handling in terms of trigger verification by remote user than the complete memory saving buffer. Indeed it can be transferred directly over the mobile network and based on its reading decision can be made if the whole event contained in the memory saving buffer is of interest or not.

Other point is that in exceptional scenarios such as a power loss or reboot of the monitoring system, this file will remain on the hard drive for future reading, but the computer memory saving buffers will be lost.

Also there is a limited memory space for the saving buffers which implies that they are overwritten by new data sooner or later. On the other hand a hard drive of several Gbytes can hold thousands of those event files.

Finally this file can also be considered as an evidence of the successful trigger acquisition, since it is clearly visible on the hard drive, which is not the case with the computer memory buffers.

III.3.2.1.3. Shape transmission

Once a controller has acquired a current shape, it informs the server over the mobile network. This information is based on Internet Protocol data packets. Each of them has a fixed size of 8192 bytes. This amount is not sufficient to hold a whole memory saving event and transmit it to server since 1 second of acquisition data with two acquisition channels acquired at 10 Msamples per second requires 40 Mbytes. Therefore several packets are exchanged between the server and the client following a procedure described below.

First packet sent from the controller to the server contains the saved file name of the event, as well its location on the monitoring system hard drive. As stated previously, this name contains important information such as:

- Monitoring system Internet Protocol address, in order to differentiate them
- Date and time of event
- Triggering channel
- Digital value of the criteria point

Therefore with the first packet arrival to the server, it already gives a preview of the most interesting part of the acquired event. Based on those information, remote user may decide to download the complete event file.

A typical file of 1500 data points per channel, with two acquisition channels, requires less than 50 kbytes of hard drive space, and is therefore sent in few seconds over the mobile network.

Once requested by the remote user, the file is split in several packets of 8192 bytes. First packet is sent from the monitoring system to the server application. If its arrival is confirmed, the sending of other parts of the file is proceeded as well.

After successful transfer, the event file is rebuilt by the server application. The current shape is displayed on the computer screen.



Figure 24 - Example of shape display by server application

If the event file seems interesting, remote user may request to receive the complete memory saving buffer. In that case samples contained in the memory are copied inside packets as well, and sent one by one to the server. Same constraints apply as for the event file sending, such as maximum packet size of 8192 bytes.

However due to the large amount of data to be sent over the mobile network, some additional functions are implemented. First of all, the packet transfer can be stopped at any time if the remote user decides that the number of samples received is satisfactory. Also some compression functions are implemented in the client application which can compress the memory samples before splitting them inside packets. Main objective is to reduce the size of the data to be sent over the mobile network.

III.3.2.1.4. Other functions

A major function implemented in the controller is the time synchronization with a Network Time Protocol (NTP) server. Indeed next to the real time current shape acquisition and transmission from the controllers to the server, it is also very important to make sure that all of the clients have the same time clock, whatever the tower they are installed at.

First of all this precise timer data is saved with the trigger event once a lightning current shape has been detected. Once the event is analyzed at the server side, and compared to other data sources, such as a lightning detection system, an accurate time of event is preferable.

But this precise timer also applies to the synchronization of controllers. Indeed two controllers or more, installed on nearby towers, can detect the same lightning event. This is possible since several arresters installed on those pylons may operate with the energy duty sharing. Or if there is a time drift between two controllers of one second or more, this same event might be registered such as two separate events, like two independent lightning strokes.

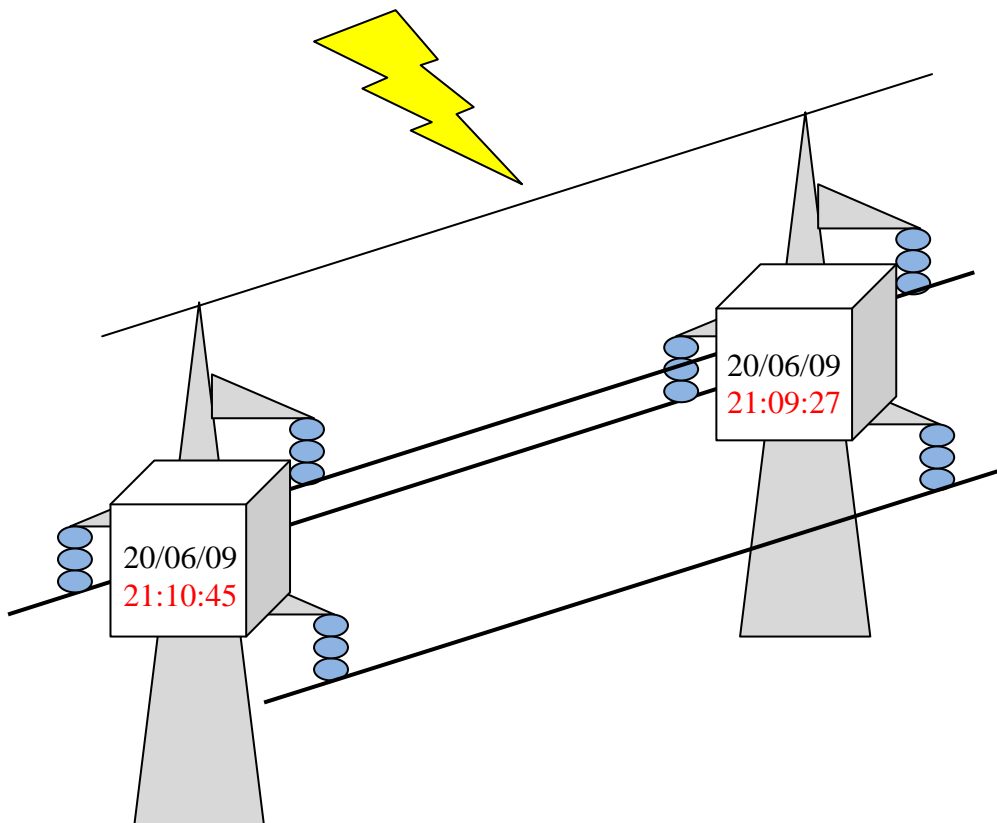


Figure 25 - Time drift issues in the arrester monitoring field

In order to avoid this, each of the controllers synchronizes its timer with a remote server. This enables the monitoring system to have a precise internal clock that is also the same for the other clients.

This process is based on an Internet Protocol packet sent by the controller to the NTP server, over any available network. In the response packet, the monitoring system receives the current precise time of the NTP server. Then it synchronizes its internal clock with the received data.

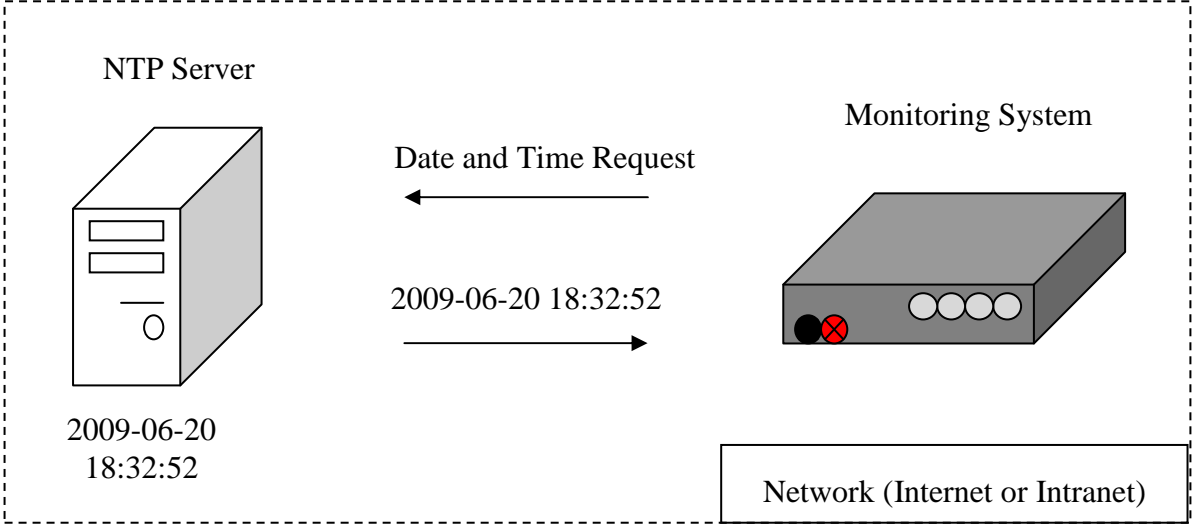


Figure 26 - Monitoring system time synchronization with a NTP server

III.3.2.2. Server side software

A server application is also developed in order to handle several controllers. It runs on almost any modern computer with Microsoft Windows operating system. Some functions have already been presented in the client shape transmission part. However the server is also in charge of other tasks.

First of all the server defines the acquisition parameters and trigger criteria of each monitoring system. Indeed the client application will not start to acquire data until the server sends it a data packet containing all of this information, listed in Table 11.

Also the server application may check at any time the present measured value of each channel of each controller by just sending a request. In the reply packet the client application sends the date and time of acquisition as well the present acquired value. This function is useful in order to check if the monitoring system is operating correctly and that there is no error or accuracy loss in the measurement.

Parameter:	Value (example):
Acquisition speed (Msamples/s/channel)	10
Number of acquisition channels	2
Input range (volts)	-5 to +5
Low threshold	2008
High threshold	2098
Nth point	50
Pre-points	100
Post-points	1400

Table 11 – Example of parameters sent by server application

The server can stop the acquisition as well, and restart it with existing or new parameters, such as different trigger thresholds.

Finally along the possibility to display the received current shape, the server application can also export this data in a raw format such as a text file. Then third party software may be used such as Microsoft Excel for the current shape displaying.

IV. Simulation

Before the correct selection of the current sensors, as well the installation of the monitoring system in real field, it is important to use a simulation model.

A single shielded 123 kV line is modelised. This line is similar to the Ston – Komolac line which is located nearby the Dubrovnik city in Croatia. Main reason for choosing this line as the simulation model is that the developed monitoring system is to be installed on that line.

Therefore the different simulations are very important in order to have a preview of the real field current shapes which may flow through the arresters. These results are used for the selection of the current transformers based on criteria such as maximum current input.

An insulation coordination study is performed with the ElectroMagnetic Transients Program EMTP_RV. This Restructured Version is actively supported by a pool of utilities such as Electricité de France and Hydro Québec, and aims to become the main software solution for various fields of interest in the power energy sector.

The study modelisation is detailed in Annex III. A preview of the simulation model is shown in Figure 27. Four towers are designed with tower number 2 being considered as the one which is to receive the monitoring system.

Scenario 1: Lightning stroke at Shield Wire at middle of Span 2

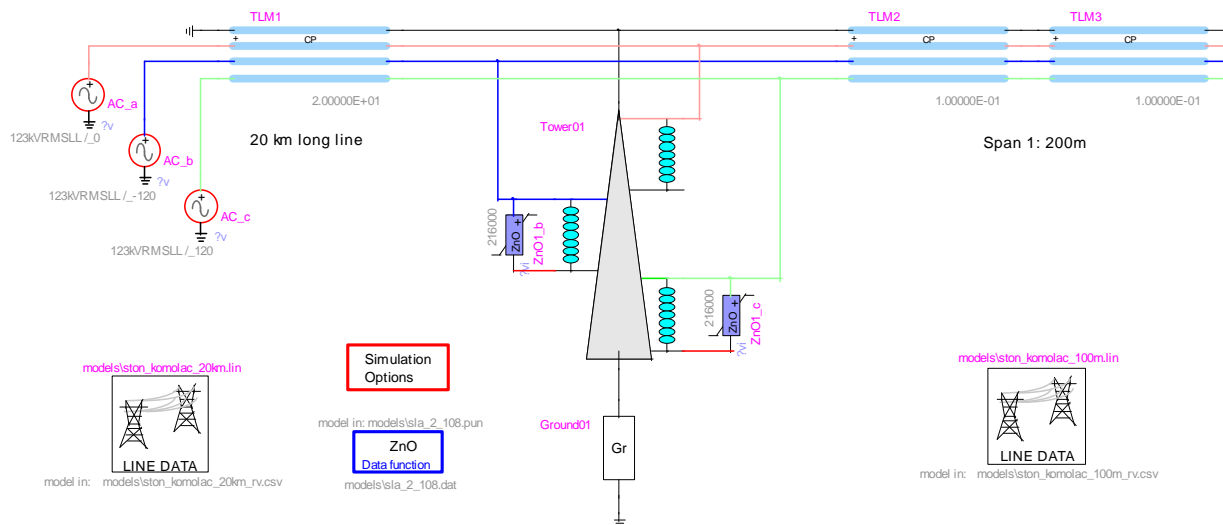


Figure 27 - EMTP_RV Simulation preview

IV.1. SIMULATION SCENARIOS

Currents flowing through the tower number 2 are monitored. Three realistic scenarios are performed in order to measure the current shapes. Realistic means that impossible situations for this line configuration like the lightning stroke hitting directly the bottom phase conductor are ignored. These scenarios are:

- Scenario number 1: Lightning stroke hitting the middle of the span 2 (between tower number 2 and 3) at Shield Wire
- Scenario number 2: Lightning stroke hitting the Tower number 2 top (so called direct hit to the tower)
- Scenario number 3: Lightning stroke hitting the middle of the span 2 (between tower number 2 and 3) at the middle phase

IV.1.1. Scenario number 1

In this scenario the lightning stroke of 200 kA hits the shield wire at the middle of the span number 2. This kind of impact is the most realistic one with the direct hit to the tower.

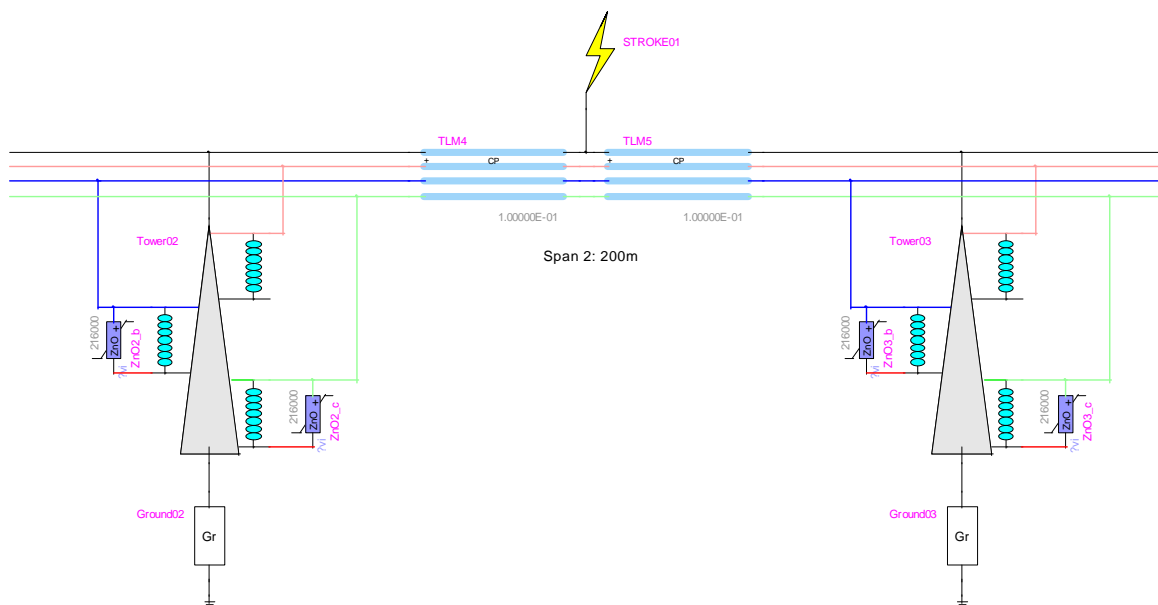


Figure 28 - EMTP_RV simulation preview of Scenario 1

IV.1.2. Scenario number 2

This scenario assumes a direct hit of the lightning stroke to the tower number 2 top. This event often produces so called backflashovers, where the transient current is transmitted from the tower to the phase conductors.

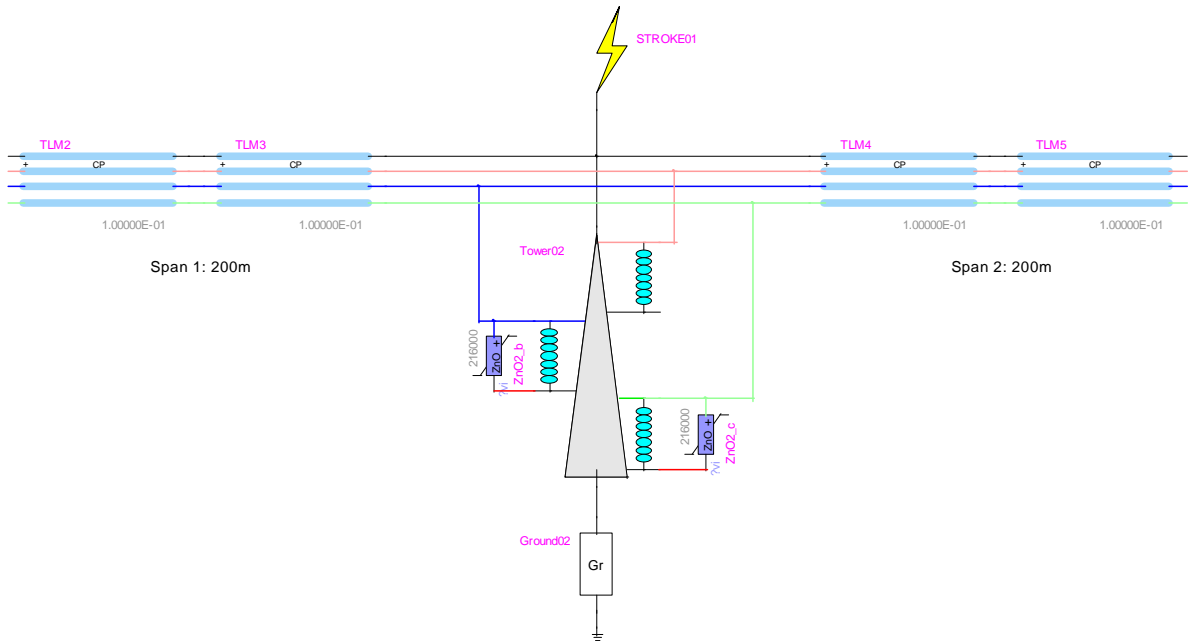


Figure 29 - EMTP_RV simulation preview of Scenario 2

IV.1.3. Scenario number 3

In this case the lightning stroke bypasses the shield wire and hits directly the middle phase conductor, at the middle of the span number 2. This event is called shielding failure. However in this simulation case only a 20 kA current peak stroke is used. This is because due to the Electrogeometric model, a higher current stroke cannot bypass the shield wire and hit the phase conductors directly [3]. Therefore 200 kA lightning stroke is not realistic for this scenario.

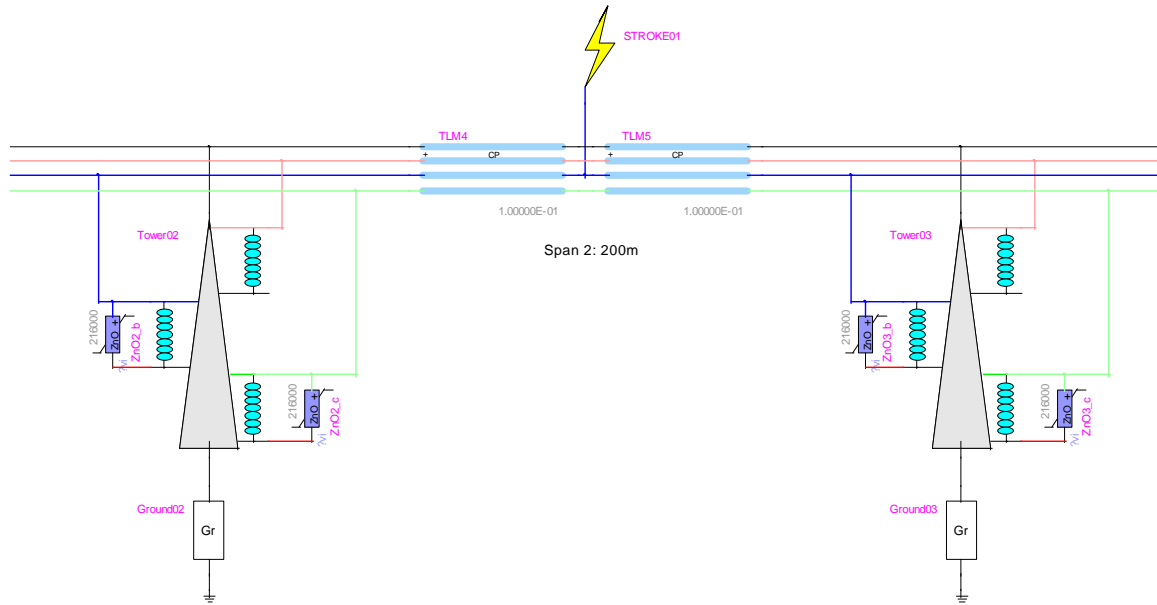


Figure 30 - EMTP_RV simulation preview of Scenario 3

IV.2. SIMULATION RESULTS

The three previous scenarios are computed and the currents flowing through the middle and the bottom phase arresters are measured at the tower number 2. Main objective is to get the shape profile of the current as well its peak since this is the data which is to be measured by the monitoring system in real field. Simulation results are given in figures below. Currents flowing through the bottom arrester are presented in red and through the middle arrester in blue.

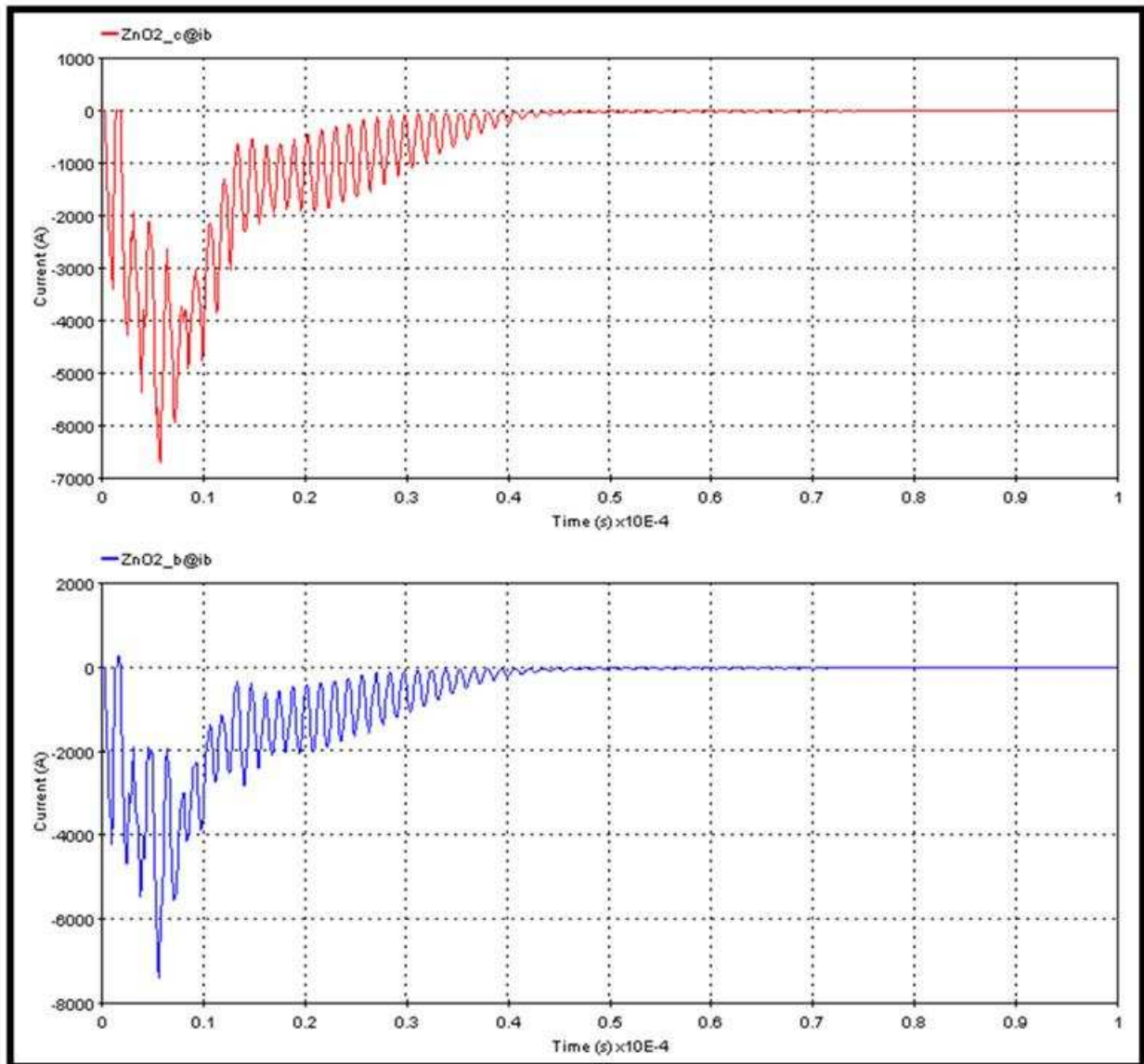


Figure 31 - Currents flowing through bottom and middle arresters in Scenario 1

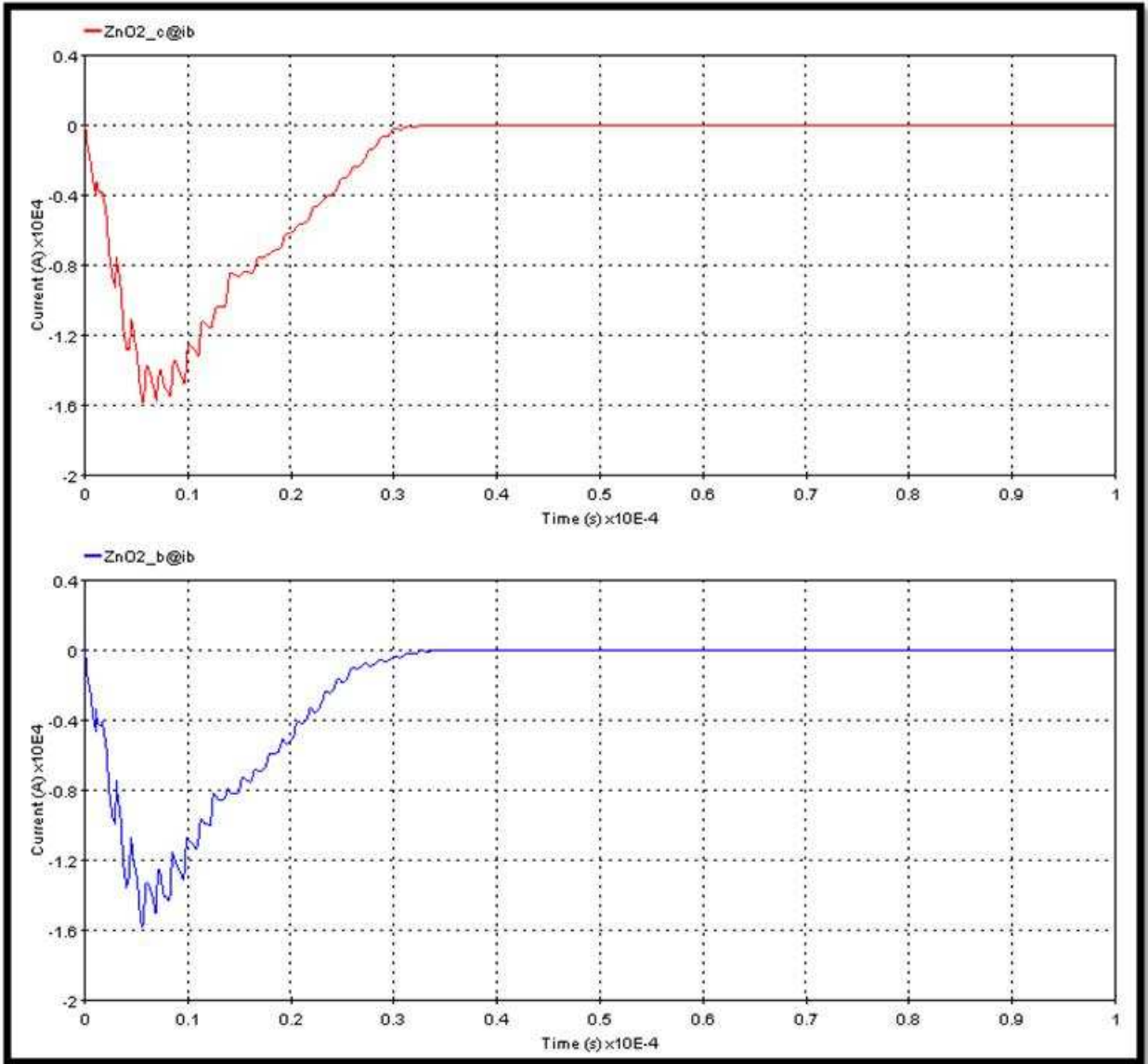


Figure 32 - Currents flowing through bottom and middle arresters in Scenario 2

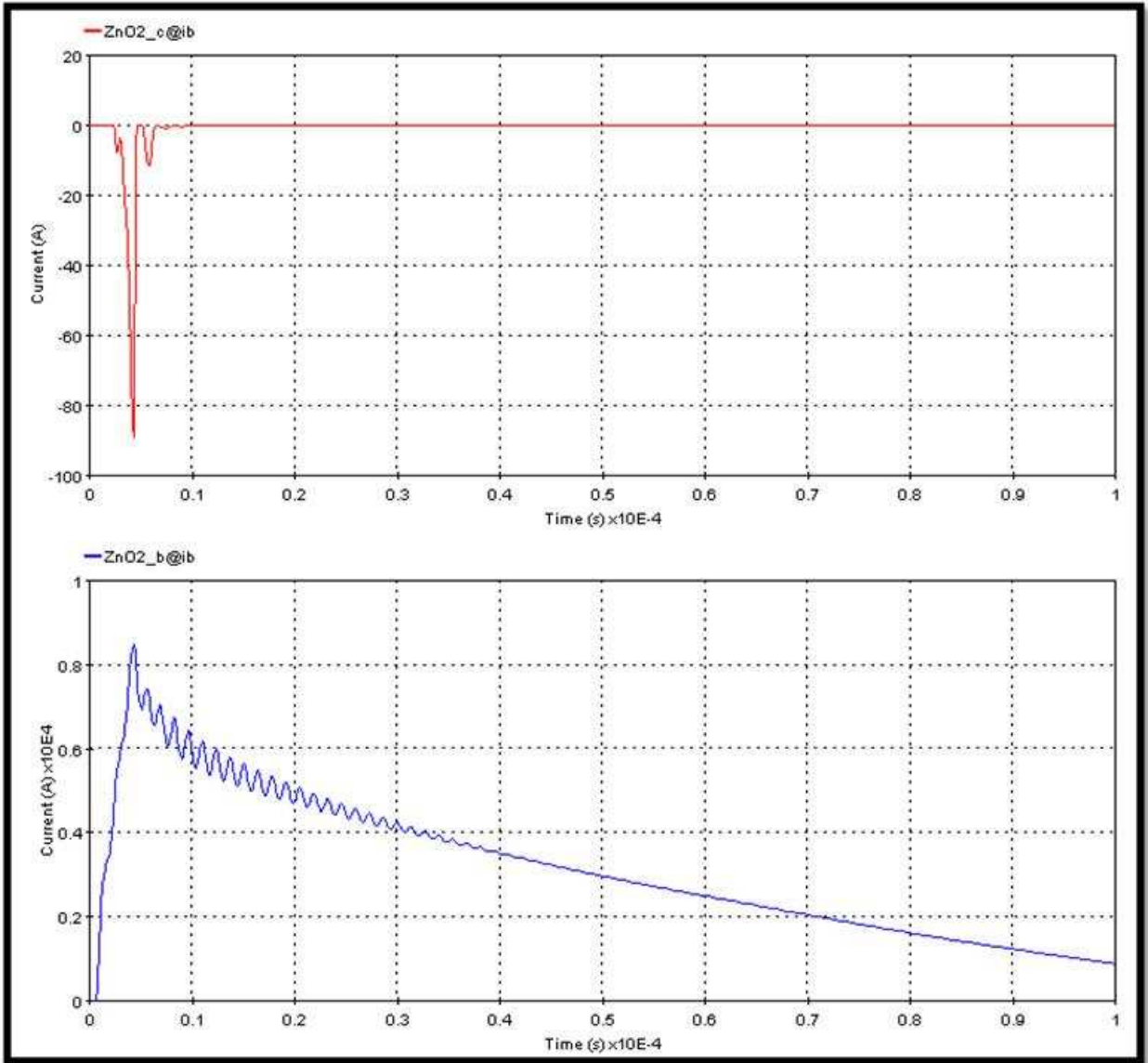


Figure 33 - Currents flowing through bottom and middle arresters in Scenario 3

A summary of the simulated absolute current peaks is given in the table below.

	Scenario 1	Scenario 2	Scenario 3
Bottom arrester	6703 A	15854 A	89 A
Middle arrester	7409 A	15843 A	8489 A

Table 12 - Absolute current peaks flowing through arresters for all scenarios

Therefore even if for the three scenarios the current shapes flowing through the arresters are very different, some similarities can be pointed out:

- The current flowing through the bottom phase arrester never exceeds 16 kA
- The current flowing through the middle phase arrester never exceeds 16 kA

IV.3. FIRST CONCLUSIONS

Although not detailed in this chapter, it is important to add that several other simulations are performed. For example the study of direct lightning hit to tower number 2 is extended (Scenario number 2) because it has the highest current flowing through studied arresters. Tower footing resistance (R_{tower}) for all pylons is varied and currents flowing through arresters are observed. Table below summarizes the results.

	$R_{tower} = 60 \text{ Ohm}$	$R_{tower} = 80 \text{ Ohm}$	$R_{tower} = 100 \text{ Ohm}$
Bottom arrester	15854 A	17496 A	18379 A
Middle arrester	15843 A	17535 A	18007 A

Table 13 - Absolute current amplitude variation as function of tower footing resistance

However obtained results have only a minor impact on the simulations conclusions presented below.

These conclusions are very important since they are related to the correct current sensor selection. Indeed the current transformer to be installed with the monitoring system has to fulfill the following criteria:

- Maximum input current of 20 kA
- Bandwidth of few MHz
- Rise time of few μs and less in order to correctly acquire transient events due to lightning with very small front time

Also the same conclusions apply to the acquisition card, which has to:

- Acquire data at speeds of few samples per microsecond in order to get the detailed shape of the lightning current

V. Testing and Installation

V.1. LABORATORY TESTING

In order to validate the simulation results, and before the real field installation, it is important to test the monitoring system in laboratory. Special care is given to both hardware and software aspects. Since the system is to be installed on a high voltage tower, its installation and maintenance is quite a difficult task. Therefore in order to avoid any failure in real field, laboratory testing is of first importance. Several points are studied such as the electromagnetic compatibility, acquisition results accuracy, and software reliability. Different scenarios are simulated thanks to the laboratory equipment.

The monitoring system is tested remotely in order to simulate the real field behavior. For this purpose a new approach is chosen with the design of a remote laboratory [31], [32], [33], [34], [35]. The configuration scenario is described below. Detailed pictures are presented in Annex V.

V.1.1. Remote Laboratory Concept

An impulse generator is used for the laboratory testing. Model name is ECOMPACT 4 from the company Haefely EMC [29]. Main characteristic of this generator is that it can fire impulses from 0,2 to 4,2 kV. At the current level, this corresponds to a 2,1 kA maximum. A positive and negative polarity can be chosen as well. Also several shapes are possible such as the standardized 8/20 μ s one [8]. This means that the current rises from 0 to 2,1 kA in 8 μ s, then falls to the half value of the peak (1,05 kA) in 20 μ s. This shape design is commonly used in the arrester acceptance test. Other characteristics of this impulse generator are presented in the table below.

Model	ECOMPACT 4
Operating mode	Burst impulse, surge impulse
Voltage range (kV)	0,2 to 4,2
Minimum duration between 2 impulses	10 seconds
Communication interface	Serial (RS232, RS485)

Table 14 - Impulse generator specifications

The ECOMPACT 4 serial interface enables the software control of the generator, thus an impulse can be generated without the need to activate front panel buttons. Haefely EMC do provide a program called EMV-Check for this purpose. Also a manual is provided with the definition of serial commands to be sent to the RS232 port of the generator and their effect on it, such as the change of the peak value of the desired shape or fire the impulse.

However for the desired testing configurations such as the automatic generation of impulses with random peaks, own software is developed. This program enables the remote control of the generator over Internet. This contribution is mandatory for the success of the remote laboratory work. Software source code is given in Annex VI.

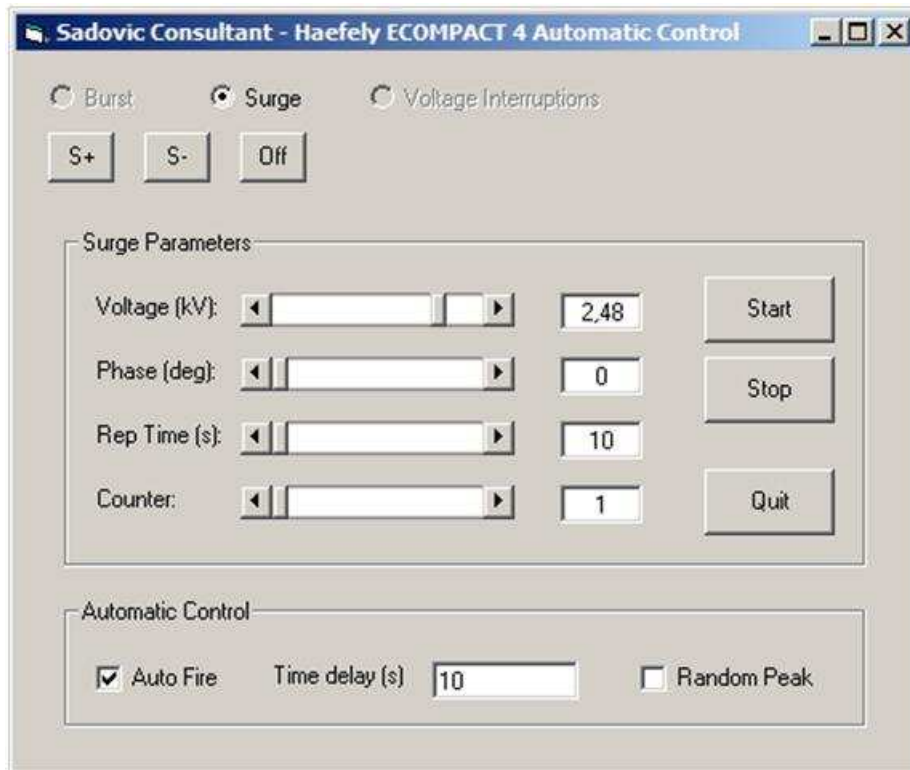


Figure 34 - Application developed for automatic control of Haefely ECOMPACT 4

Testing configuration for this remote laboratory is presented in Figure 35 and is described below. The ECOMPACT 4 RS232 interface is connected to a Serial to Ethernet convertor. This device enables that the commands controlling the generator can be sent over the network cable, since it converts them to the serial ones. The convertor is connected to an Internet ready network port, enabling the remote control of the ECOMPACT 4 with the developed software.

Output of the impulse generator is flowing through a current transformer presented previously. This sensor has a 20 kA maximum peak input and an output ratio of 0,025 V/A. This current transformer is chosen for the monitoring system testing since it is to be installed in real field and simulations have validated it.

Since the generator can fire impulses of 2 kA, this maximum value corresponds to 50 volts at the current transformer level. Therefore attenuation with a ratio of 1/10 is used for the voltage dividers at the sensor output, in order to prevent an overvoltage at the acquisition card input.

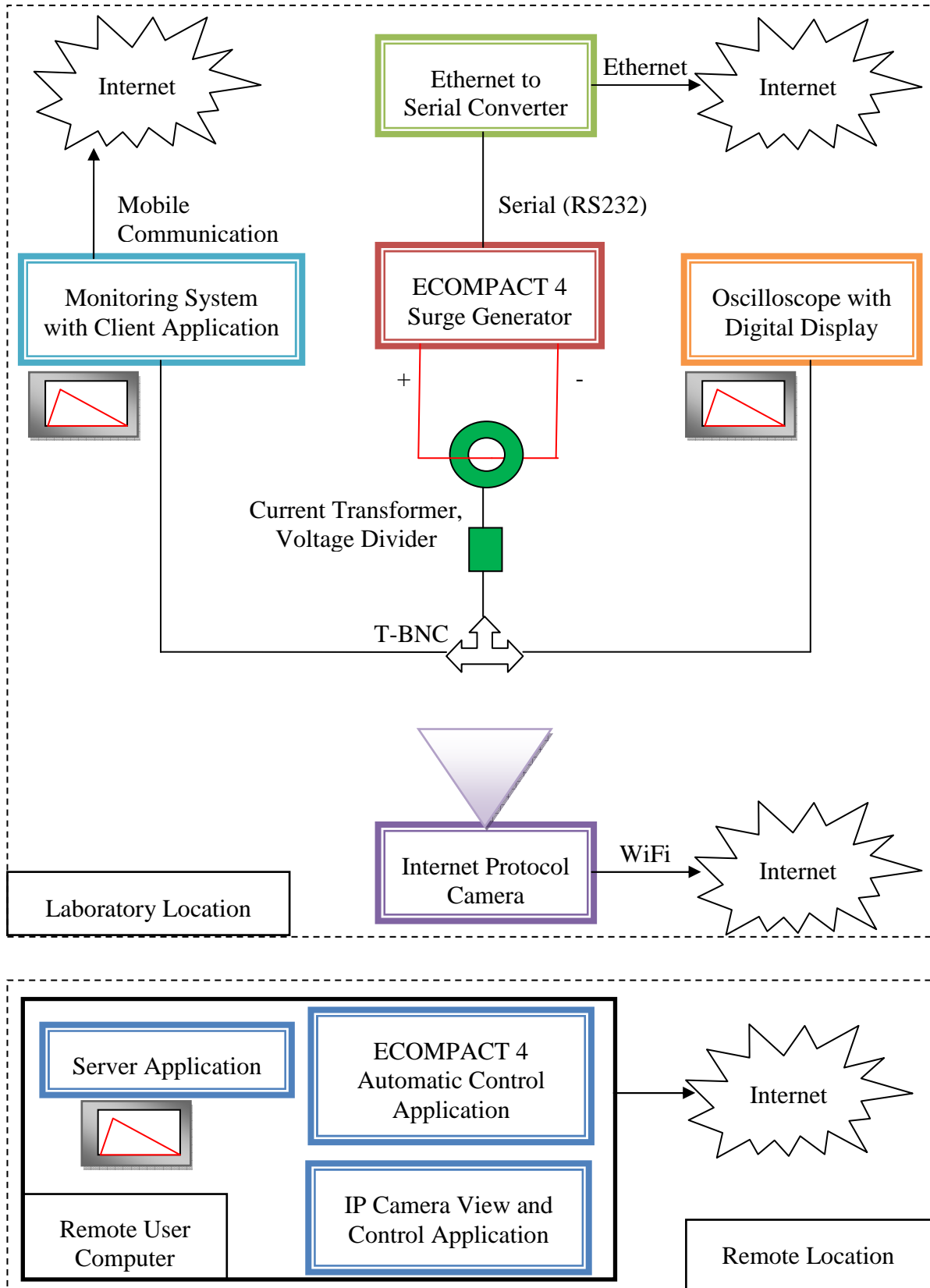


Figure 35 - Monitoring System Laboratory Testing Setup

The output of the voltage divider is split into two with a T-BNC. This is because the ECOMPACT 4 only offers a digital display with some values of the generated shape, without its real profile. Therefore next to the monitoring system an oscilloscope is required in order to see the generated shape. The voltage divider output is connected to the monitoring system acquisition card on one side and to the oscilloscope input on the other one.

Oscilloscope is set into trigger mode in order to acquire the generated transient current shape and display it.

The monitoring system is running with the client application ready to acquire data. It waits for the server command of acquisition parameters and threshold levels. Connection is made to the Internet over the mobile network in order to send to the remote laboratory user the acquired shapes.

Finally an Internet Protocol Camera is installed in front of the laboratory equipment and is connected to the Internet by WiFi. It has a so called Pan-Tilt-Zoom function enabling its control and zooming at distance. Main purpose of the camera installation is to remotely follow the experiment.

On a distant location, the remote laboratory user is connected with its computer to the Internet. Three applications are running on it.

First of all, the server application that defines the acquisition parameters of the monitoring system and the threshold levels as well. This program is also in charge of receiving the controllers acquired shapes and displaying them.

Then the ECOMPACT 4 automatic control software that operates the impulse generator is running as well.

Finally, the remote camera viewing program is used in order to follow the experiment in real time and at distance. Also the oscilloscope display is zoomed in order to compare the acquired and received shape by the server application with the one generated in laboratory.

Several experiments are performed, and are described below.

V.1.2. Lightning first leader acquisition testing

First experiment consists of the generation of a single 8/20 μ s impulse, with a low peak current. This preliminary test is important in order to check that the remote laboratory is operational with equipment responding to desired commands. Also the low amplitude of the first impulse is used to verify that the chosen thresholds are defined correctly. Indeed if this generated impulse is acquired correctly by the monitoring system and sent to the server, all the other ones with higher peaks shall be recorded as well. With this first test being successful, the testing can proceed with a more difficult task presented below.

Second experiment consists of random generation of current shapes with different peaks. This is possible thanks to own developed software for the ECOMPACT 4 automatic control. Several impulses with random current peaks varying from 100 A to 2 kA are generated. Duration between two impulses is also fixed by the program. Main objective is to make sure that the monitoring system will acquire all of the impulses and send them to the server over the mobile network.

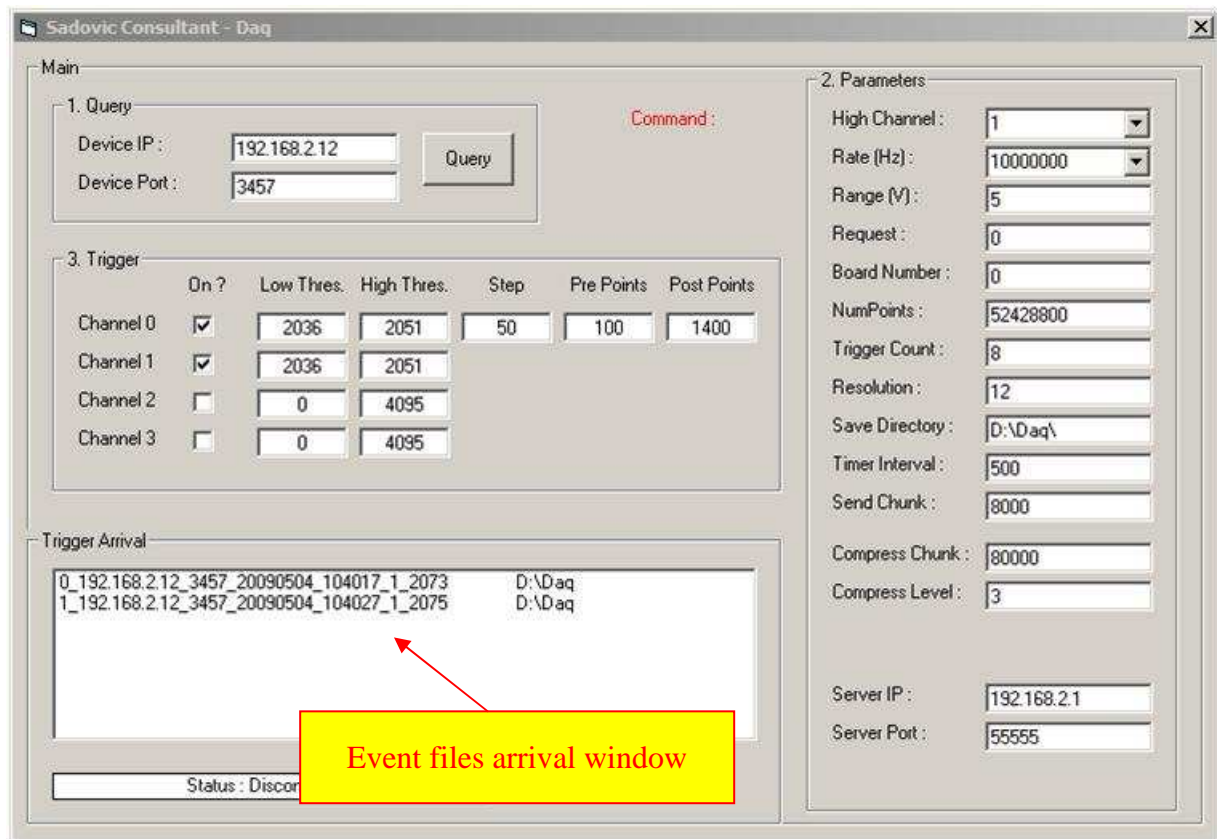


Figure 36 - View of the server application with successful trigger arrivals

Experiment is satisfactory if at its end the number of acquired shapes and received by the server application is equal to the number of generated ones. It is also important to see if the results are accurate when correlated to the current transformer output ratio as well the voltage dividers.

Both of the experiments are successful and the remote laboratory operation has been demonstrated during several conferences in real time and at distance [32], [33], [34]. Detailed pictures are presented in Annex V.

V.1.3. Multicomponents acquisition testing

As described earlier in its characteristics, the ECOMPACT 4 generator can produce an impulse every 10 seconds. Its shape is similar to the lightning current expected in real field. Indeed in terms of duration and amplitude, the generated impulse varies from 100 A to 2 kA during few dozens of microseconds. But these parameters only correspond to the first component of the lightning. Although this primary current shape acquisition is very important in terms of energy duty, other transients may occur hundreds of milliseconds after the leader due to the subsequent strokes.

Introduced monitoring system has to acquire them as well, and therefore a different generator is required for this purpose. It must be able to generate two consecutive transients every few milliseconds since this cannot be done with the ECOMPACT 4.

The second impulse generator used for hardware testing is the DDS-3005 from company Hantek [30]. It is a multipurpose arbitrary waveform signal generator commonly used in a laboratory. It can produce at its output different voltage shapes such as sinusoid, square, trapezoid or ramp. Also a user-defined waveform can be generated. Main specifications are given in the table below.

Model	DDS-3005
Frequency	5 MHz
Amplitude	10 volts
Vertical resolution	14 bits

Table 15 - Arbitrary waveform generator specifications

However this device doesn't simulate the lightning shape in terms of amplitude since it generates a voltage shape of few volts at its output. Also the produced shape is not necessarily similar to the lightning one. Nevertheless it can be connected directly to the acquisition card for testing purposes without the current transformer and the voltage dividers. Main goal remains the acquisition of two and more consecutive impulses with an interval of hundreds of milliseconds, even though they are not similar to the lightning current shape.

A simple sinusoid waveform is generated with peak value of 5 volts and frequency of 5 Hz. Threshold is carefully chosen in order to trigger only on specific parts of the generated shapes, but every hundreds of milliseconds. This simulates the multicomponents of the lightning with a typical duration of 100 ms and more between two subsequent strokes.

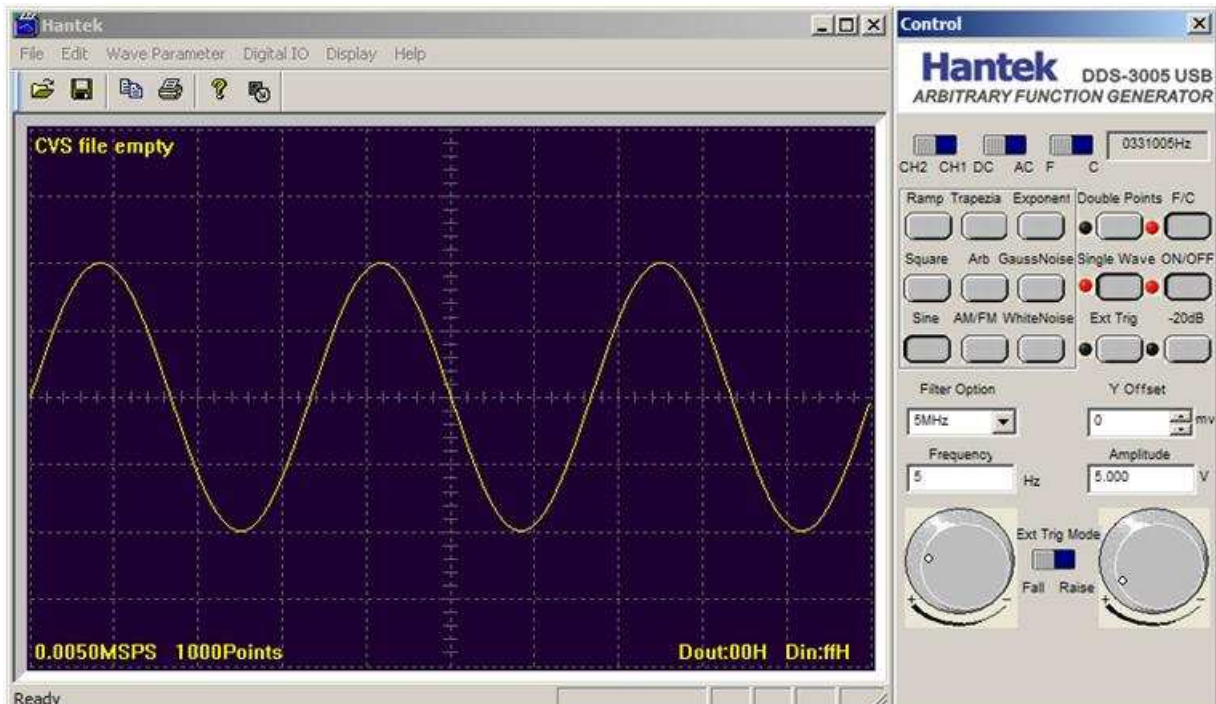


Figure 37 - Generated shape for multicomponents acquisition testing

A typical threshold is just a single voltage value below the sinusoid peak, such as 4,9 volts. Therefore the trigger criterion is met every hundred of ms and the monitoring system has to acquire all of those events. This experiment is successful as well.

V.1.4. Accuracy of the measurement

Another point is the length of the coaxial cable connecting the current transformer output to the acquisition card. Five meters are used since it is the maximum length that shall be used in practice. This is a possible distance such as the connection of the system to a distant sensor like the one monitoring the top phase arrester.

The objective of the experiment is to see if the current transformer output ratio of 0,025 V/A is maintained at the cable end. For this scenario an oscilloscope is used to measure the voltage. An impulse of 1 kA is generated and correlated to the output ratio.

Although coaxial cable has a loss factor, the small length has almost no effects on the results and shall not be taken into account for the measurements.

V.1.5. Mobile communication testing

The purpose of this test is to see if the monitoring system can communicate over the mobile network with a telecom base station with the default internal antenna. Indeed since the communication card is installed inside the EMC enclosure, it is uncertain if the radio waves will pass through it. Keeping this internal antenna would be interesting because it avoids the installation of an external one mounted on the tower, with additional cabling and transient protection.

This experiment is realized by installing the monitoring system inside the enclosure. Connection is made to the mobile network. Another computer is also connected to the Internet in order to see if the monitoring system is online. This simple test is possible with a so called ping command. Indeed if the second computer is connected, this software command gives this information as well the traveling time of this data packet between the two devices.

```
root@sadovic:~# ping client1.sadovic.com
PING client1.sadovic.com (90.94.21.8): 56 data bytes
64 bytes from 90.94.21.8: seq=0 ttl=111 time=548.193 ms
64 bytes from 90.94.21.8: seq=1 ttl=111 time=697.345 ms
64 bytes from 90.94.21.8: seq=2 ttl=111 time=672.720 ms
64 bytes from 90.94.21.8: seq=3 ttl=111 time=651.867 ms
64 bytes from 90.94.21.8: seq=4 ttl=111 time=436.299 ms
64 bytes from 90.94.21.8: seq=5 ttl=111 time=454.870 ms

--- client1.sadovic.com ping statistics ---
6 packets transmitted, 6 packets received, 0% packet loss
round-trip min/avg/max = 436.299/576.882/697.345 ms
root@sadovic:~#
```

Figure 38 - Mobile communication testing

Results of the simulation are the described below. With the internal antenna, if the system is kept outside the enclosure, the communication quality is fine enough to allow current shapes transmission. By closing the device inside, the link with the telecom base station remains stable with a quality loss and dependant on the antenna position. Therefore the conclusion of this experiment is that the integrated internal antenna of the communication card can be used inside the enclosure in order to establish a reliable connection with the network. External antenna is not anymore mandatory.

V.2. REAL FIELD INSTALLATION

The proposed monitoring system has the opportunity to be installed in real field. Chosen line is the Ston – Komolac one in Croatia, and has been introduced in the simulation part. This first installation is of primary interest since it enables to finally verify if the monitoring system is working successfully and to get real field results. Several steps were necessary for the installation and are detailed below.

V.2.1. Tower selection

Two monitoring systems are installed on two towers of the Ston – Komolac line. This real field application implies one system per pylon. Before their installation the two towers among the 144 available have been selected following some criteria.

First of all the results acquired by the existing monitors EXCOUNT-II from ABB show which towers are the most affected by the lightning strokes. Useful information is the frequency at which the tower is hit by the lightning and with what current peaks. Also the same data from the neighboring towers are of interest.

Also the tower shall have at least two arresters installed, one on the bottom and one on the middle phase conductor. This is because the monitoring system can handle up to four acquisition inputs, so it is interesting to acquire more data results with two channels rather than one. However if the tower of interest has only one arrester but is heavily affected by the lightning it is still possible to select this tower and install one more arrester.

Third criterion is the footing resistance of the tower. The higher its value, the higher is the probability of arrester operation due to backflashover. Previously measured values give an idea of the footing resistance of each tower of this line, but this measurement is weather dependant and not very accurate. Also this criterion has already been taken into account with the arresters installation and therefore the towers with two arresters are expected to have a higher footing resistance.

Also some minor point is the proximity of a telecom base station to the tower. Although a range of few kilometers is enough for the communication between the monitoring system and the server via the base station, a clear line of sight and shorter distances are preferable but not mandatory. This can speed up the arrival of current shapes for example.

Finally the ease of access to the tower by ground is considered. Installation line is located in a severe environment with only a few towers being accessible directly by road.

Therefore based mainly on the first two criteria, as well the last one, the following towers have been selected:

- Tower number 38
- Tower number 110

Some information concerning them is detailed in the table below:

	Tower 38	Tower 110
Footing resistance	60,3 Ohm	30,2 Ohm
Arresters installed	2	2
EXCOUNT-II installed	YES	YES

Table 16 - Monitoring system installation towers data

V.2.2. Installation equipment

V.2.2.1. Current sensors

Current sensors from Pearson Electronics, Inc. have to be installed around the ground wire that connects the bottom base of the arrester to the tower structure. However several points have to be considered.

First of all the chosen current sensor is not a clamp-on type, thus it cannot be installed directly to the existing arresters ground wire. This means that the arrester has to be disconnected first from the tower, in order to mount the sensor on the ground wire. Only then the arrester can be put back in operation.

Also the ground wire is quite flexible to allow the movement of the arrester around its top base because of heavy wind in the region. Although this hanging is a good idea to prevent the arrester mechanical failure like disconnection due to wind, it makes the sensor installation more difficult. Indeed while surrounded by the current transformer, the ground wire has to keep its flexibility without damaging the sensor.

Finally the current transformer output cable has to resist interferences. This is done by the installation of protecting cable around the coaxial output, which is only grounded at the enclosure end in order to prevent the flowing of induced current. Also the sensor is installed in the way that the output coaxial cable is in parallel to the tower structure and therefore in case of lightning current flowing through the pylon to the earth, interferences to the transformer output are limited.

V.2.2.2. Solar panel

Solar panel has also to be fixed strongly to the tower structure due to heavy winds. Also it has to be oriented to the south in order to improve its power output.

And even if snow is quite rare in the region, the chosen installation angle of the panel is quite important in order to avoid the possible accumulation of snow on it.

Battery and charge controller are inside the enclosure. The solar output is also protected by the same protecting cable as for the current transformers ones. It is grounded at the enclosure end in order to prevent the flowing of induced current. A lightning arrester is also installed inside the enclosure on the solar panel output cable in order to protect the charge controller and therefore the rest of the equipment.

V.2.2.3. Communication antenna

Installation of external antennas, for the mobile and wireless communication, was planned initially, and had to be fixed on the enclosure. Lightning arresters for the communication cards protection were provided as well. However based on laboratory testing results, the external antennas were not anymore mandatory, and decision was taken to not install them. Therefore both of the mobile and wireless communications are based on the internal antennas of the cards. This reduces the number of devices involved in installation.

V.2.2.4. Enclosure

The enclosure is installed on the tower structure. It is strongly fixed to it in order to avoid vibrations due to wind.

The interior of the enclosure contains the following equipment:

- Acquisition system
- Charge controller
- Battery
- Voltage Dividers
- Lightning arrester for the solar panel

V.2.3. Installation procedure

A major requirement for the system installation is that the line is not under operation. Indeed present Croatian regulation forbids the live line working. Therefore it was necessary to obtain a time schedule when the system may be installed. Two half days were chosen, one per monitoring device.

Maintenance team from HEP Transmission Split, the Croatian utility, was in charge of the system transportation and mounting. Both of the chosen towers are located in very difficult access areas, with rock terrain.

Nevertheless the installation of the two monitoring systems was successful. Detailed pictures are presented in Annex VII.

VI. Results and conclusion

VI.1. FIELD RESULTS

The monitoring system has already successfully acquired transient current shapes. The most interesting of them are presented below. The first one has an absolute current peak of 1,26 kA. This event was acquired on the 20 June 2009 at 21:10:39 (GMT+1 time zone) at tower number 38. Bottom phase is in red and middle one in blue. Presented time step is 20 μ s.

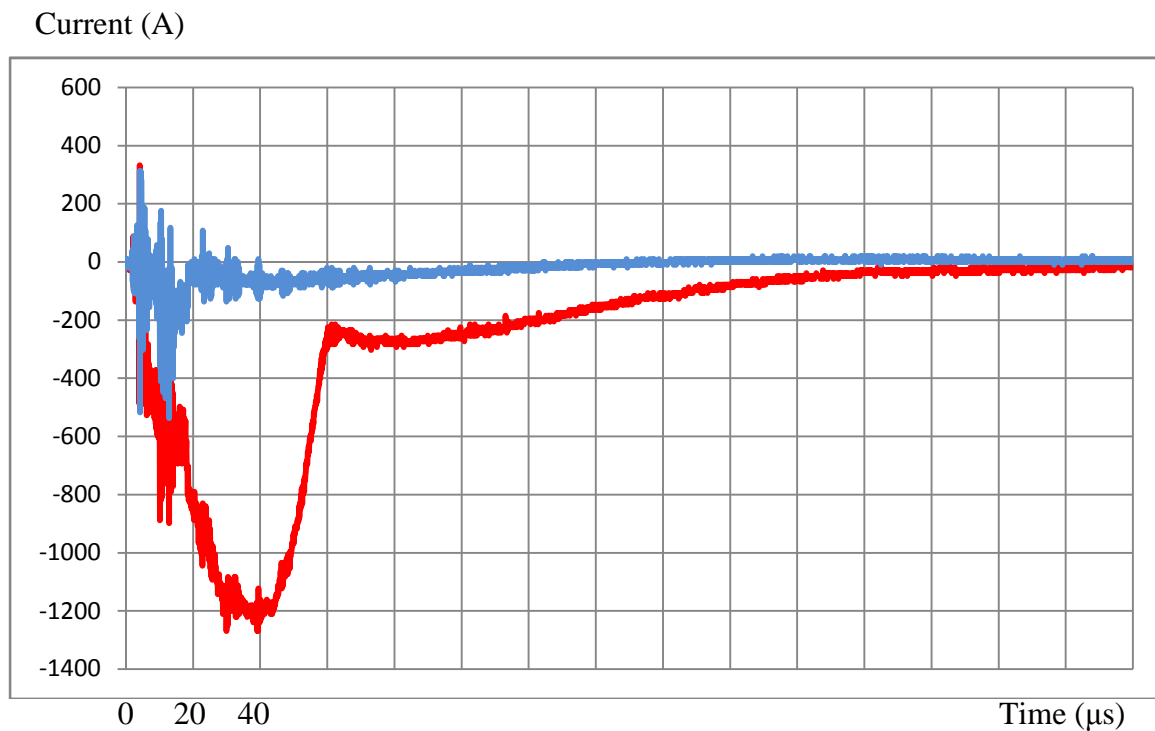


Figure 39 - Real field transient current measurement (1/5)

The second one has an absolute amplitude of 5,24 kA. This event was acquired on the 14 September 2009 at 05:35:34 (GMT+1 time zone) at tower number 38.

The third one has a smaller amplitude and shorter duration compared to the previous one. This event was acquired on the 06 November 2009 at 09:17:28 (GMT+1 time zone) at tower number 38.

The fourth one introduces the multiplicity. This event was acquired on the 06 November 2009 at 10:32:13 (GMT+1 time zone) at tower number 38.

The fifth one has an absolute amplitude of 1,69 kA. This event was acquired on the 05 January 2010 at 14:46:48 (GMT+1 time zone) at tower number 110.

Current (A)

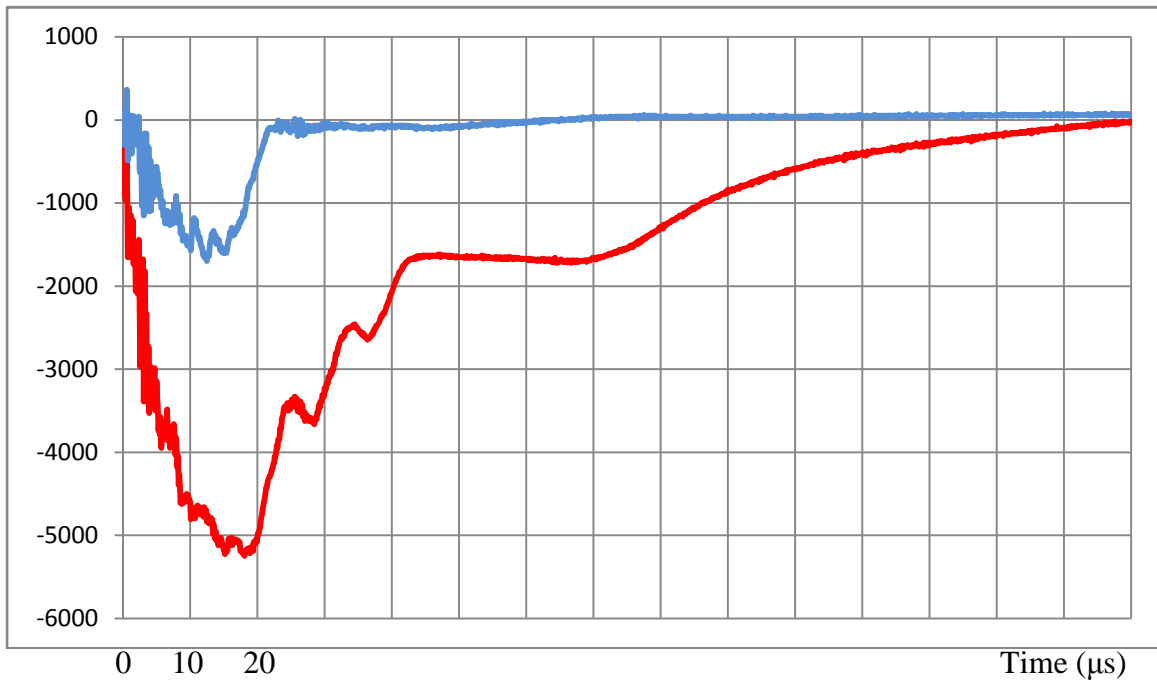


Figure 40 - Real field transient current measurement (2/5)

Current (A)

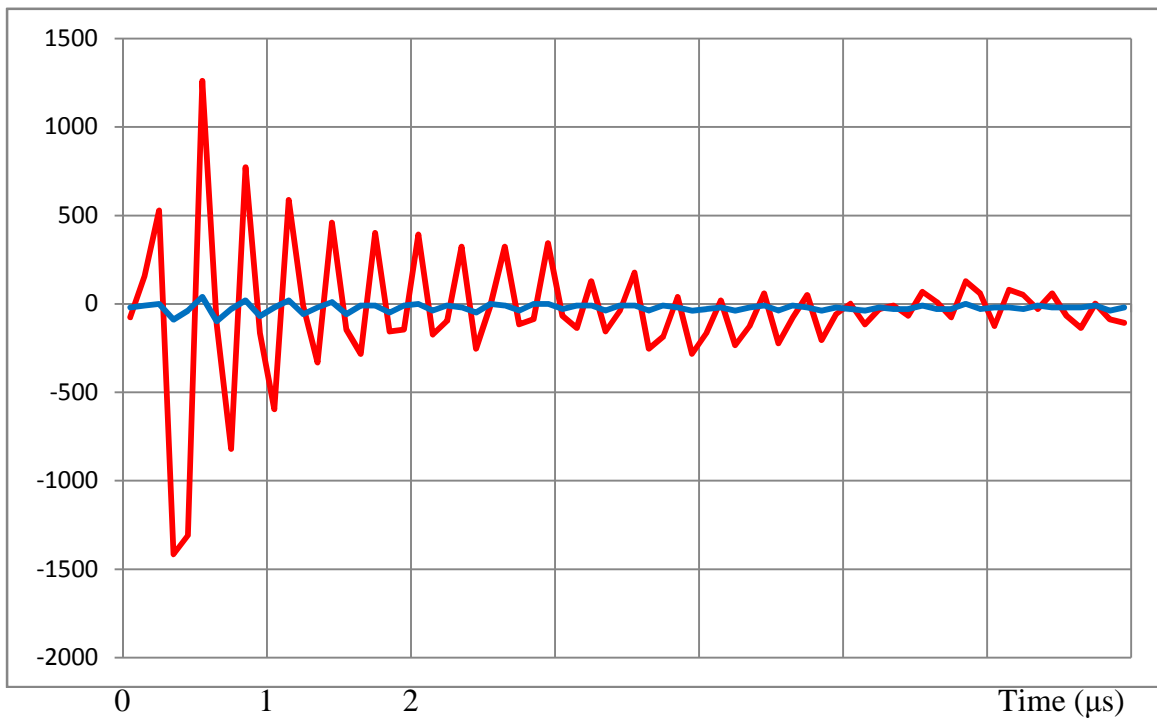


Figure 41 - Real field transient current measurement (3/5)

Current (A)

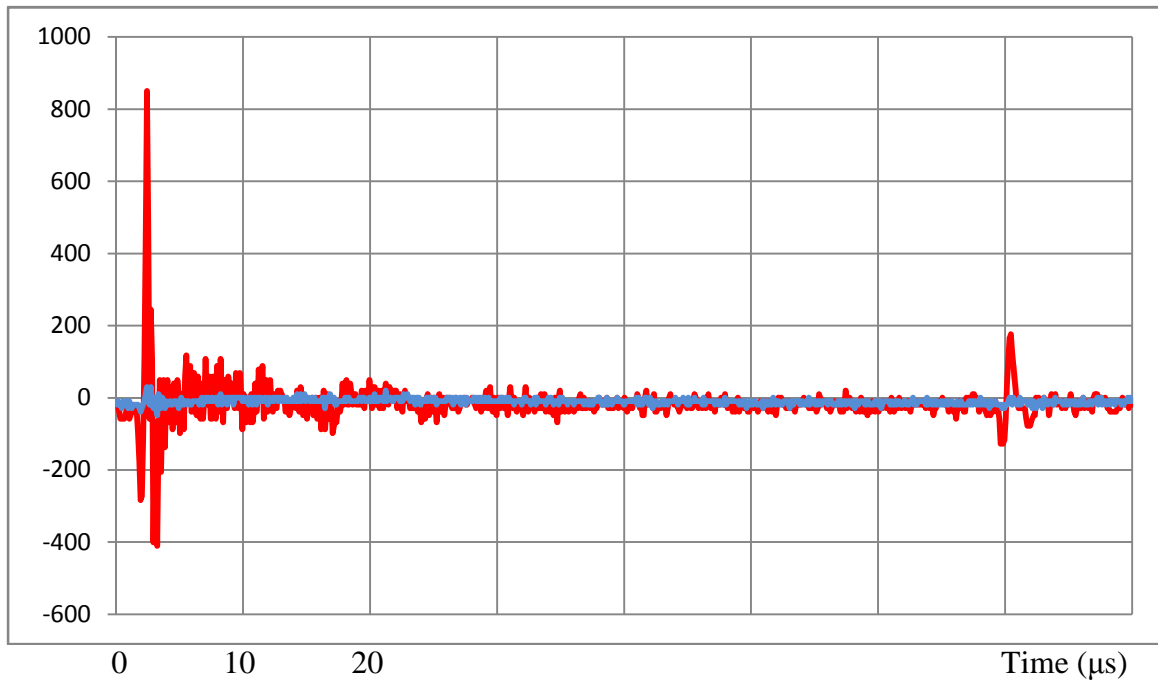


Figure 42 - Real field transient current measurement (4/5)

Current (A)

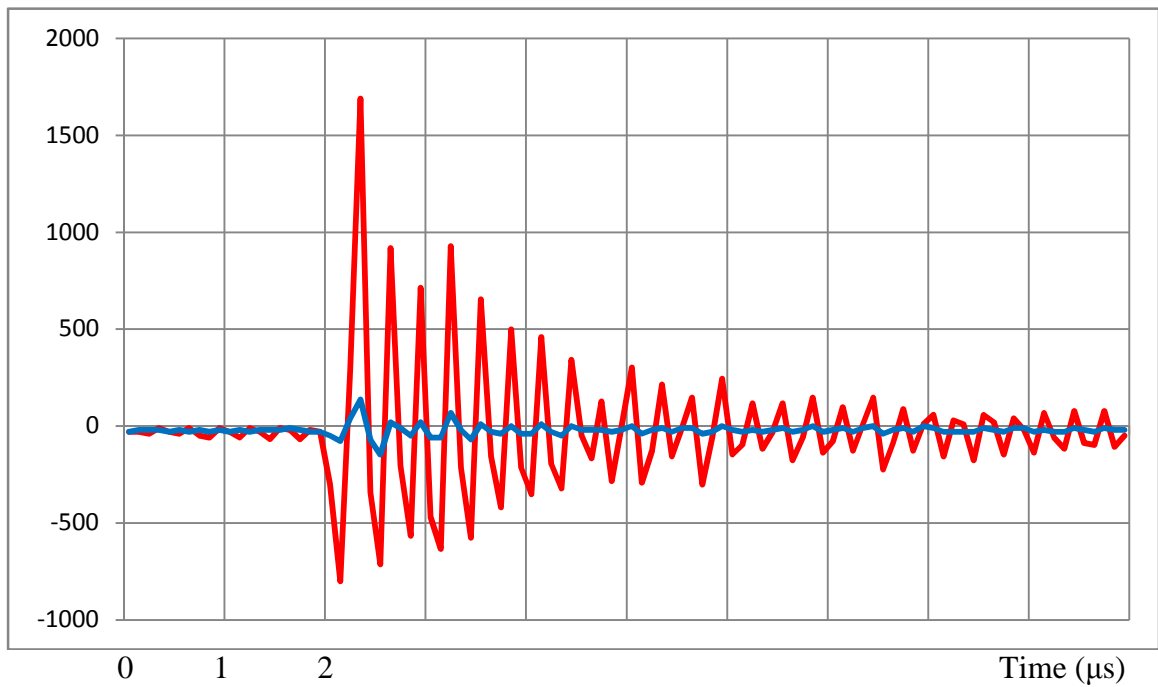


Figure 43 - Real field transient current measurement (5/5)

Table below presents monitoring system results on tower number 38 from the 28 May 2009 to the 23 June 2009. Only events with current peaks higher than 100 A are shown.

Date	Time	Peak (A)
2009-05-28	04:56:45	-205,07
2009-06-02	09:27:02	-683,59
2009-06-02	09:28:33	-253,90
2009-06-02	09:28:35	-634,76
2009-06-02	09:30:36	-117,18
2009-06-20	21:10:39	-1269,53
2009-06-20	21:22:21	-341,79
2009-06-20	21:25:59	-224,60
2009-06-20	21:27:53	-214,84
2009-06-20	21:29:45	341,79
2009-06-20	21:29:46	312,5
2009-06-20	21:31:57	-156,25
2009-06-22	06:24:27	107,42
2009-06-23	12:06:46	-107,42
2009-06-23	12:07:57	-146,48

Table 17 - Monitoring system results (Tower 38, Dates: 28 May 2009 – 23 June 2009)

ABB EXCOUNT-II results are also compared for the same tower and dates in order to see if both of the monitoring devices have recorded similar events. Points of interest are the date and time of the acquisition, as well the amplitude of the transient current.

Date	Time	Phase	Range (A)
2009-05-30	00:25:49	B	10-99
2009-05-30	00:27:22	B	1000-4999
2009-06-02	07:11:06	C	10-99
2009-06-02	07:12:39	C	10-99
2009-06-15	11:29:22	B	1000-4999
2009-06-15	11:29:23	B	10-99
2009-06-15	11:29:23	B	10-99
2009-06-15	11:41:04	B	10-99
2009-06-20	18:16:24	C	1000-4999

Table 18 - ABB EXCOUNT-II readings (Tower 38, Dates: 28 May 2009 – 23 June 2009)

First interesting observation is that it seems that both the monitoring system and the ABB EXCOUNT-II recorded this same lightning event with a current peak higher than 1 kA. Phase is correct as well the date. However there is a time delay of nearly 3 hours between the two results.

In order to clear this difference between the results of both devices, relay protection operations are compared for the considered line and dates. They are presented in the table below.

Date	Time	Fault Distance to Ston (km)	Fault Distance to Komolac (km)
2009-05-28	02:21:45	28,1	18
2009-05-28	02:34:44	36,5	Not Available
2009-06-02	09:28:45	26,7	Not Available
2009-06-20	21:10:48	9,7	37
2009-06-20	21:21:11	4,7	42
2009-06-20	21:22:29	15,1	Not Available
2009-06-23	13:38:55	46,5	2

Table 19 - Relay protection operation (Dates: 28 May 2009 – 23 June 2009)

Relay protection operation comparison gives reason to our monitoring system time with a delay of 9 seconds.

Nevertheless it is not mandatory that the ABB EXCOUNT-II delay is due to time drift. This device might have been incorrectly configured with its internal clock being synchronized with a wrong time from the beginning. In all cases the NTP server synchronization functionality of the proposed monitoring system has been successfully verified and the acquisition results timing can be trusted.

Energy duty calculation can be computed for the previous transient shape, as detailed below. All the time - current values of that event are known. Equations 5, 6, 7, 8 are used. Integration time step is of 100 ns and corresponds to the acquisition time step. Voltage discharge curve of the installed arrester is given in Table 20.

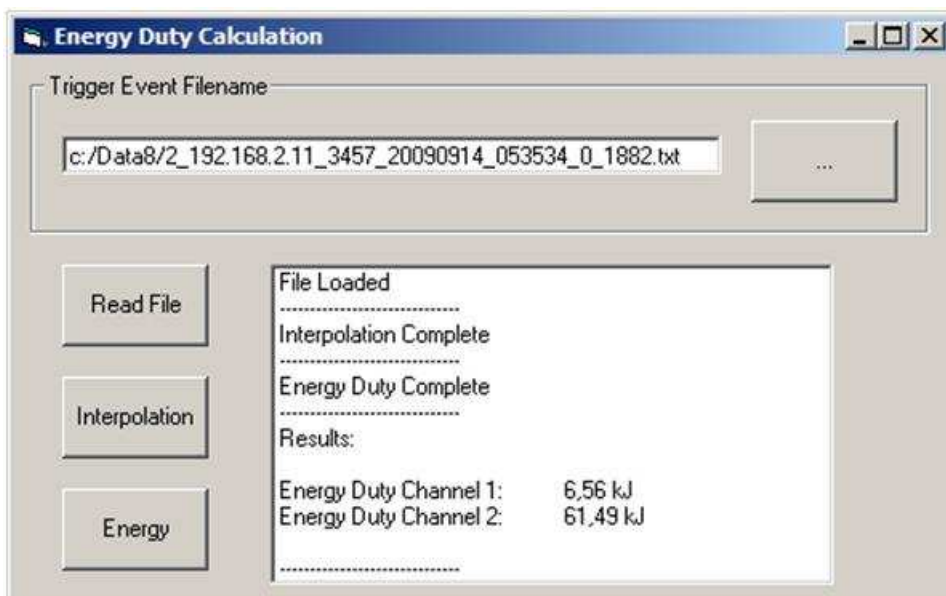


Figure 44 - Application developed for arrester energy duty calculation

Own developed simple software tool is used. It contains the data points of the transient shape as well of the voltage discharge curve ones. Total energy duty for the bottom phase arrester for the first transient event is calculated and is equal to 15,83 kJ. Same calculation gives 61,49 kJ for the second transient event. Conclusion is that those transient events have not deteriorated the monitored surge arrester, based on energy duty tests in Annex II.

VI.2. CONCLUSION

The proposed monitoring system has been successfully tested in laboratory, and managed to acquire real field transient currents. Measured results are obtained from a real line with real lightning activity. No artificially triggered lightning is involved.

Acquisition of the real current shape discharged through the arrester permitted the calculation of its energy duty. This operation is active all the time. With the number of recorded events as well their quality, the developed triggering algorithm operation is successful.

Remote and real time operation offers several advantages in terms of the gathering of results and system diagnosis. Both mobile and wireless communications are working successfully in a high voltage environment, and at the same time.

Monitoring system accurate time synchronization has been verified when compared with the relay protection operation. Timing of the acquired events can be trusted and compared with lightning location systems.

Remote laboratory testing permitted the validation of the monitoring system. Experiments are operated at distance with remote control of the generation equipment and viewing thanks to the cameras. Next to the testing of own developed monitoring system, the remote laboratory is useful as a promotion tool to potential clients demonstrating that this device is working.

Own developed applications for different purposes involved in this monitoring system have been successfully verified. This included the client application for trigger detection, the server application, the ECOMPACT 4 automatic control software and the energy duty calculation program.

The measured results and energy duty calculations offer better understanding of the real stresses the arrester is exposed to in service.

For the correct selection of arresters and validation of simulation software, much more real field results are needed. This monitoring system enables their acquisition. Transient shapes with high current amplitudes and longer duration are of primary interest for this, since they produce a higher electrical stress to the arrester.

During the different phases of the development of this monitoring system, new knowledge has been acquired in various fields. In the acquisition field, special care has been

given to the correct sensor and acquisition card selection, their calibration and the correct installation of those sensitive electronics devices in a high voltage environment.

In the telecommunication field, it was important to make sure that the mobile communication never fails otherwise the results would be unreachable.

In the solar power supply field, monitoring system behavior has been observed during summer and winter seasons and conclusions have been made regarding its correct dimensioning in terms of rated power of the panels, charge controller maximum input current and battery capacity.

Finally software has been used extensively. On one side the simulation programs were of primary importance for the correct design of the monitoring systems, such as the current transformer selection.

But also own developed software required programming knowledge. Various applications have been developed for the acquisition of transient events, the display of the acquired results, the calculation of line surge arrester energy duty and the automatic control of a remote generator.

The new aim of this thesis work is the installation of new monitoring systems on various lines all around the world. This would improve the general knowledge in the lightning field by the increase of the number of acquired results in terms of quantity but also from a qualitative point of view. Indeed the monitoring systems may acquire transient events affecting different line designs, but also the lightning parameters would differ for a given region, such as polarity, duration, front time, distribution, multiplicity.

Next to the discharged current, other parameters may be monitored as well. A short term possibility is the upgrade of existing equipment, such as the leakage current monitors.

Finally, the developed monitoring system is not only limited to the line surge arresters. Thanks to its data acquisition, computation and communication possibilities, other devices may be monitored by using the adequate sensors, such as the current transformers. This is the case for example for the station surge arrester.

VII. Future developments

The proposed monitoring system already operates successfully in real field. However there is still place for improvement, in terms of technological breakthrough and installation configurations. Several proposals are detailed below.

VII.1. ARRESTER ENERGY DUTY SHARING

The proposed monitoring system permits to study the energy duty sharing between several arresters installed on few consecutives towers. Ideally this can be done with two or three systems installed on neighboring towers. Since up to four acquisition channels can be measured per system, three can represent the arrester of each phase, and the fourth a high current peak sensor installed on tower top. This sensor would measure the total lightning current flowing through tower.

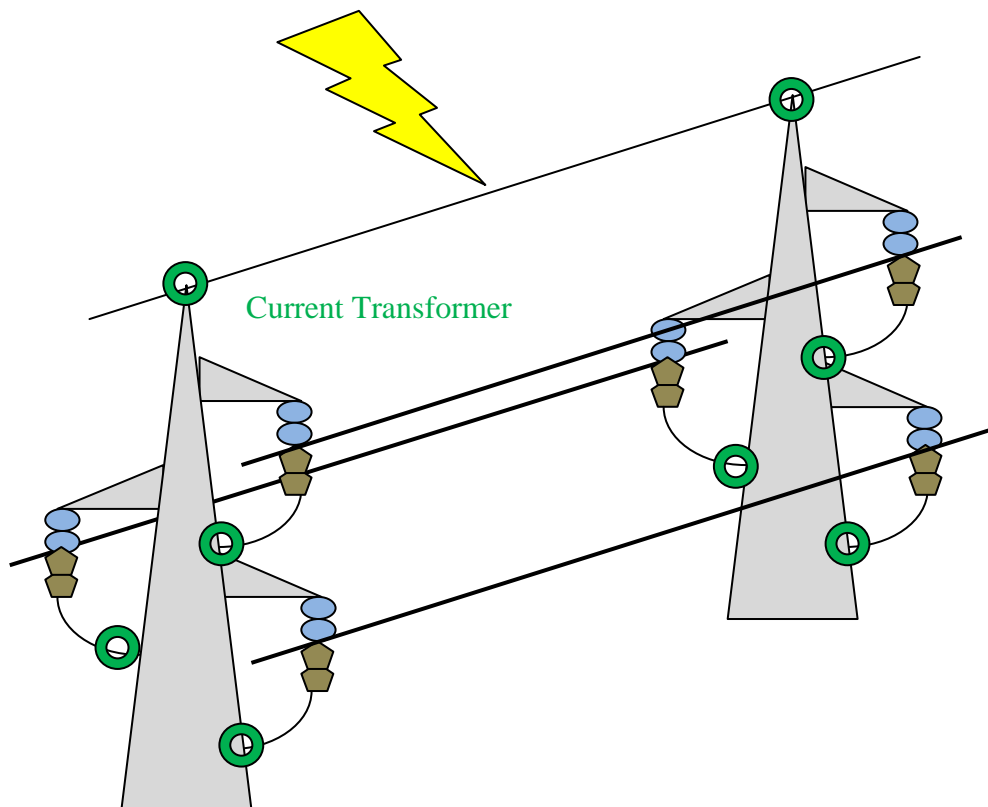


Figure 45 - Proposed configuration for the study of arrester energy duty sharing

With this proposed configuration and the monitoring systems, all currents flowing through the towers and the surge arresters would be measured, in order to study the energy duty sharing among them. This information is of primary interest for the correct arrester selection in terms of IEC Class.

VII.2. GPS TIME SYNCHRONIZATION

Proposed NTP synchronization over the Internet of the monitoring systems is an acceptable solution in this scenario where both of the controllers are installed nearby in the sense of the same transmission line, region, country or time zone. Also compared to the existing devices such as ABB EXCOUNT-II, this method shows clearly some advantages as described previously. However for the future system development some points shall be taken into account.

First of all, the NTP synchronization requires the network connection of the monitoring systems to a common time server, over the Internet or the Intranet of the utility. This implies that this computer is working continuously 24 hours per day and 7 days per week. Also it shall have its own time very accurate by synchronizing it with another NTP server or by other methods such as GPS.

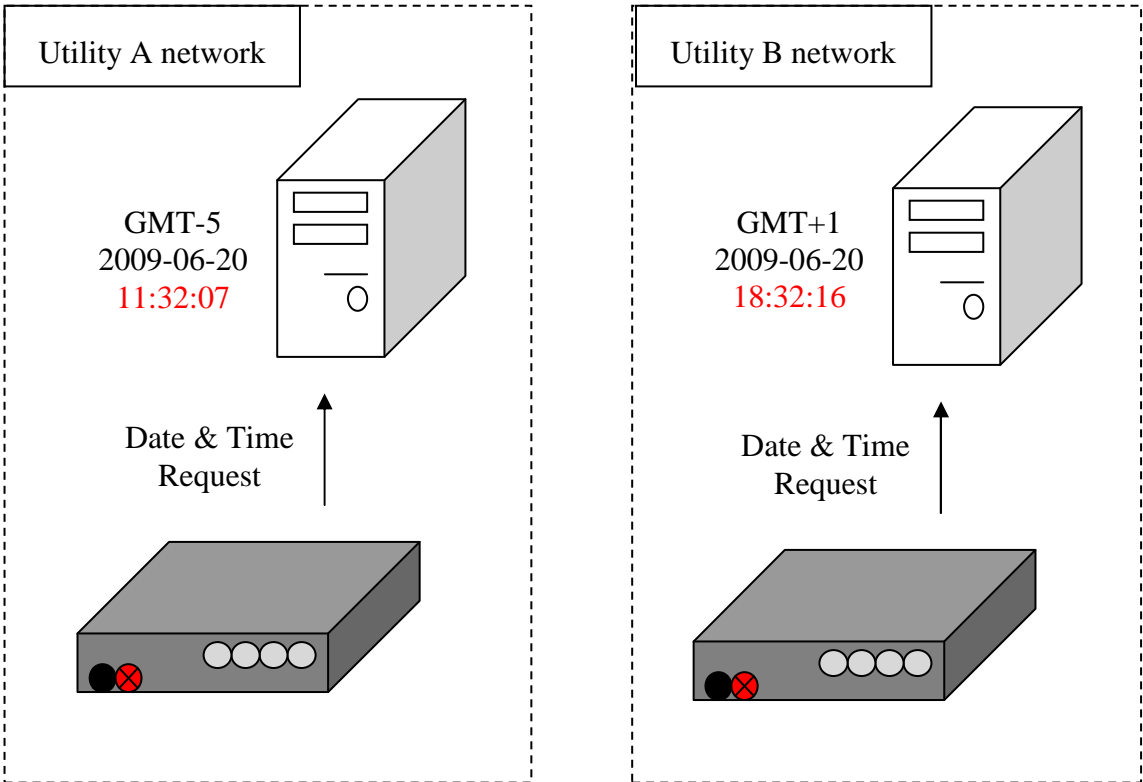


Figure 46 - Time drift issues with monitoring systems installed for different utilities

Also with the installation of several monitoring systems on different transmission lines for different utilities, located in different countries and time zones, controller's synchronization might be difficult. Indeed in the case that some of them have access to the Internet while others are connected directly to the utility network, each of these devices may have to connect to different NTP servers. For example they may be a part of different networks that cannot communicate with each other such as utilities ones, because of security and privacy purpose. But since two and more NTP servers do not have necessarily the same accurate timings, this may lead to a time drift between the monitoring systems.

Therefore a better solution for the midterm is the individual time synchronization of each monitoring system by GPS. This would guarantee an accurate timing for each controller whatever the tower, utility, country and time zone it is installed. Also whatever the connection of the monitoring system to Internet or the utility network, GPS synchronization is an ideal solution since it avoids time drifting issues with several NTP servers. And even with GPS the controller doesn't need to be connected to a network but can work in a so called offline mode.

Since the main part of the monitoring system is the industrial motherboard, the most interesting GPS receiver is probably the one with USB port, since it allows easy connection to the controller for the communication and power. Only requirement for the receiver is that its antenna is installed outdoors and with no obstacles above it.

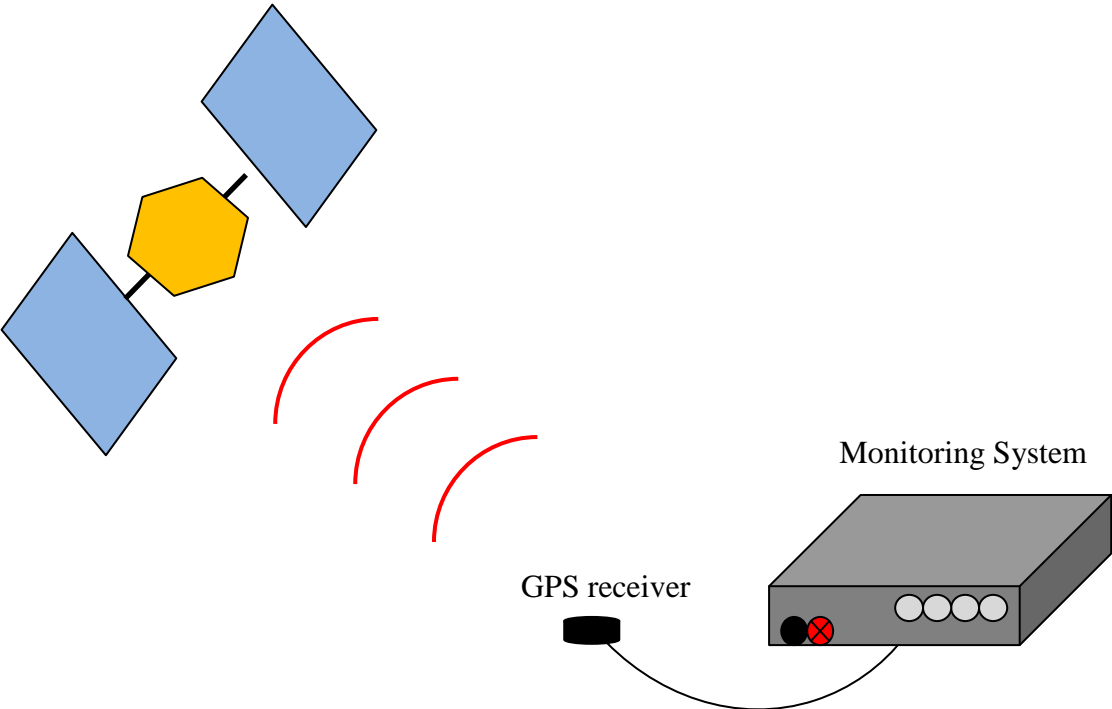


Figure 47 - Monitoring system time synchronization over GPS

VII.3. WIRELESS COMMUNICATION ALONG TOWERS

Another point of interest for the future system development is the wireless communication along towers. Indeed in present situation controllers are communicating mainly over the mobile network, and this implies some limitations.

First of all, each monitoring system has to connect to the telecom provider base stations with adequate modem and a SIM card. This induces some additional costs in the terms of equipment required for mobile communication as well a monthly connection fee to be paid per system.

Next to the price of mobile communication, another concern is reliability of the link. Indeed monitoring system's communication is dependant of the telecom base station and if this one fails because of lightning for example, the controller is not anymore accessible. Same goes with connection parameters such as the access point name of the mobile network. The monitoring system has to specify it in its software in order to connect to the right telecom provider and therefore to Internet. If this provider decides to make some changes to those parameters, connection to the controller might be lost once again.

Finally the privacy of transmitted data is another issue. Although all the information transmitted between the monitoring systems and the server can be encrypted over a virtual private network, it is still travelling over the Internet. And some utilities may consider this type of data as confidential and therefore mobile communication using external networks is not welcome.

Therefore in order to improve cost effectiveness, reliability and privacy of the monitoring system, wireless communication shall be the preferred solution whenever possible. Main goal is to connect the controllers directly to the utility network. In that case two scenarios are to be considered.

On one side, lines that are already equipped with fiber optics network of the utility. This is the case mainly with shielded transmission lines where the optical cable is installed along the shield wire. Connection to this cable and therefore to the utility network is accessible on some towers with a junction box where the fiber optics are cut and connected between them. Typical section of this optical cable or the distance between two junction boxes is of few kilometers.

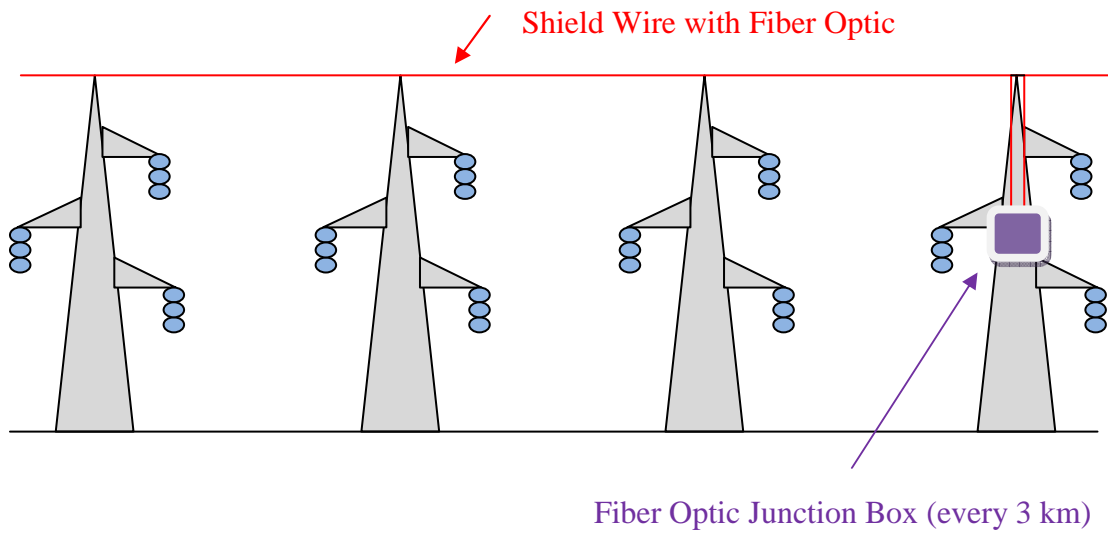


Figure 48 - Fiber optics along a transmission line

On the second one, lines that are installed without fiber optics cable. This is the case mainly with distribution lines as well transmission lines with no shield wire.

In the first scenario, wireless communication is required for the connection of the monitoring system to the nearby tower with a junction box. At this tower, wireless signal is converted to fiber optics with adequate modem, in order to connect the controller to the utility network.

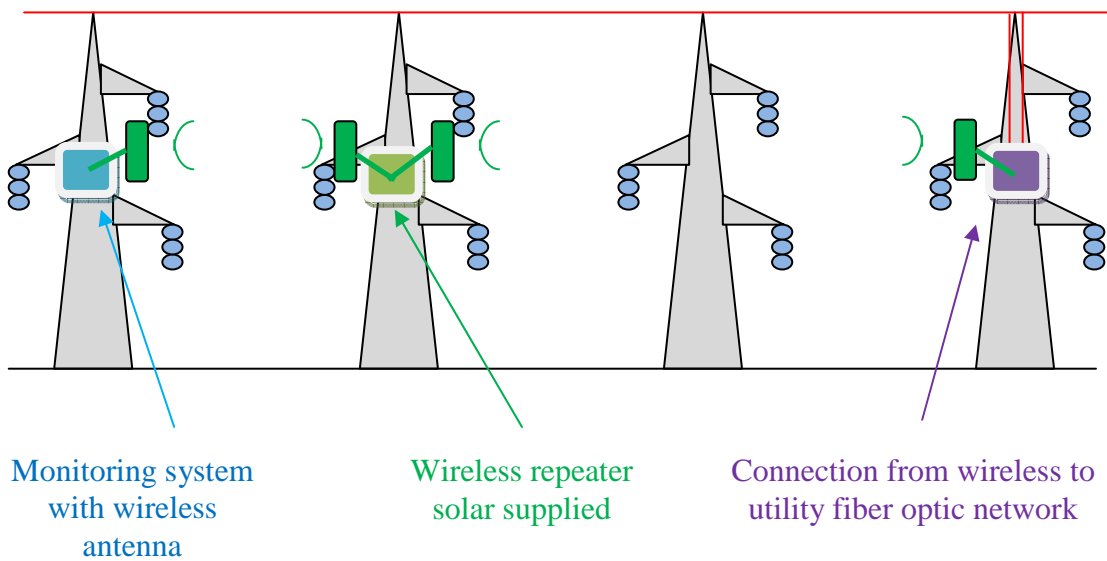


Figure 49 - Application of wireless communication next to fiber optics

In the second scenario, wireless communication implies full coverage of the line from the tower of interest to the nearest substation connected to the utility network. In that case several wireless modems are to be installed along the line in order to transmit data.

Whatever the scenario, typical tower connection point consists of two wireless modems. It is solar supplied with an overall power consumption lower than 8 watts. First modem behaves as a client and connects this tower to the previous one. Second modem behaves as a wireless access point and permits the connection to it of the next tower.

Since each wireless modem has a transmit range of a few kilometers, the connection points don't need to be installed on each consecutive tower. Only requirement is a direct line of sight between the modems in order to maintain a good quality link. And since sections of towers are aligned because of installation constraints, one wireless link between two connection points can cover several towers at once.

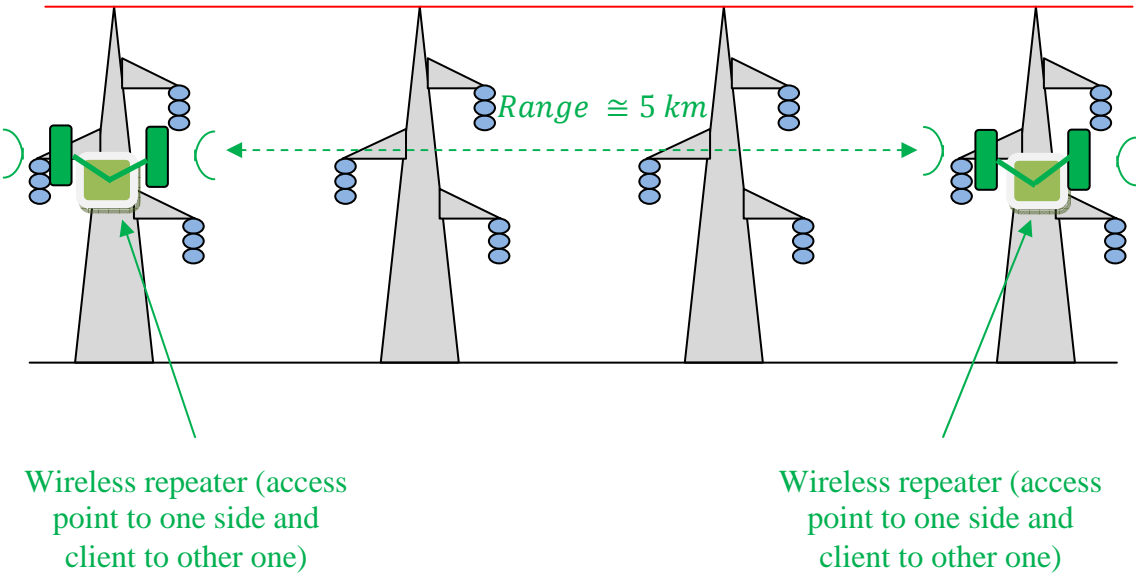


Figure 50 - Application of wireless communication along whole line

Main objective is to install those repeaters at strategic towers in order to link this wireless network to the utility one, wherever it is already present through a junction box on a tower or in a substation. Once the signal coverage is satisfactory, monitoring systems can connect to it by wireless with own modem, and communicate with the server.

VII.4. EXISTING EQUIPMENT USE AND UPGRADE

For the future development of this type of monitoring, one of the possibilities is to use existing devices already installed in real field, and upgrade them with new functionalities.

This is the case of the surge counter devices with an auxiliary port such as the Tyco SC13. Indeed its output connector gives the instant measurement of the total leakage current of the monitored arrester. By connecting it as a sensor to the proposed monitoring system, instead of the current transformers, a much powerful device is designed.

For example, the communication capabilities of the controller enable that the surge counter data can be accessed over any available network. Indeed the total leakage current is acquired with the acquisition card through the auxiliary port, and the resulting shape can be received on demand or based on trigger criteria by remote user. Main advantage is that there is no more need to send a technician on site in order to read instant total leakage measurement value on the surge counter screen.

Also triggering capabilities of the monitoring system with its accurate time add new functionalities to the existing device. In case of arrester operation, a more important current than the total leakage one flows through the surge counter. During this event, the measurement at the auxiliary output is higher than the usual one. By selecting correctly the trigger threshold values at the entrance of the acquisition card, that arrester operation can be registered thanks to the triggering function of the monitoring system. And that event is saved with accurate time due to the controller's synchronization by NTP or GPS.

Therefore this upgraded monitoring device is able to register the event of arrester operation and this with accurate time. Number of discharges can be counted by the controller itself, and transmitted to the server application over the network.

VIII. Summary

Line surge arresters are devices used to improve transmission line lightning performance. Electrically, they are installed in parallel to the line insulators, with the main function to prevent line insulation flashover. This technology is today used worldwide as a standard solution for line lightning performance improvement of transmission and distribution lines.

In Chapter II electrical stresses a surge arrester is exposed to were presented. Lightning and switching overvoltages main characteristics were described in terms of amplitude and duration. Then the line surge arrester was detailed, with special care being given to its energy capability regarding the design and installation configuration. Lightning parameters such as amplitude, duration, multiplicity, polarity and distribution were described as well and correlated to the energy duty of the arrester. Topics such as correct arrester selection for a particular line and validation of software simulation results were discussed.

In Chapter III existing surge arrester monitoring devices and current research projects were studied. Their characteristics regarding the measurement of the real electrical stresses were underlined. Then the proposed monitoring system has been extensively described in order to present the new possibilities it offers. Both hardware and software parts were detailed, with a special care given to the own developed triggering algorithm for the successful electrical stresses results gathering.

In Chapter IV a simulation model of a particular overhead line was designed and results were presented regarding estimated stresses line surge arrester is exposed to. ElectroMagnetic Transients Program (EMTP_RV) software has been used for that purpose. Results of this study demonstrated that for the designed line configuration, selected surge arresters, their position and chosen lightning parameters, electrical stresses would be absorbed successfully. This simulation was of primary interest for the correct design of the proposed monitoring system in terms of current transformer and acquisition card selection.

In Chapter V the laboratory testing of the monitoring system was presented. This included the remote control of the impulse generator equipment as well the remote viewing of the experiment thanks to digital cameras. This original laboratory testing was presented during several conferences in order to demonstrate the correct operation of the proposed monitoring system.

Once successfully verified in laboratory, two monitoring systems have been installed on a pilot line, which is very similar to the previously simulated one. Therefore all the conclusions made thanks to the software simulation and laboratory testing apply for this installation in terms of correct design of the monitoring system.

In Chapter VI the first results acquired by the two monitoring systems were presented. Those real electrical stresses affecting the line surge arresters were measured in the real field and are due to real lightning activity. Next to the interesting current shapes illustrated, arrester energy duty was computed for each event thanks to own developed application. Conclusion is made regarding the arrester condition.

In Chapter VII are introduced the next available steps in the future development of this monitoring device. This covered topics such as an original configuration of the system installation, where line surge arresters on subsequent towers are monitored as well the tower itself, and which may lead to interesting results regarding the energy duty sharing. Also hardware upgrade possibilities of the monitoring device were presented such as wireless communication along towers and GPS time synchronization for even more accurate results.

With this summary of all of the chapters, final conclusions can be made regarding this thesis work, and are presented below.

The proposed monitoring system has successfully acquired real field transient currents. Measured results are obtained from a real line with real lightning activity. No artificially triggered lightning is involved.

The measured results and energy duty calculations offer better understanding of the real stresses the arrester is exposed to in service.

For the correct selection of arresters and validation of simulation software, much more real field results are needed. The proposed monitoring system enables their acquisition. Transient shapes with high current amplitudes and longer duration are of primary interest for this, since they produce a higher electrical stress to the arrester.

Up to now and based on present real stresses measurements, line surge arresters installed on the monitored line can be stated as correctly chosen in terms of energy capability.

IX. References

- [01] E. Kuffel, W.S. Zaengl, J. Kuffel:
“High Voltage Engineering” Fundamentals, Second Edition
Butterworth-Heinemann, 2000.
- [02] Hugh M. Ryan:
“High voltage engineering and testing” 2nd edition
The Institution of Electrical Engineers, IEE POWER AND ENERGY SERIES 32,
2001.
- [03] CIGRE:
“Guide to Procedures for Estimating the Lightning Performance of Transmission Lines”
CIGRE brochure 63, October 1991.
- [04] CIGRE:
“Characterization of Lightning for Applications in Electric Power Systems”
Task Force 33.01.02, Lightning Location Systems, December 2000.
- [05] IEEE:
“IEEE Guide for Improving the Lightning Performance of Transmission Lines”
IEEE Std. 1243-1997, 1997.
- [06] IEEE:
“IEEE Guide for Improving the Lightning Performance of Electric Power Overhead
Distribution Lines”
IEEE Std. 1410, 2004.
- [07] IEEE:
“IEEE Standard for Metal-Oxide Surge Arresters for AC Power Circuits (> 1 kV)”
IEEE Std. C62.11, 2005.

- [08] IEC:
“IEC 60099-4 Standard: Surge arresters - Part 4: Metal-oxide surge arresters without gaps for a.c. systems”
International Electrotechnical Commission, 2009.
- [09] IEC:
“IEC 60099-5 Standard - Amendment 1: Surge arresters – Part 5: Selection and application recommendations – Section 1: General”
International Electrotechnical Commission, 1999.
- [10] IEC:
60071.4: “Insulation Coordination – Part 4: Computational guide to insulation coordination and modelling of electrical networks”.
- [11] IEEE:
TF on Fast Front Transients, “Modeling guidelines for fast transients”,
IEEE Trans. On Power Delivery, vol. 11, no. 1, pp. 493-506, January 1996.
- [12] CIGRE:
WG 33-02, “Guidelines for Representation of Network Elements when Calculating Transients”, 1990.
- [13] T. Klein, W. Kohler, K. Few, W. Schmidt, R. Bebensee:
“A New Monitoring System for metal Oxide Surge Arresters”
High Voltage Engineering Symposium, 22-27 August 1999, Conference Publication No. 467, IEEE.
- [14] Volker Hinrichsen:
“Monitoring of High Voltage Metal Oxide Surge Arresters”
VI Jornadas Internacionales de Aislamiento Eléctrico Bilbao, 22./23.10.1997, Paper 6.4.

- [15] Y. Matsumoto, O. Sakuma, K. Shinjo, M. Saiki, T. Wakai, T. Sakai, H. Nagasaka, H. Motoyama, and M. Ishii:
“Measurement of lightning surges on test transmission line equipped with arresters struck by natural and triggered lightning”
IEEE Trans. Power Del., vol. 11, no. 2, pp. 996–1002, Apr. 1996.
- [16] T. Wakai, N. Itamoto, T. Sakai, M. Ishii:
“Evaluation of Transmission Line Arresters Against Winter Lightning”
IEEE Transactions on Power Delivery, Vol. 15, No. 2, pp. 684 - 690, April 2000.
- [17] P. P. Barker, R.T. Monaco, D.J. Kvaltine, D. E. Parrish:
“Characteristics of lightning surges measured at metal oxide distribution arresters”
IEEE Transactions on Power Delivery, Vol. 8, No.1, , pp. 301 - 310, January 1993.
- [18] Jens Schoene, Martin A. Uman, Vladimir A. Rakov, Angel G. Mata, Carlos T. Mata, Keith J. Rambo, Jason Jerauld, Douglas M. Jordan, and George H. Schnetzer:
“Direct Lightning Strikes to Test Power Distribution Line - Part I: Experiment and Overall Results”
IEEE Transactions on Power Delivery, Vol. 22, No. 4, October 2007.
- [19] M.I. Femandez, K.J. Rambo, V.A. Rakov, M.A. Uman:
“Performance of MOV Arresters During Very Close, Direct Lightning Strikes to a Power Distribution System”
IEEE Transactions on Power Delivery, Vol. 14, No. 2, April 1999.
- [20] C. T. Mata, V. A. Rakov, and M. A. Uman:
“Division of lightning current and charge among multiple arresters and grounds of a power distribution line”
Proc. 26th Int. Conf. Lightning Protection, Krakow, Poland, pp. 585–590, Sep. 2 - 6, 2002.

- [21] C. T. Mata, V. A. Rakov, K. J. Rambo, P. Diaz, R. Rey, M. A. Uman:
 “Measurement of the division of lightning return stroke current among the multiple arresters and grounds of a power distribution line”
 IEEE Trans. Power Del., Vol. 18, No. 4, pp. 1203 - 1208, Oct. 2003.
- [22] Alexandre Piantini, Thaís Ohara, Acácio Silva Neto, Jorge M. Janiszewski, Ruy A. C. Altafim, R. A. Roncolato:
 “A Full-Scale System for Lightning Data Acquisition, With special Reference to Induced Voltages on Distribution Lines”
 GROUND’2002: International Conference on Grounding and Earthing and 3rd Brazilian Workshop on Atmospheric Electricity, Rio de Janeiro - Brazil November 4-7, 2002.
- [23] P. Barker, T. Short, H. Mercure, S. Cyr, J. Brien:
 “Surge arrester energy duty considerations following from triggered lightning Experiments”
 IEEE winter Power Meeting, Panel session on Transmission Line Surge Arrester Application Experience, 1988.
- [24] Tyco Electronics, Bowthorpe EMP, Surge Counters Type SC12 & SC13 datasheet.
- [25] Siemens Surge Counter 3EX5 030, Surge Monitor 3EX5 050, technical specification.
- [26] ABB High Voltage Surge Arresters Buyer’s Guide – Section EXCOUNT-II.
- [27] Measurement Computing PCI-DAS4020/16, user’s manual.
- [28] Pearson Electronics, Inc., Pearson current monitor model 3025 datasheet.
- [29] Haefely EMC Technology, ECOMPACT 4 Transient Immunity Test Station datasheet.
- [30] Hantek Electronic co., Ltd., DDS-3005 Arbitrary Waveform Generator user manual.

- [31] S. Sadovic, T. Sadovic:
“Line Surge Arrester Monitoring System”
2005 Höfler’s Days, Portorož, Slovenia, 6-8.11.2005.
- [32] S. Sadovic, T. Sadovic, I. Uglešić, V. Milardić, B. Filipović-Grčić:
“Information Technology In High Voltage Measurements”
17th International Expert Meeting, May 13th - 15th 2008, Maribor, Slovenia.
- [33] M. Muhr, T. Sadovic:
“Real-Time Remote Monitoring of Line Surge Arresters”
CIGRE Colloquium, Cavtat, Croatia, 26.05.2008.
- [34] M. Muhr, T. Sadovic, S. Sadovic:
“Real-Time Remote Experiment In High Voltage Lab”
The 9th Höfler's Days, Portorož, Slovenia, 02-04.11.2008.
- [35] M. Muhr, T. Sadovic, S. Sadovic:
“Real-Time Remote Experiment In High Voltage Lab”
The 16th International Symposium on High Voltage Engineering, Cape Town, South Africa, 24 to 28 August 2009.
- [36] T. Sadovic, S. Sadovic:
“Transmission Line Lightning Performance”
Simulation & Analysis of Power System Transients with EMTP_RV, Dubrovnik, Croatia, 27-29.04.2009.
- [37] S. Pack, M. Kompacher, M. Muhr, I. Hübl, M. Marketz, R. Schmaranz:
“Analyses and practical measures to reduce lightning-caused outages on a 110 kV overhead line”
XVth International Symposium on High Voltage Engineering, University of Ljubljana, Elektroinštitut Milan Vidmar, Ljubljana, Slovenia, August 27-31, 2007.

- [38] S. Pack, M. Muhr, I. Hübl, M. Marketz, R. Schmaranz:
“Possibilities and remedial measures to reduce lightning-caused outages in a distribution network”
19th International Conference on Electricity Distribution, Vienna, Austria, 2007.
- [39] M. Muhr, S. Pack, M. Kompacher:
“Möglichkeiten und Maßnahmen zur Reduzierung der Fehlerhäufigkeit einer 110 kV Hochgebirgsleitung”
Scientific Report, VA03332.
- [40] T. Judendorfer, S. Pack, M. Muhr:
“Line arrester application on a 110 kV high alpine overhead line to reduce lightning caused outages”
Application of Line Surge arresters in Power Distribution and Transmission Systems, Colloquium Cavtat, Croatia, 25-29 May 2008.
- [41] Ignaz Hübl, Michael Marketz and Robert Schmaranz, KELAG Netz GmbH, and Stephan Pack and Michael Muhr, TU Graz:
“Three Techniques to Mitigate Lightning”
Transmission & Distribution World, March 2008.
- [42] A. Xemard, J. Michaud, F. Maciela, T. Lassaigne, F. Sauvegrain, P. Auriol, J. G. Roumy, O. Saad, Q. Bui Van, A. Dutil:
“Reduction of the number of double-circuit flashovers on a 400 kV overhead line”
Application of Line Surge arresters in Power Distribution and Transmission Systems, Colloquium Cavtat, Croatia, 25-29 May 2008.
- [43] S. Bojic, I. Dolic, A. Sekso, J. Radovanovic, D. Škarica:
“First Experience in Monitoring of Line Surge Arresters Installed on 110 kV Transmission Line Ston – Komolac in Croatia”
Application of Line Surge arresters in Power Distribution and Transmission Systems, Colloquium Cavtat, Croatia, 25 - 29 May 2008.

- [44] Iryani M. Rawi, M. Pauzi Yahaya:
“Pilot Study on the Use of Gapless Transmission Line Arresters (TLA) as an Alternative to Gapped TLA in TNB Transmission System”
Application of Line Surge arresters in Power Distribution and Transmission Systems, Colloquium Cavtat, Croatia, 25-29 May 2008.
- [45] I. Uglešić, V. Milardić, B. Filipović-Grcić, A. Tokić:
“Evaluation of Energy Stress on Line Arresters”
Application of Line Surge arresters in Power Distribution and Transmission Systems, Colloquium Cavtat, Croatia, 25-29 May 2008.
- [46] M. Puharić, M. Mešić, M. Lovrić, J. Radovanović, S. Sadović:
“Lightning Performance Improvement of 123 kV Line Ston – Komolac by Use of Line Surge Arresters”
Application of Line Surge arresters in Power Distribution and Transmission Systems, Colloquium Cavtat, Croatia, 25-29 May 2008.
- [47] M. Puharić, M. Lovrić, J. Radovanović, Z. Čosić, S. Sadović:
“Line Surge Arrester Application Pilot Project”
27th International Conference on Lightning Protection, ICLP 2004, Avignon, France, 2004.
- [48] S. Sadović, R. Joulie, S. Tartier, E. Brocard:
“Line Surge Arresters and Unbalanced Insulation in the Reduction of Double Circuit Outages on a 225 kV Transmission Line”
X International Symposium on High Voltage Engineering, August 25-29, 1997, Montréal, Canada.
- [49] S. Sadović, R. Joulie, S. Tartier, E. Brocard:
“Use of Line Surge Arresters for the Improvement of the Lightning Performance of 63 kV and 90 kV Shielded and Unshielded Transmission Lines”
IEEE Transactions on Power Delivery, vol. 12, no. 3, July 1997, pp. 1232 – 1240.

- [50] D. Loudon, K. Halsan, U. Jonsson, D. Karlsson, L. Strenstrøm, J. Lundquist:
“A compact 420 kV line utilizing line surge arresters for areas with low isokeraunic levels”
CIGRE Paris Session 22/33/36-08, 1998.
- [51] A. Xemard, S. Sadovic, I. Uglesic, J. A. Martinez, L. Prikler:
“Developments on the line surge arresters application guide prepared by the CIGRE WG C4 301”
Symposium CIGRE Zagreb 2007.
- [52] A. Xémard, S. Denetière, J. Michaud, P.Y. Valentin, Q. Bui-Van, A. Dutil, M. Giroux, J. Mahseredjian:
“Methodology for the calculation of the lightning flashover rate of a line with or without line surge arresters”
CIGRE Paris Session 2006, Paper No C4-101.
- [53] W. A. Chisholm, S. Sadovic, C.J. Pon, J. Levine:
“Guidelines for Installation of Surge Arresters on Sub-Transmission and Transmission Lines using Different Structure Designs at Voltages from 69 kV to 345 kV”
CEA Technologies Project T033700-3312, Montreal, Canada, 2005.
- [54] S. Sadovic, G. Couret, Z. Abidin, M. Puharic, L. Peter:
“Quality of Service Improvement of the Compact Lines by the Use of Line Surge Arresters”
CIGRE 5th Southern Africa Regional Conference, Cape Town, South Africa, 2005.
- [55] S. Sadović:
“Can we use surge arrester monitoring data in the high voltage equipment maintenance Management”
Edvard Höfler's Days, Milan Vidmar Institute, Potroř, Slovenia, 2002.

- [56] M. Babuder, M. Kenda, P. Kotar, E. Brocard, S. Tartier, R. Joulie, S. Sadovic:
“Lightning Performance Improvement of 123 kV Transmission Line by use of Line Surge Arresters”
XI International Symposium on High Voltage Engineering, London, U.K., August 1999.
- [57] Hinrichen, V., Scholl, G., Schubert, M., Ostertag, T.:
“Online Monitoring of High-Voltage Metal-Oxide Surge Arresters by Wireless Passive Surface Acoustic Wave (SAW) Temperature Sensors”
Proceedings of The 11th International Symposium on High-Voltage Engineering, London, UK, August 23-27, 1999.
- [58] C. Heinrich, V. Hinrichsen:
“Diagnostics and monitoring of metal oxide surge arresters in high voltage networks – comparison of existing and newly developed procedures”
IEEE Transactions Power Delivery, vol. 16, n° 1, pp. 138 - 143, 2001.
- [59] M. Kobayashi, H. Sasaki, and K. Nakada:
“Rocket-triggered lightning experiments on zinc oxide arresters and their applications to Power transmission lines”
Elect. Eng. Japan., Vol. 122, No. 4, 1998.
- [60] Guilherme M. Corrêa, Silvério Visacro, André M. N. Teixeira. Lothar Ruhnke, Vladislav Mazur:
“The Response of Tower to Nearby Lightning: Resent Improvements in the Measuring System”
IX International Symposium on Lightning Protection, 26th-30th November 2007 – Foz do Iguaçu, Brazil.
- [61] Volker Hinrichsen:
“Testing Requirements and actual IEC Work on Transmission Line Arresters”
Application of Line Surge arresters in Power Distribution and Transmission Systems, Colloquium Cavtat, Croatia, 25-29 May 2008.

X. Annexes

X.1. ANNEX I – ARRESTER ENERGY DUTY CALCULATION

When the surge arrester operates, a transient current shape flows through it. Energy dissipated through the arrester is correlated to this discharged current in terms of amplitude and duration. Indeed by integrating over time the transient shape profile, and if the current-voltage characteristic of the arrester is known, its energy duty can be calculated.

The energy duty of a surge arrester is given by the equation below.

$$E = \int_{T1}^{T2} U(|I(t)|) * |I(t)| dt$$

Where:

E is the energy dissipated through the arrester

I(t) is the lightning transient current shape value

U(I) is the arrester voltage value for given current, based on its current–voltage characteristic

T1 is the lightning transient current shape start time

T2 is the lightning transient current shape end time

Equation 5 - Energy duty of a surge arrester calculation

First of all, at each time step of the integration, the present absolute current value has to be multiplied with its voltage value based on the voltage discharge curve. Based on Equation 5, arrester energy duty for the given integration time step is calculated by the trapezoid rule estimation formula below.

$$E_t = \frac{U(|i_t|) * |i_t| + U(|i_{t+1}|) * |i_{t+1}|}{2} Dt$$

Where:

E_t is the energy duty in kJ between time step t and t+1.

Dt is the integration time step in seconds

i_t is the current value at instant t

U(i_t) is the voltage value for given current i_t, based on arrester current–voltage characteristic

Equation 6 - Trapezoid rule applied to energy duty calculation at each time step

Absolute values of the current are used since the energy has a positive value even in the case of a negative transient current.

However the voltage discharge curve table has a limited number of known values for a given current. For each present absolute current value, its closest upper and lower currents values are found inside this table. Then the interpolation formula below is applied in order to calculate the voltage for the given current:

$$U(|I_i|) = \frac{U(I_2) - U(I_1)}{I_2 - I_1} (|I_i| - I_1) + U(I_1), \text{ with } I_1 \leq |I_i| \leq I_2$$

Equation 7 - Interpolation applied to voltage discharge curve

Therefore the total energy duty of the arrester can be calculated, and is given by the formula below:

$$E = \sum_{t=0}^{T_{max}} E_t, \text{ with } T_{max} = T_{rise} + 2 * (T_{tail} - T_{rise})$$

Equation 8 - Total energy duty calculation

With a more realistic current shape, such as the ones acquired in this thesis, the default integration time step corresponds to the time step of the acquisition.

Line surge arrester used on the pilot line is IEC class II gapless surge arrester having the following voltage discharge curve, given in Figure 51 and Table 20.

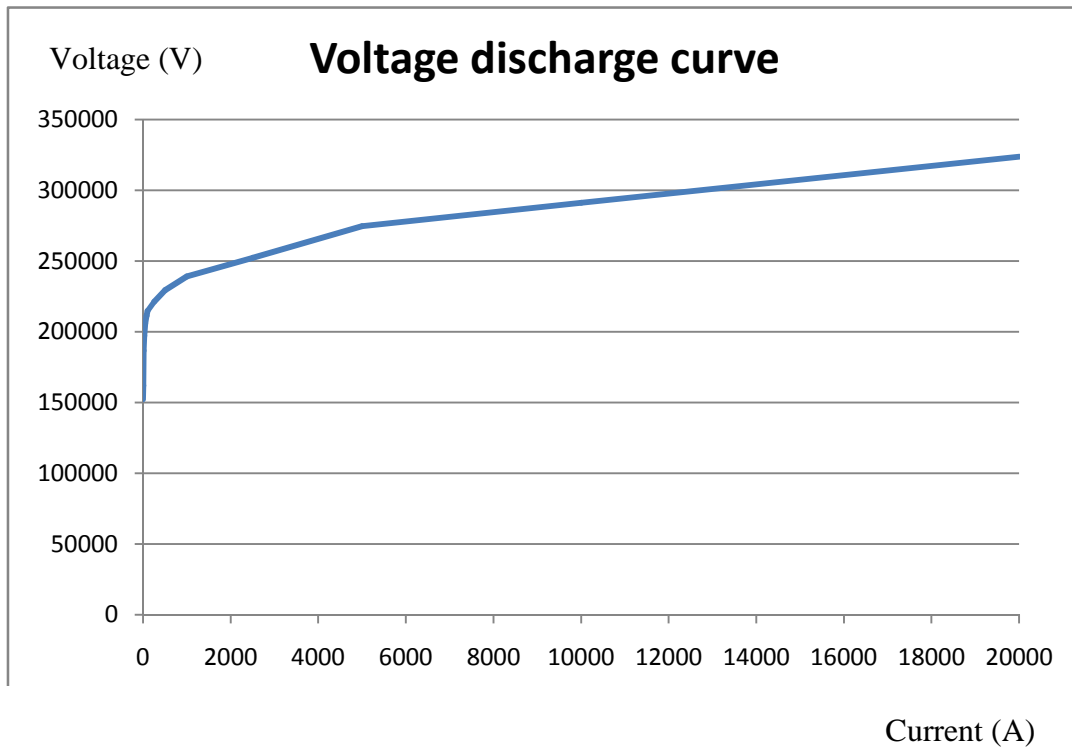


Figure 51 - Arresters voltage discharge curve example

Current (A)	Voltage (V)
0,001	152300
1	161900
10	186600
25	197300
50	205900
75	211200
100	214700
250	221200
500	229400
1000	239200
2500	252100
5000	274700
10000	291200
20000	323600

Table 20 – Voltage discharge curve data

X.2. ANNEX II – SURGE ARRESTER OPERATING DUTY TESTS

Operating duty test is a very important test for the arrester energy capability assessment. The main requirement is that arrester passes these tests without thermal runaway. It is important that the arrester section being tested has both a transient and a steady state heat dissipation capability equal or higher than for the complete arrester.

Very important parameter for the operating duty test is power losses. Taking into account that this test is performed on the new blocks, it is necessary to simulate influence of the metal oxide blocks ageing in the service. This is done by the introduction of the elevated rated and continuous operation voltages (U_r^* and U_c^*). These (elevated) rated voltages should produce the same power losses on the new blocks as normal rated and continuous operating voltages on the aged blocks. The procedure for the determination of the elevated rated and continuous operated voltage is described in IEC 60099-4 [8].

The operating duty test consists of the following sequences:

- Initial measurements
- Conditioning
- Application of impulses
- Measurement and examination

For IEC Class II [like the one installed on the pilot line] so called “Switching surge operating duty test” applies. Test procedure is presented in Table 21. It is also graphically presented in Figures 52, 53 and 54. The equivalent injected energy for the single impulses or for the group of impulses for the considered arrester ($U_{\text{rated}} = 108 \text{ kV}$) is also presented on these figures.

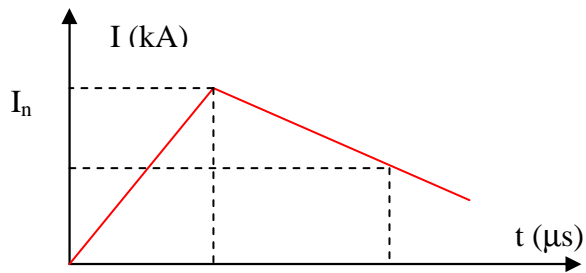
Initial measurement: Figure 52	The lightning impulse residual voltage at nominal discharge current of each three test samples is determined at ambient temperature.
Conditioning: Figure 52 Figure 53	<p>First part of the conditioning:</p> <ul style="list-style-type: none"> - Twenty 8/20 lightning current impulses having a peak equal to the nominal discharge current are applied. - The test sample energized at 1,2 times the continuous operating voltage. - Impulses are applied in four groups of five impulses. - Interval between impulses: 50 to 60 s. - Interval between groups: 25 to 30 min (no need to have block energized during this period). <p>Second part of the conditioning:</p> <ul style="list-style-type: none"> - Application of two 4/10 100 kA high current impulses. - Samples are not energized. - Cooling to ambient temperature before the second impulse.
Application of impulses: Figure 54	<ul style="list-style-type: none"> - The temperature of the complete section shall be $60^{\circ}\text{C} \pm 3^{\circ}\text{C}$. - Two long duration (rectangular) current impulses with the peak values related to the line discharge class. - Time interval between the impulses shall be 50 s to 60 s. - As soon as possible (<100 ms) the elevated rated voltage U_r^* has to be applied for 10 s. - After 10 s of U_r^*, the elevated continuous operating voltage U_c^* is applied immediately for 30 min. - Voltage and current shapes are monitored during the application of the second impulse. - The current and voltage shall be registered continuously during the power frequency application.
Final measurement:	<ul style="list-style-type: none"> - After the test sample has cooled to near ambient temperature, the lightning impulse residual voltage measurement at nominal discharge current is performed.

Table 21 - Switching surge operating duty test based on IEC 60099-4 Standard

NOMINAL CURRENT CONDITIONING: [4 x 5 x (I_n , 8/20 μ s)]

I_n - Nominal discharge current:

$I_n = 10$ kA



RESIDUAL VOLTAGE
(I_n , 8/20 μ s)

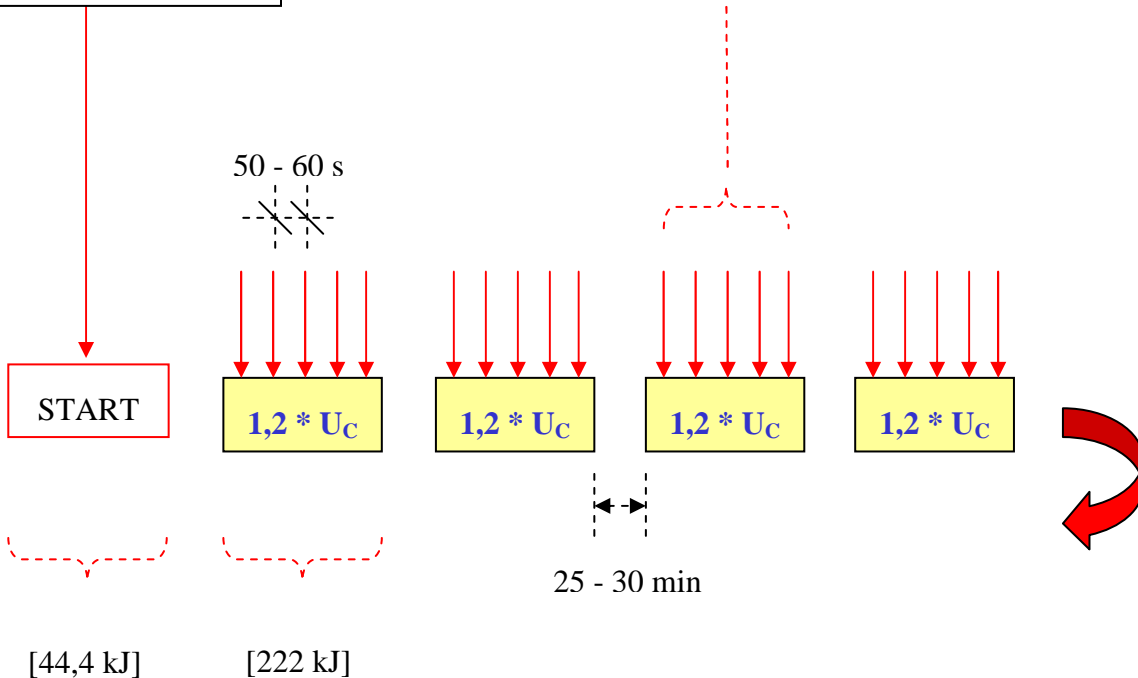


Figure 52 - Switching surge operating duty test: Conditioning

HIGH CURRENT IMPULSE CONDITIONING: [4 x 5 x (100 kA, 8/20 μ s)]

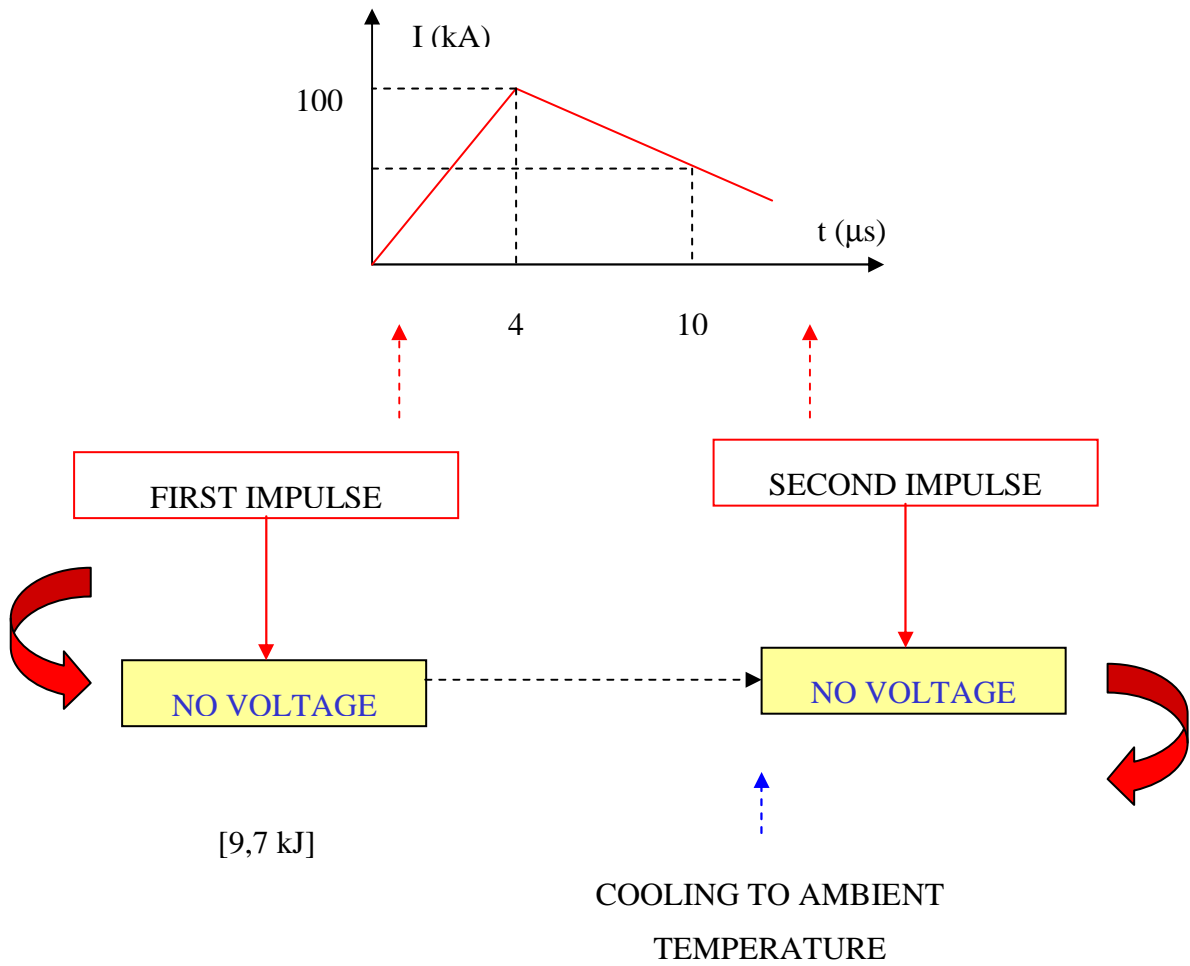


Figure 53 - Switching surge operating duty test: High current impulse conditioning

APPLICATION OF IMPULSES:

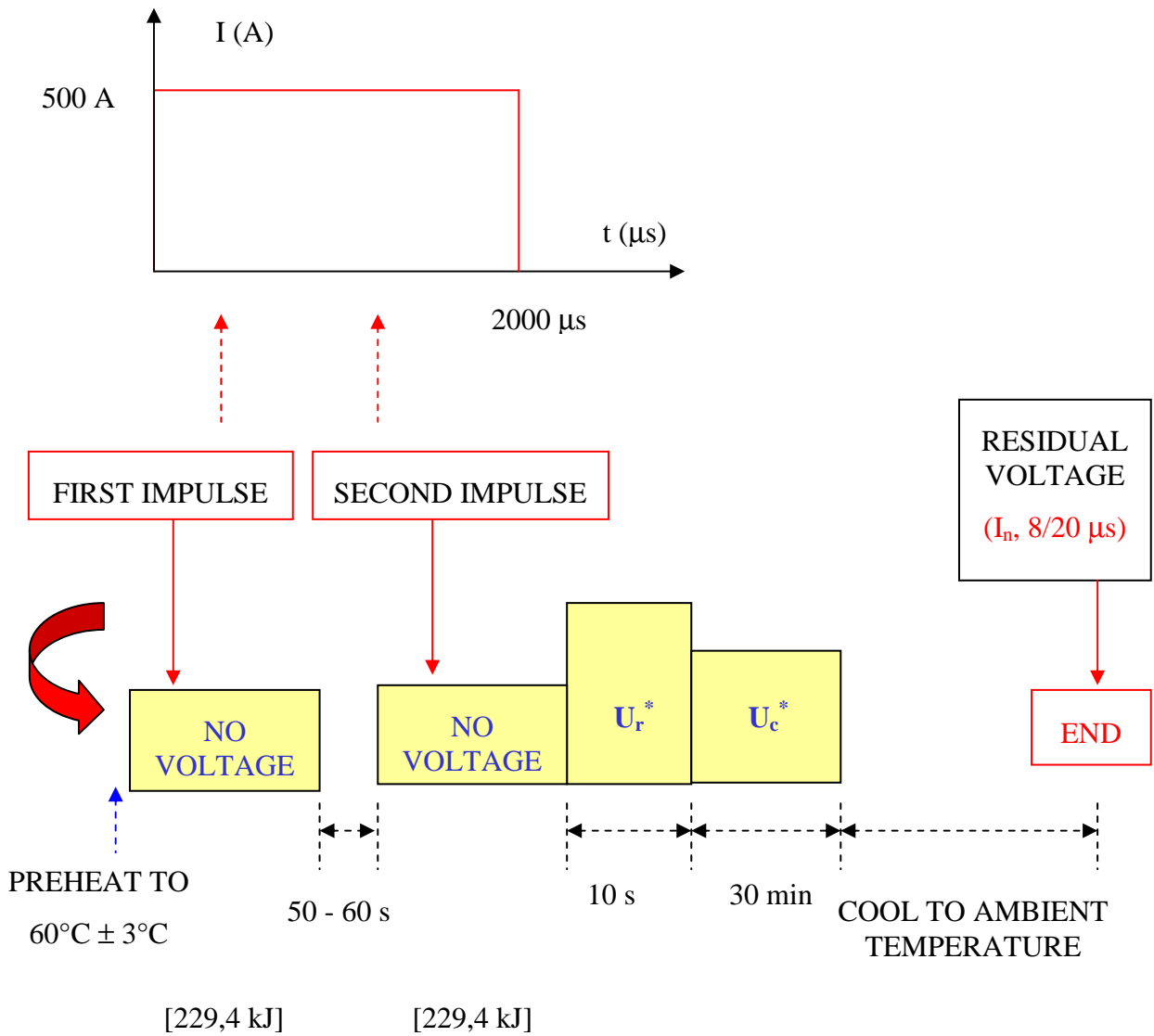


Figure 54 - Switching surge operating duty test: Application of impulses

Test evaluation:

The arrester has passed the test if thermal stability is achieved, if the change in residual voltage measured before and after the test is not changed by more than 5 % and if examination of the test samples after the test reveals no evidence of puncture, flashover or cracking of the resistors.

Energy duty:

The equivalent injected energy for the single impulses or for the group of impulses for the considered arrester is given in Figures 52, 53 and 54. As expected, the highest energy is injected by the rectangular impulse [500 A, 2000 μ s]. Taking into account that two rectangular impulses are injected in short time (with 50 - 60 seconds interval between impulses there is no time for cooling) we can consider that the total energy injected by these two impulses is:

$$W = 2 * 229,4 = 458,8 \text{ kJ}$$

So called 'relative energy capability' of the considered arrester, expressed on the rated voltage base is:

$$W_t = \frac{458,8}{108} = 4,248 \text{ kJ/kV}_{rated}$$

For this IEC class the surge arrester manufacturer declares relative energy capability of 5 kJ/kV_{rated}.

X.3. ANNEX III – SIMULATION STUDY WITH EMTP_RV

The simulation model includes four towers, with tower number 2 being the tower of interest where the currents flowing through the arresters are being monitored. Each tower has arresters installed on bottom and middle phase. Long lines are used at the beginning and the end of the simulated line in order to avoid reflections. A voltage source is also used at the entrance of the line.

Simulation parameters to be modelised carefully are:

- Lightning stroke current shape and its point of impact
- Line model with phase conductors and shield wire
- Tower model with insulators
- Tower footing resistance
- Arrester model and position

Each of these models is detailed below in order to justify the accuracy of the simulation with the selected parameters. Different values used for the modeling have been calculated based on real parameters [36].

1. Lightning stroke modelisation

Lightning stroke is simulated as a current source which is connected to the point of interest.

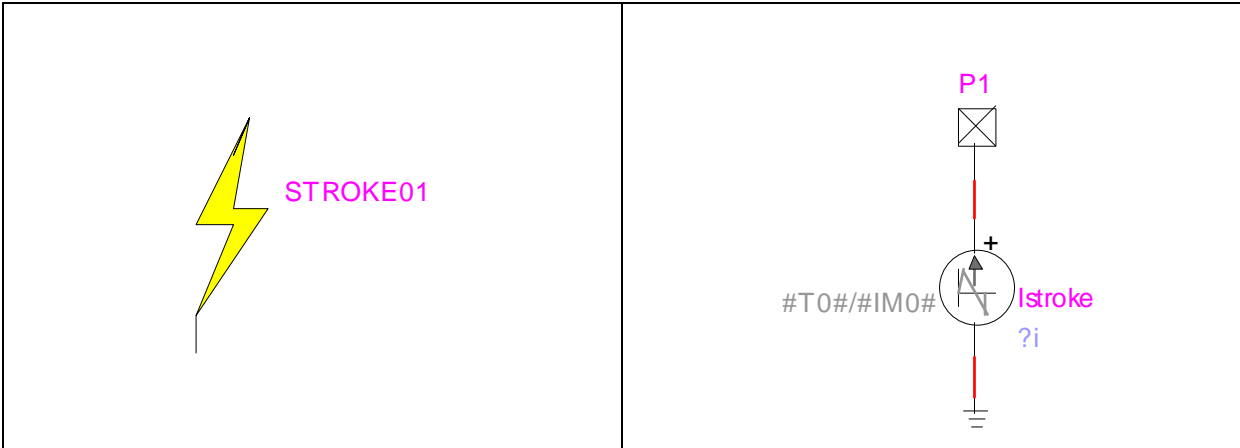


Figure 55 - Lightning stroke model (left) and sub-circuit modelisation (right)

As recommended by CIGRE [3], the following median values shall be used for the lightning stroke model:

- Front time: 3.8 μs
- Peak current: 33 kA
- Tail time: 75 μs
- Tail current: 16.5 kA

However, since the worst lightning case has to be taken into account, the simulation model has the following profile:

- Front time: 4 μs
- Peak current: 200 kA
- Tail time: 75 μs
- Tail current: 100 kA

Also the impact position of the stroke is studied. Several cases are simulated:

- Middle of the span at Shield Wire
- Tower top
- Middle of the span at middle phase

2. Line model

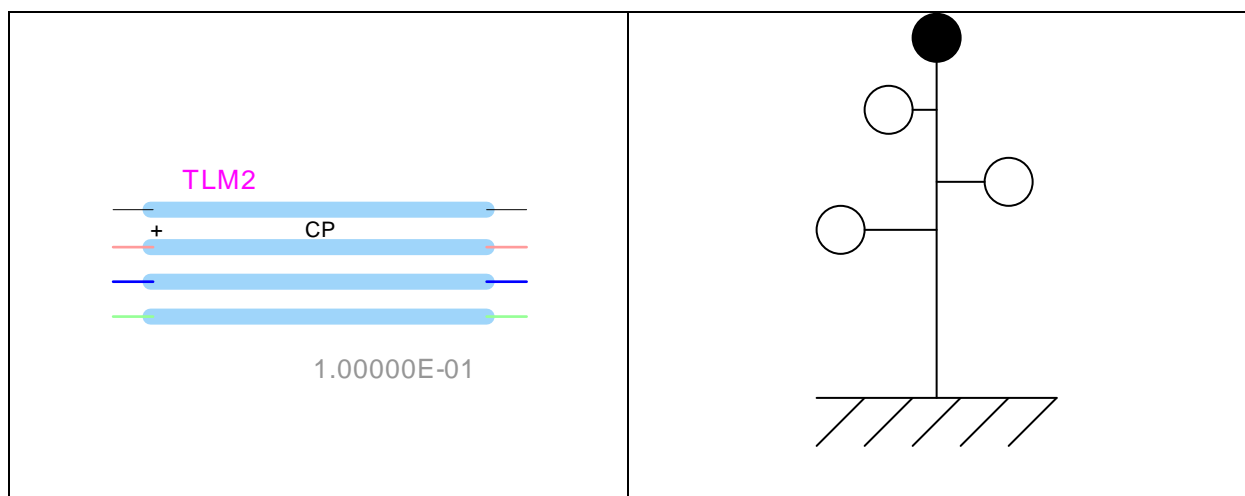


Figure 56 - Line model

Line model data is designed similar to the real line Ston – Komolac, which is a 123 kV single shielded line supplying Dubrovnik city in Croatia.

Wire	#	DC Resistance [Ohm/km]	Outside diameter [cm]	X [m]	Y [m]	Y at midspan [m]
1 (Shield Wire)	4	0.4555	0.9	0	28.9	21.3
2 (Phase A)	1	0.1444	1.708	2.5	22.7	14.1
3 (Phase B)	2	0.1444	1.708	-3	20.5	11.9
4 (Phase C)	3	0.1444	1.708	3.5	18.3	9.7

Table 22 - Input data for the simulated line

Span or line length between two towers is considered as a mean value of 200 meters.

3. Tower model with insulators

Tower

Tower is designed as a sub-circuit with insulators, impedances between phases and line element as tower length. Several pins are sorted out the sub-circuit in order to easily connect an arrester in parallel to the phase conductor insulators or measure the nodes voltages at some interesting points.

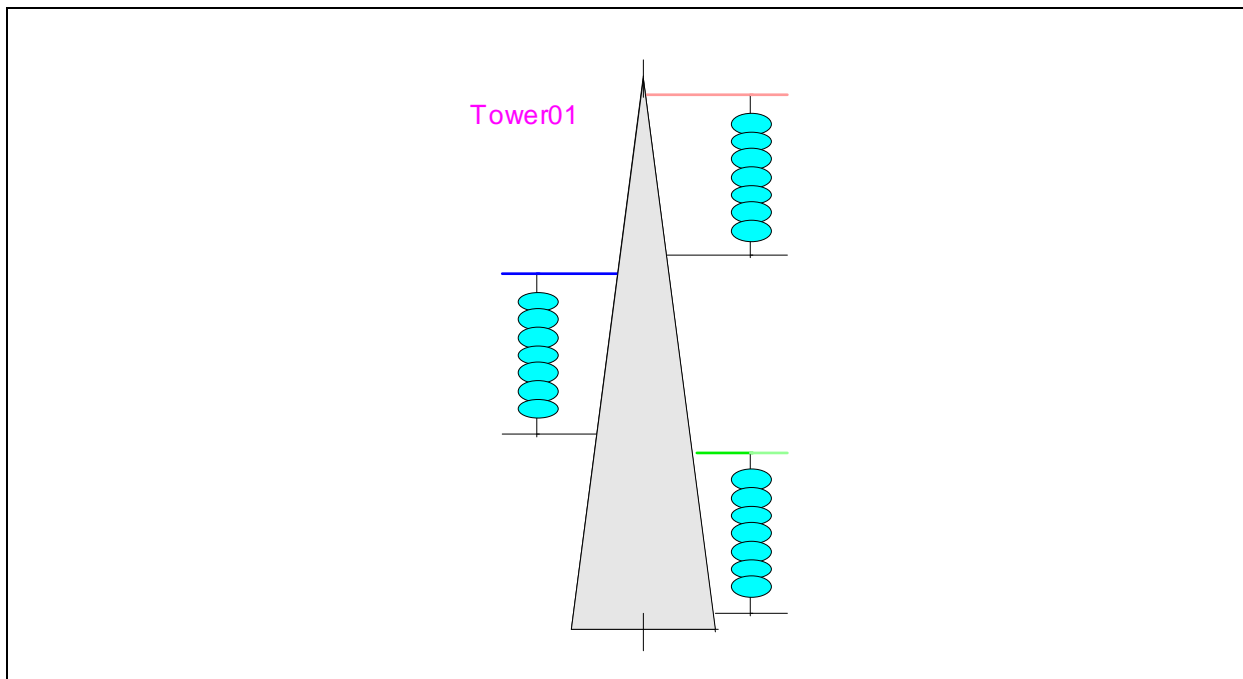


Figure 57 - Tower model

Sub-circuit:

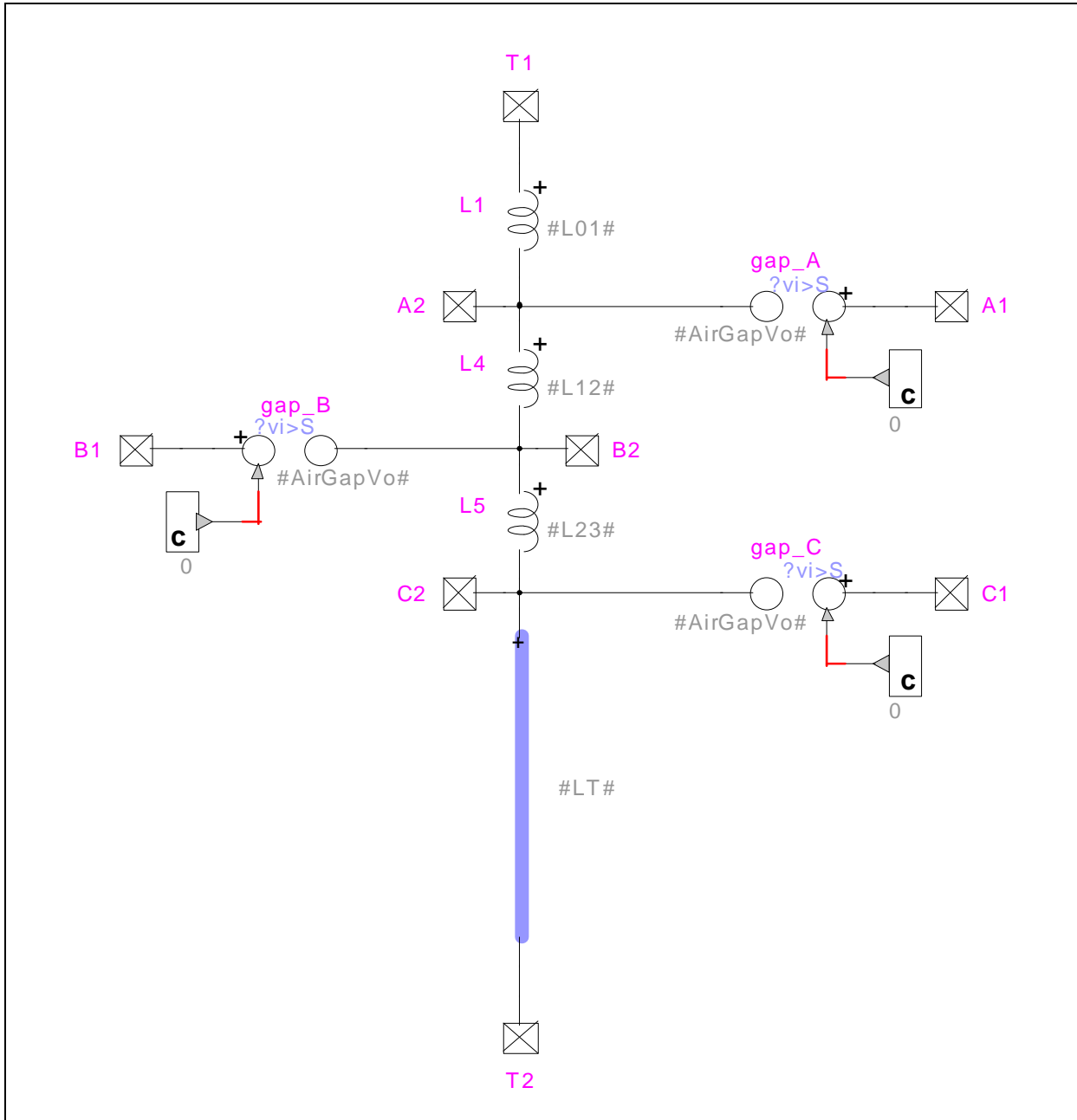


Figure 58 - Tower sub-circuit

Example of data used in computations for the chosen line tower is given below:

- $L01 = 2.8e-6$; // Inductance between GW & phase A (H)
- $L12 = 1.37e-6$; // Inductance between A & B (H)
- $L23 = 1.37e-6$; // Inductance between B & C (H)
- $LT = 20$; // Tower Length (m)
- $ZT = 184$; // Tower Impedance (Ohm)

Insulators

Insulators are modelised as Air Gap elements.

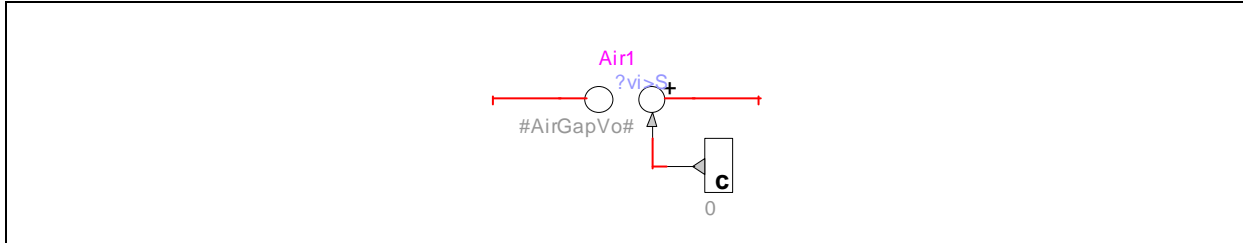


Figure 59 - Insulator model

Flashover occurs when the following integral becomes greater or equal to D:

$$\int_{t_0}^t (|V_{gap}(t)| - V_0)^k dt \geq D$$

Where:

t_0 is the time-point from which v_{gap} became greater than V_0 .

V_0 is the minimum voltage to be exceeded before any breakdown process can start.

When the voltage v_{gap} goes below V_0 the integral is reset. The gap is an ideal open switch before flashover and becomes an ideal closed switch after flashover. The gap stays closed after flashover until the control signal becomes greater than 0, in which case it will reset (open) the gap.

Equation 9 - Air gap EMTP_RV model flashover criteria

Example for a 1-meter long insulator modelisation:

- $V_0 = 495000$; // Air Gap V_0 (V)
- $K = 1$; // Air Gap K
- $D = 0.2045$; // Air Gap D

4. Tower footing resistance

Non-linear soil ionization tower footing resistance model is used [3], [5]. Note that this model is much more realistic than a fixed resistance value.

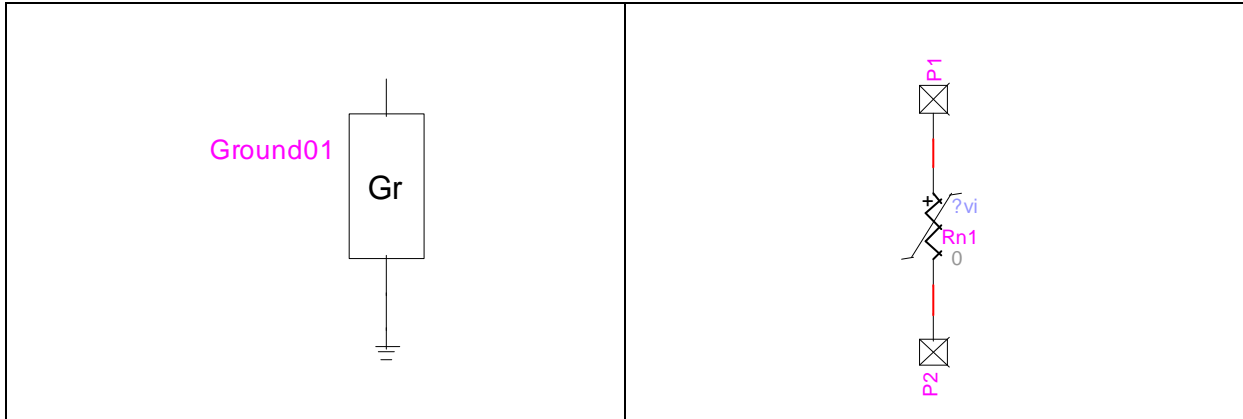


Figure 60 - Tower footing soil ionization model

This model is defined by the following equations:

$$R_i = \frac{R_{lc}}{\sqrt{\left(1 + \frac{I}{I_g}\right)}}$$

$$I_g = \frac{\rho E_g}{2\pi R_{lc}^2}$$

Where:

R_{lc} is the low current tower footing resistance (Ω)

R_i is the tower footing impulse resistance (Ω)

ρ is the soil resistivity (Ωm)

I is the impulse current (kA)

I_g is the soil ionization limit current (kA)

E_g is the soil ionization critical electric field (kV/m) - [$E_g = 400$ (kV/m)]

Equation 10 - Tower footing soil ionization

Example of a 20 Ω tower footing resistance with a soil resistivity of 400 Ωm :

Current (kA)	Voltage (kV)
-100	-1247
-90	-1158
-80	-1065
-70	-966
-60	-861
-50	-748
-40	-626
-30	-494
-20	-348
-10	-185
0	0
10	185
20	348
30	494
40	626
50	748
60	861
70	966
80	1065
90	1158
100	1247

Table 23 - Current / Voltage characteristics of a 20 Ω tower footing resistance

The higher the current, the lower is the tower footing resistance. Indeed instead of a fixed value of 20 Ω , tower footing resistance goes from 18 Ω for smaller kA currents to 12 Ω for 100 kA.

Simulation data is based on real field measurement for this line. Example of the measured data is given in the table below.

Tower Number	Footing resistance (Ohm)
36	46,5
37	51,3
38	60,3
39	35,4
40	50,2

Table 24 - Tower footing resistance measurement example

For the different simulations, soil resistivity was considered as equal to 30 times the footing resistance. For example, the following input data was used for the tower footing resistance model:

- RLC = 60; // Tower footing resistance (Ohm)
- ROhmm = 1800; // Soil resistivity (Ohm-m)

5. Arrester model

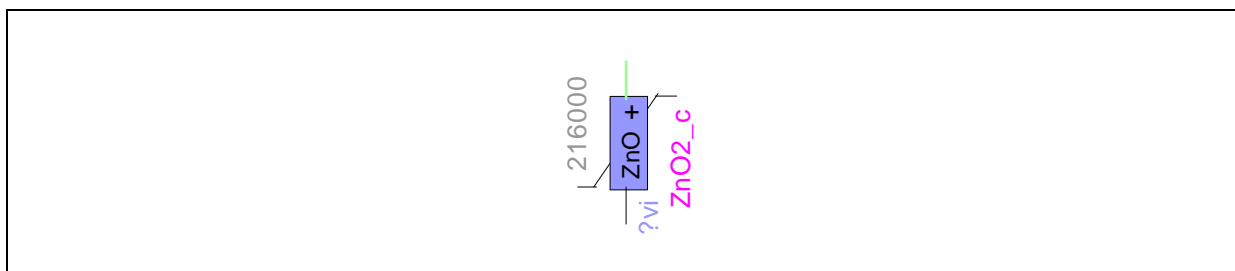


Figure 61 - Arrester model

Arrester model data is taken similar to the arresters used on the Ston – Komolac line. Sediver is the manufacturer of the arresters. Chosen model reference is IEC Class II and it has a voltage rating of 108 kV, with the following Current/Voltage profile:

Current (A)	Voltage (V)
1000	239000
2500	252000
5000	275000
10000	291000
20000	324000
40000	357000

Table 25 - Current / Voltage characteristics of the simulated arrester

Since the monitoring system is to be installed on the towers with two arresters to get more results, the simulation model includes towers with two arresters.

Connecting the arrester to the desired phase of the selected tower is as simple as connecting its both ends to the insulator pins. An example of a simulation tower equipped with two arresters (bottom and middle phase) is presented below.

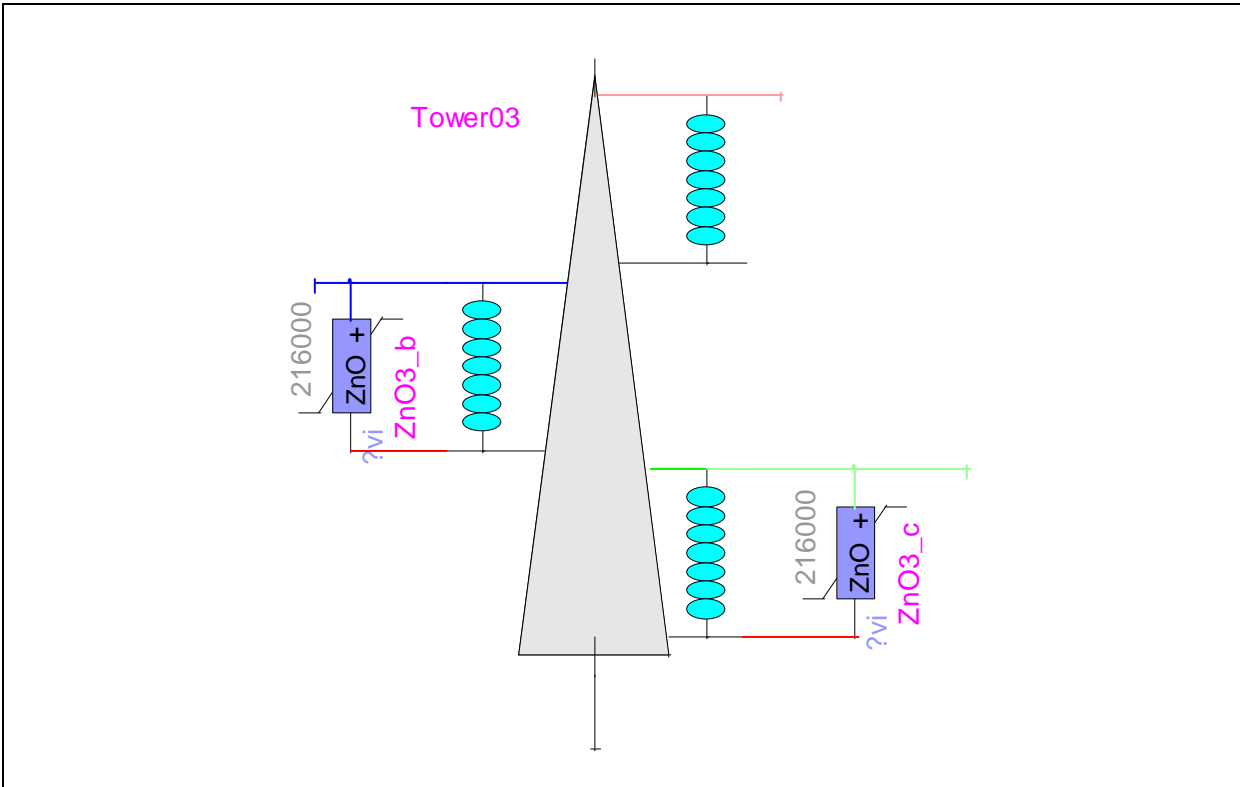


Figure 62 - Tower model equipped with arresters on bottom and middle phase

6. Others

Voltage Source

Voltage of the line is modelised by an AC voltage source at the beginning of the line.

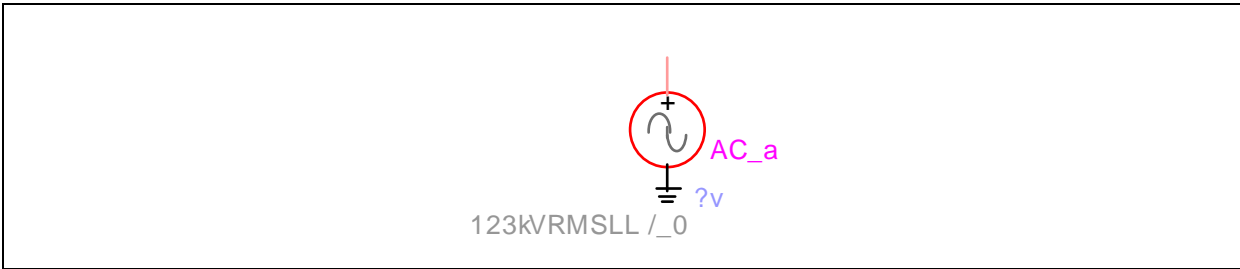


Figure 63 - Line source model

Long lines because of reflections

Long lines of 20 km are used at the beginning and the end of the tower network in order to avoid reflections. Same line model is used as for the spans between towers.

Simulation options (time step & duration)

Simulation time step is set to 50 ns, and simulation duration is 100 μ s.

Full scale simulation model

Scenario 1: Lightning stroke at Shield Wire at middle of Span 2

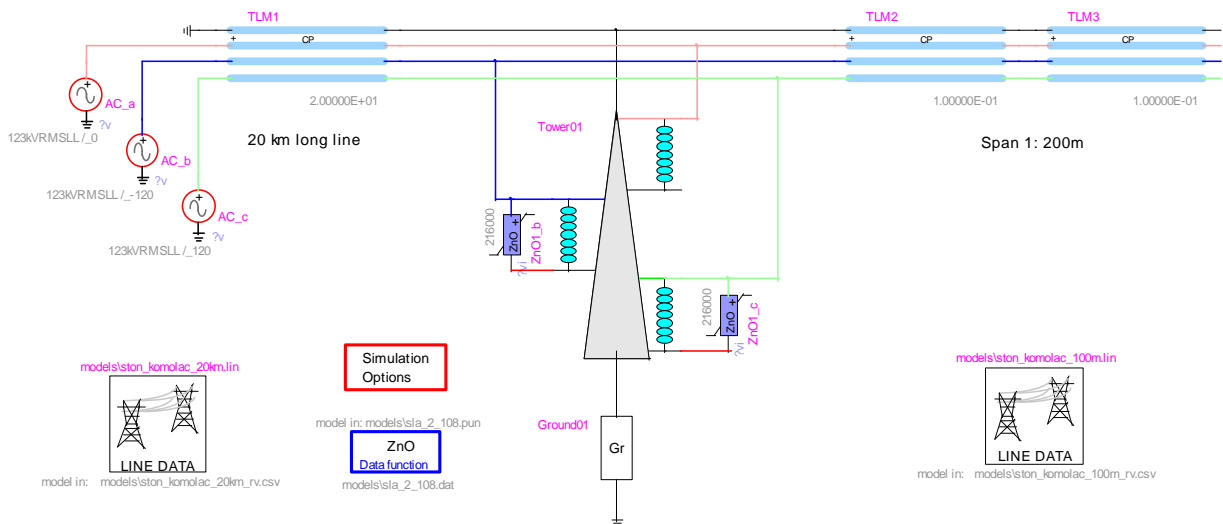


Figure 64 - EMTP_RV full scale simulation preview (part 1/3)

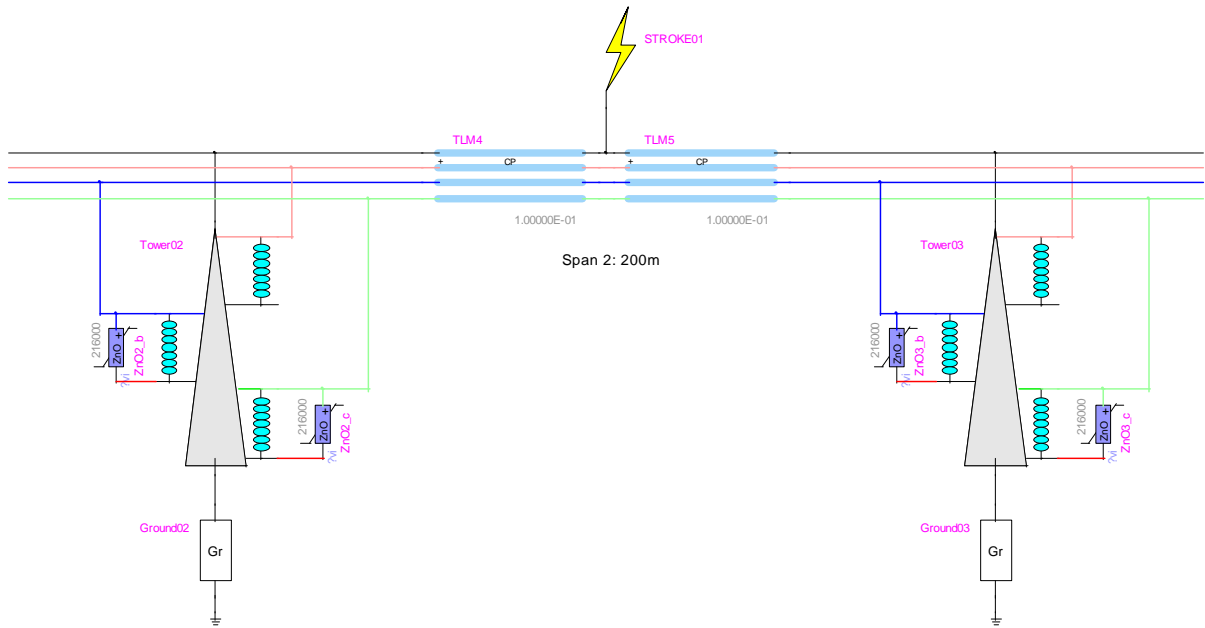


Figure 65 - EMTP_RV full scale simulation preview (part 2/3)

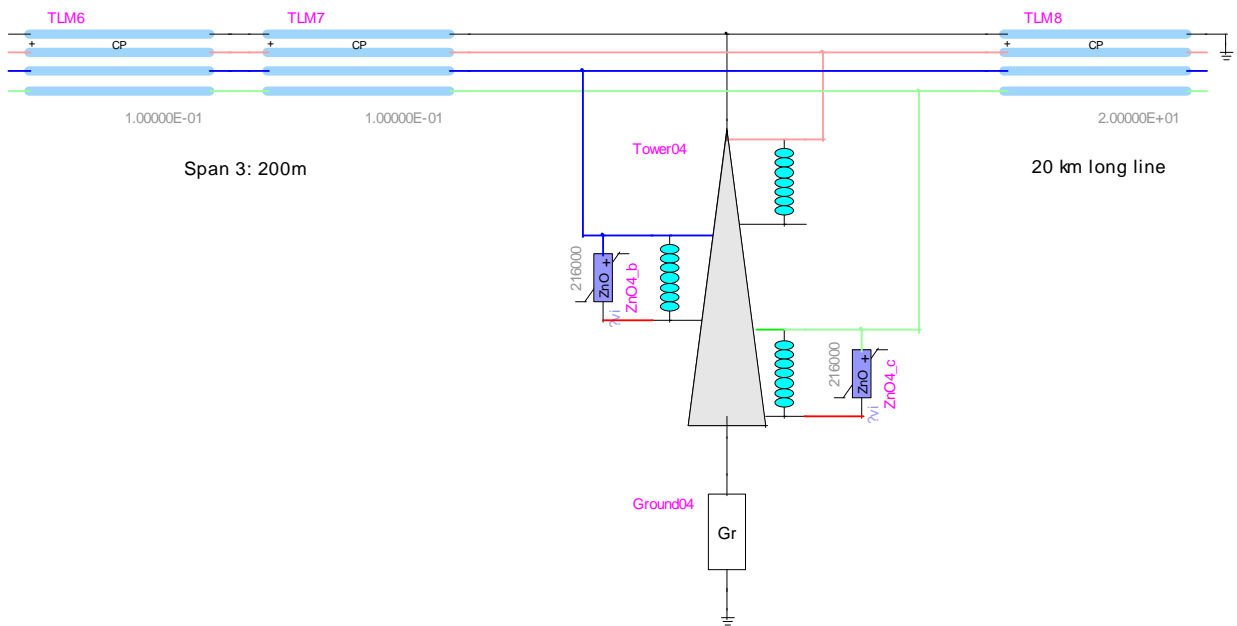


Figure 66 - EMTP_RV full scale simulation preview (part 3/3)

X.4. ANNEX IV - MONITORING SYSTEM SOLAR POWER REQUIREMENTS CALCULATION

This annex details the calculation procedure required for correct selection of solar panel nominal power, battery capacity and charge controller current input and output levels, based on monitoring system power consumption.

First of all, the main controller which consists of the industrial motherboard, memory and compact flash disk requires 14 watts under load. This is the maximum power consumption which corresponds to the board processor running at full speed. Next to the controller, the acquisition card consumes 8 watts. This is only valid when two acquisition channels are used. Four acquisition inputs require up to 10 watts. Finally the communication card for the mobile network requires 2 watts while sending and receiving data. Therefore for a typical monitoring system designed to monitor two acquisition channels such as two arresters on a tower, the power consumption is given in the table below.

Controller (board, memory, hard drive)	14 watts
Acquisition card	8 watts
Communication card	2 watts
Total power consumption	24 watts

Table 26 - Typical monitoring system power consumption

This system has a power consumption of 24 watts.

Since the monitoring device is supplied by 12 volts DC, this means that it requires 2 A per hour. This information is very important in the correct selection of the solar panel, battery and charge controller.

With the total power consumption known, the easiest parameter to define is the battery. During night time, the monitoring system is exclusively supplied by the battery. Thus for half of the day, or for 12 hours without sun, the power requirements are the following:

$$2 * 12 = 24 Ah$$

Theoretically this means that a battery with a capacity of 24 Ah and more would be enough to supply the system during nighttime. However an important parameter to take into account is the discharge frequency. This is because even the new generation of solar batteries using the Absorbed Glass Mat (AGM) technology has a limited lifetime. Indeed the number of discharging cycles and the percentage of the daily discharge compared to total capacity determine the number of days the battery can operate. An example of this lifetime expectancy is given in the table below.

Discharge percentage	Number of cycles
10	5000
25	2000
50	1000
80	600

Table 27 - Typical lifetime of an AGM battery

Therefore the higher is the capacity of the battery, the higher is its lifetime. Thus for a monitoring system consuming 24 watts, a battery of 200 Ah shall guarantee proper operation during few years.

Next to the battery, the solar panels have to be defined. They have a double function while the day is clear. They have to supply the system during the 12 hours of daytime. But also at the same time they have to resupply the battery so the system can operate during nighttime. Both of these operations are simultaneous and are controlled by the charge controller.

In order to determine the nominal power of the solar panels, next to the power requirements of the system it is important to know the solar value of the installation region. This number is easily found with several solar maps. Considered region has a solar index of 3.

The monitoring system consumes 24 watts. Therefore for 24 hours it will require:

$$24 * 24 = 576 W$$

Daily consumption is around 600 watts.

In a region with a solar index value of 3, this would require solar panels with the following nominal power:

$$\frac{600}{3} = 200 W$$

In order to obtain 200 watts of nominal power, several panels can be combined such as 2 panels of 100 watts for example.

The last device to determine is the charge controller. It is defined by two parameters:

- Maximum current at its input (coming from the solar panel)
- Maximum current at its outputs (monitoring system and battery)

A 12 volts solar panel with 200 watts nominal power produces a current of 16,7 A during the peak of the day. Therefore the maximum input current of the charge controller shall be 17 A or more.

X.5. ANNEX V – LABORATORY TESTING

The following annex presents different pictures of the laboratory testing for the lightning first leader and multicomponents acquisition.

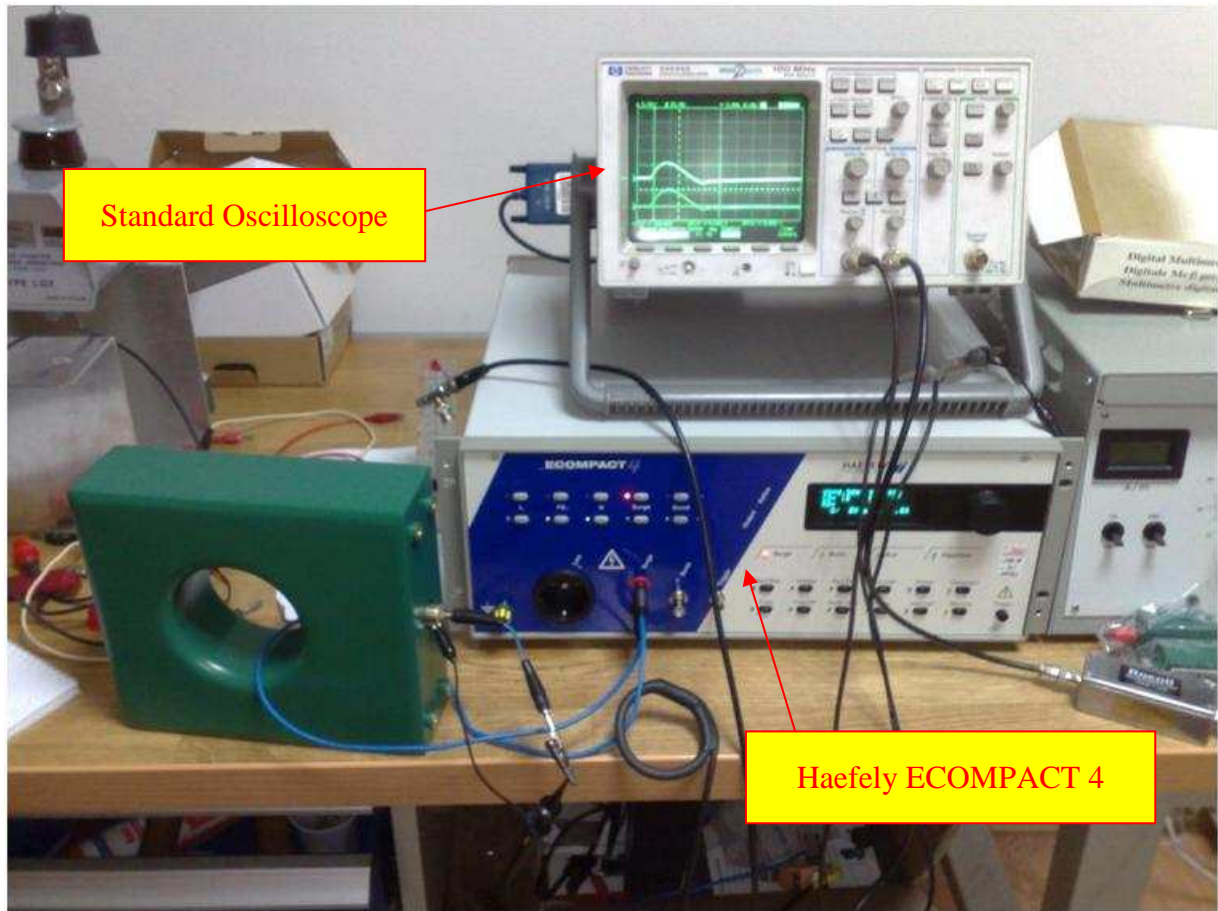


Figure 67 - Laboratory setup for the ECOMPACT 4 generated shape acquisition

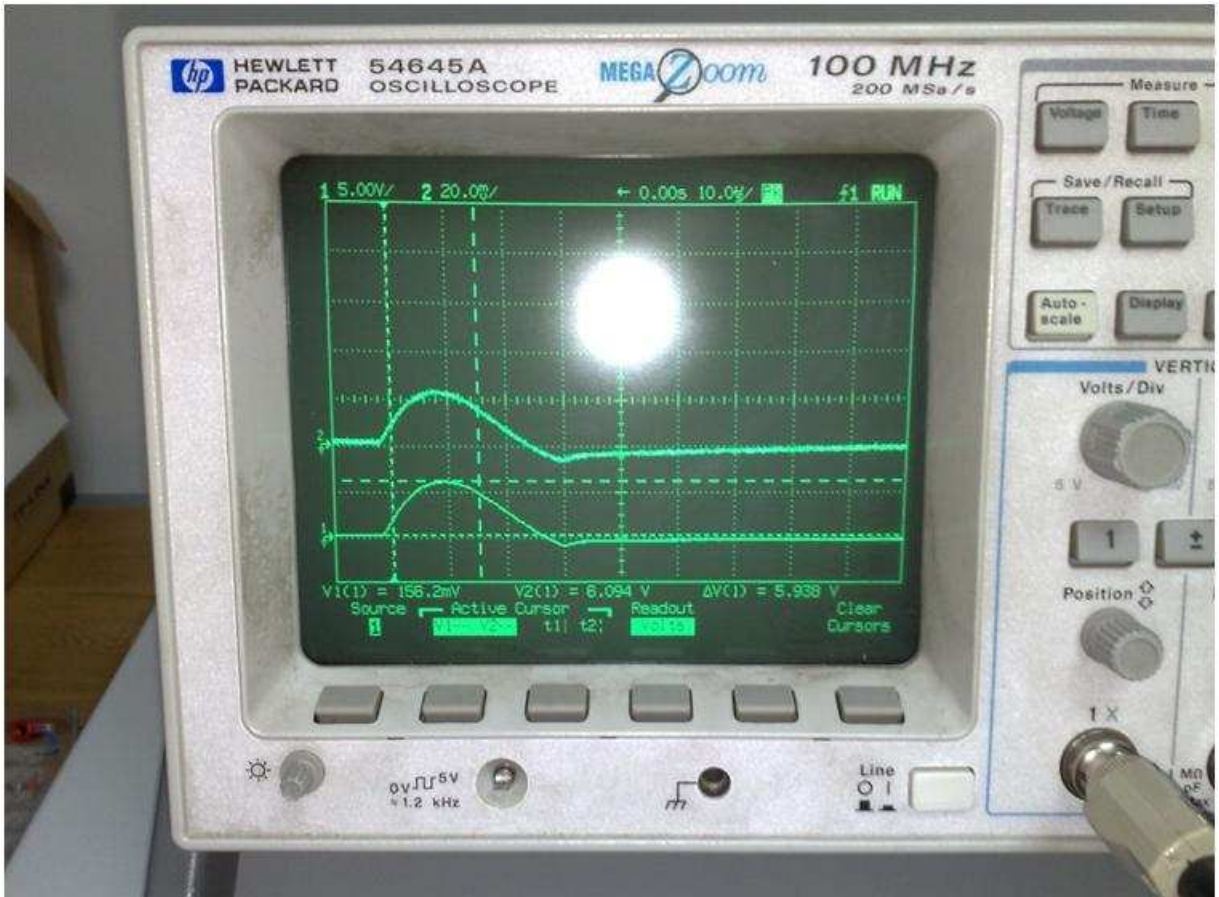


Figure 68 - Oscilloscope view of the generated shape in laboratory

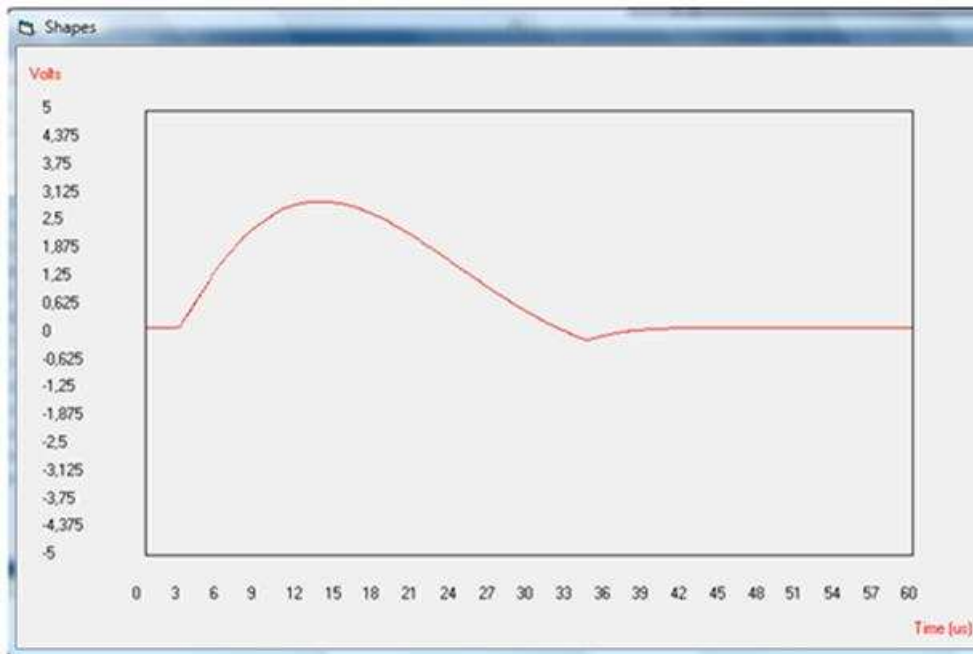


Figure 69 - Current shape acquired by the monitoring system and transmitted to server

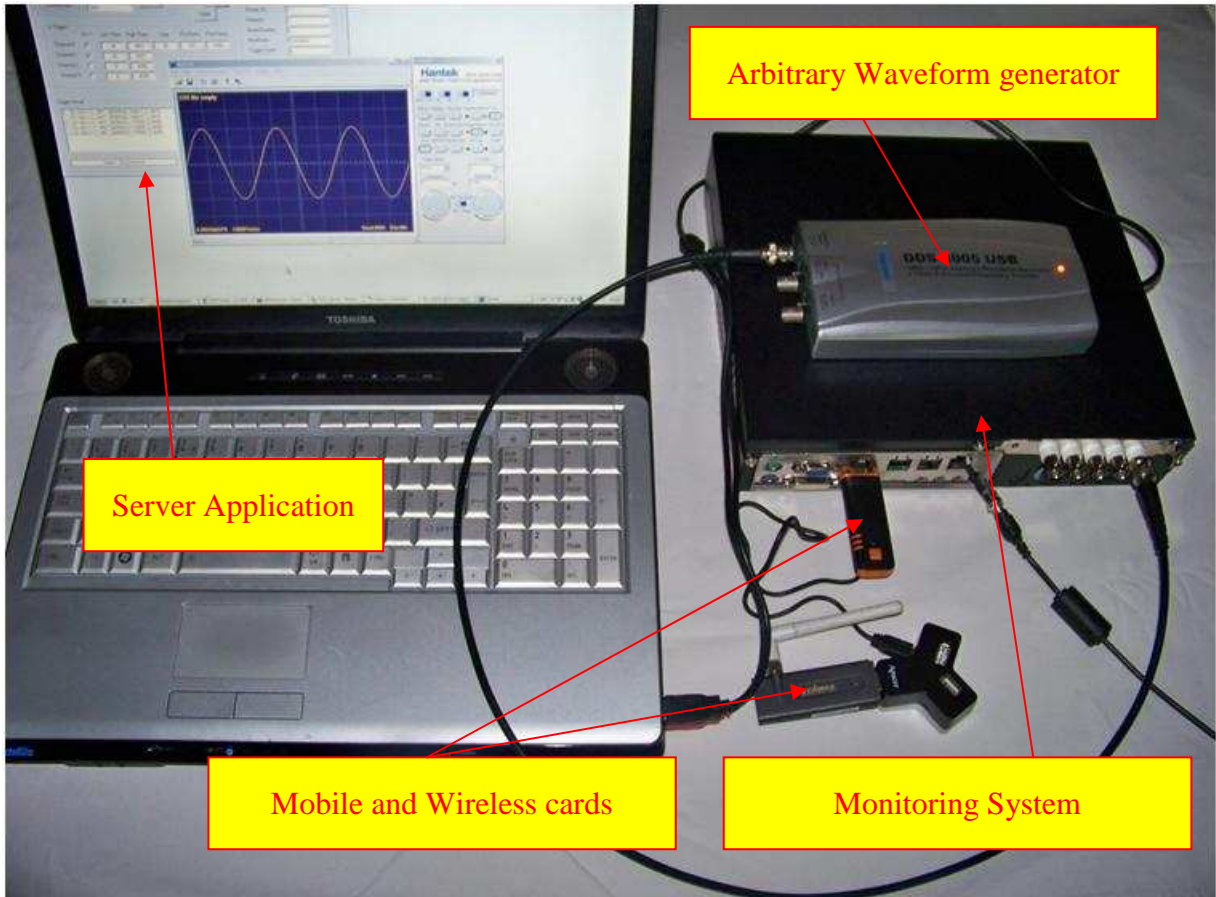


Figure 70 - Multicomponents acquisition test setup

X.6. ANNEX VI – ECOMPACT 4 AUTOMATIC CONTROL SOFTWARE SOURCE CODE

This annex gives the complete source code of the ECOMPACT 4 automatic control software. Programming language is Microsoft Visual Basic 6.0.

```
Public Sub procWaitTimer(sngWaitForSeconds As Single)

    Dim Start

    Start = Timer

    Do While Timer < Start + sngWaitForSeconds
        DoEvents
    Loop

End Sub

Private Function Haefely_Fire() As String

    Dim SendString As String
    Dim EndString1 As String
    Dim EndString2 As Integer
    Dim EndString3 As String

    SendString = Chr(&H34) & Chr(&H41)
    SendString = SendString & Replace(Format(tbxVoltage.Text, "0.00"), ",", ".")
    SendString = SendString & Format(tbxCounter.Text, "000")
    SendString = SendString & Format(tbxPhase.Text, "000")
    SendString = SendString & Format(tbxRepTime.Text, "000")

    EndString1 = Format(tbxVoltage.Text, "0.00")
    EndString2 = Val(Left(EndString1, 1)) + Val(Mid(EndString1, 3, 1)) + Val(Right(EndString1, 1))
    EndString3 = Hex(229 + EndString2)

    SendString = SendString & EndString3 & Chr(&HD)

    Haefely_Fire = SendString

End Function
```

```
Private Function Haefely_Protocol_On() As String
```

```
    Dim SendString As String
```

```
    SendString = Chr(&H34) & Chr(&H79) & Chr(&H41) & Chr(&H44) & Chr(&HD)
```

```
    Haefely_Protocol_On = SendString
```

```
End Function
```

```
Private Function Haefely_Protocol_Off() As String
```

```
    Dim SendString As String
```

```
    SendString = Chr(&H34) & Chr(&H61) & Chr(&H39) & Chr(&H35) & Chr(&HD)
```

```
    Haefely_Protocol_Off = SendString
```

```
End Function
```

```
Private Function Haefely_Stop_1() As String
```

```
    Dim SendString As String
```

```
    SendString = Chr(&H34) & Chr(&H53) & Chr(&H31) & Chr(&H30) & Chr(&H45) & _  
                Chr(&H38) & Chr(&HD)
```

```
    Haefely_Stop_1 = SendString
```

```
End Function
```

```
Private Function Haefely_Stop_2() As String
```

```
    Dim SendString As String
```

```
    SendString = Chr(&H34) & Chr(&H53) & Chr(&H30) & Chr(&H30) & Chr(&H45) & _  
                Chr(&H37) & Chr(&HD)
```

```
    Haefely_Stop_2 = SendString
```

End Function

Private Function Haefely_Surge_Plus() As String

Dim SendString As String

```
SendString = Chr(&H34) & Chr(&H4F) & _  
    Chr(&H30) & Chr(&H30) & Chr(&H30) & Chr(&H31) & _  
    Chr(&H30) & Chr(&H30) & Chr(&H30) & Chr(&H30) & _  
    Chr(&H30) & Chr(&H34) & Chr(&HD)
```

Haefely_Surge_Plus = SendString

End Function

Private Function Haefely_Surge_Minus() As String

Dim SendString As String

```
SendString = Chr(&H34) & Chr(&H4F) & _  
    Chr(&H30) & Chr(&H30) & Chr(&H30) & Chr(&H30) & _  
    Chr(&H30) & Chr(&H30) & Chr(&H30) & Chr(&H31) & _  
    Chr(&H30) & Chr(&H34) & Chr(&HD)
```

Haefely_Surge_Minus = SendString

End Function

Private Function Haefely_Surge_Off() As String

Dim SendString As String

```
SendString = Chr(&H34) & Chr(&H4F) & _  
    Chr(&H30) & Chr(&H30) & Chr(&H30) & Chr(&H30) & _  
    Chr(&H30) & Chr(&H30) & Chr(&H30) & Chr(&H30) & _  
    Chr(&H30) & Chr(&H33) & Chr(&HD)
```

Haefely_Surge_Off = SendString

End Function

Private Sub Haefely_Send_Command(ByVal SendString As String, ByVal TimeToWait As Single)

 Winsock1.SendData SendString

 procWaitTimer (TimeToWait)

End Sub

Private Sub cmdSurgeMinus_Click()

 Winsock1.Connect

 Call Haefely_Send_Command(Haefely_Protocol_On(), 1)

 Call Haefely_Send_Command(Haefely_Surge_Minus(), 1)

 Winsock1.Close

End Sub

Private Sub cmdSurgeOff_Click()

 Winsock1.Connect

 Call Haefely_Send_Command(Haefely_Protocol_On(), 1)

 Call Haefely_Send_Command(Haefely_Surge_Off(), 1)

 Winsock1.Close

End Sub

Private Sub cmdSurgePlus_Click()

 Winsock1.Connect

 Call Haefely_Send_Command(Haefely_Protocol_On(), 1)

 Call Haefely_Send_Command(Haefely_Surge_Plus(), 1)

 Winsock1.Close

End Sub

```

Private Sub Form_Load()

    Winsock1.Close
    With Winsock1
        .Protocol = sckUDPProtocol
        .RemoteHost = "10.243.128.140"
        .RemotePort = 2005
    End With

End Sub

Private Sub Haefely_Start()

    Winsock1.Connect

    Call Haefely_Send_Command(Haefely_Protocol_On(), 1)

    Call Haefely_Send_Command(Haefely_Fire(), 0.1)

    Call Haefely_Send_Command(Haefely_Protocol_On(), 1)

    Call Haefely_Send_Command(Haefely_Stop_1(), 0.4)

    Call Haefely_Send_Command(Haefely_Protocol_On(), 1)

    Winsock1.Close

    If chkAutoFire.Value = Checked Then
        procWaitTimer (Val(tbxSecondsToWait.Text))
        If chkRandomPeak.Value = Checked Then
            scrVoltage.Value = 200 + Rnd(4200 - 200)
            tbxVoltage.Text = scrVoltage.Value / 1000
        End If
        Call Haefely_Start
    End If

End Sub

Private Sub cmdStart_Click()

    Call Haefely_Start

```

```

End Sub

Private Sub cmdStop_Click()
    Winsock1.Connect
    Call Haefely_Send_Command(Haefely_Stop_2(), 1)
    Winsock1.Close
End Sub

Private Sub cmdQuit_Click()
    Winsock1.Close
    End
End Sub

Private Sub Form_Unload(Cancel As Integer)
    Winsock1.Close
End Sub

Private Sub scrVoltage_Change()
    tbxVoltage.Text = scrVoltage.Value / 1000
End Sub

Private Sub scrPhase_Change()
    tbxPhase.Text = scrPhase.Value
End Sub

Private Sub scrRepTime_Change()
    tbxRepTime.Text = scrRepTime.Value
End Sub

Private Sub scrCounter_Change()
    tbxCounter.Text = scrCounter.Value
End Sub

Private Sub Winsock1_DataArrival(ByVal bytesTotal As Long)
    Dim data As String
    Winsock1.GetData data
End Sub

```

X.7. ANNEX VII – MONITORING SYSTEM INSTALLATION IN REAL FIELD

The following annex presents several pictures of the monitoring system first installation in real field.



Figure 71 - Difficult access area to towers

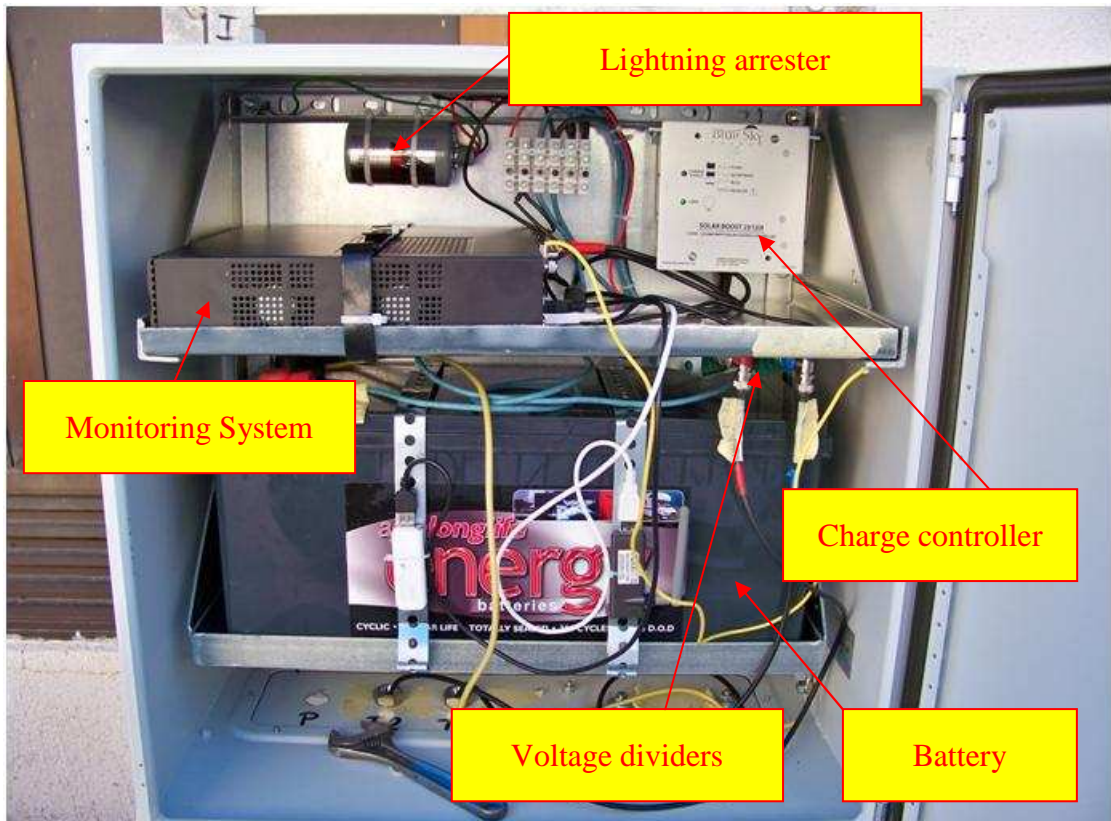


Figure 72 - Interior view of the EMC enclosure

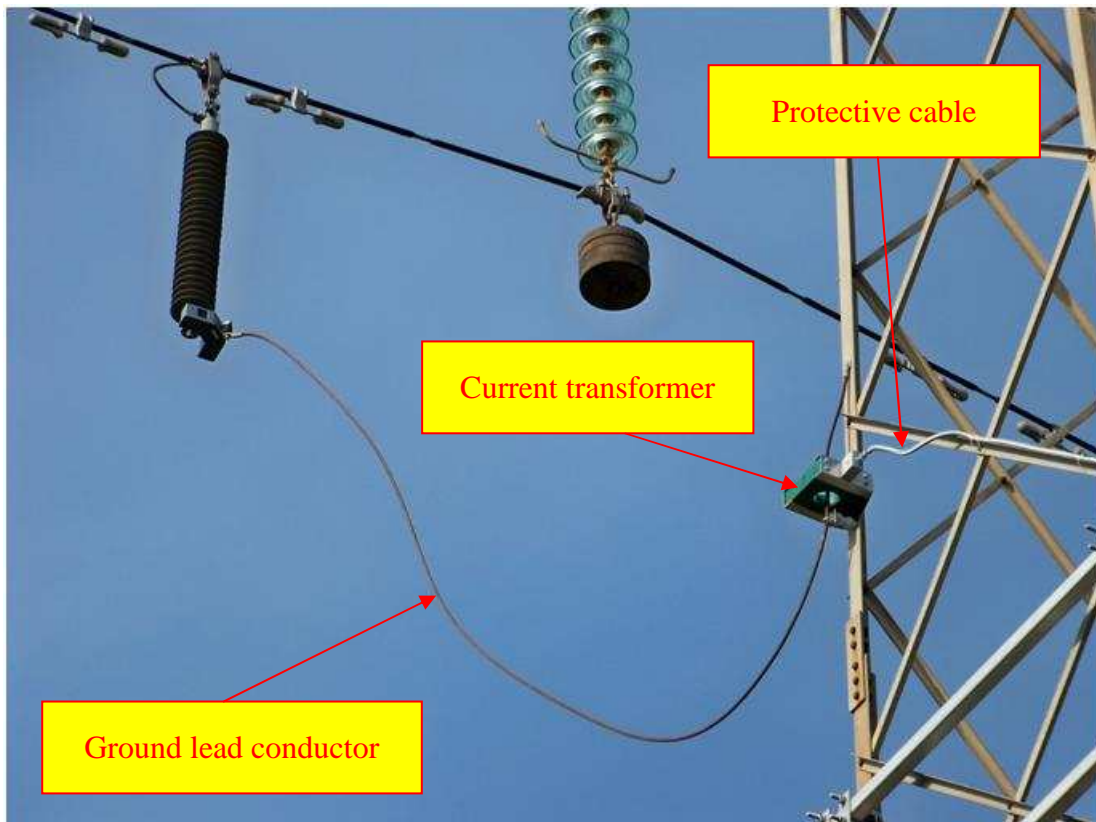


Figure 73 - Current transformer installation over the ground lead conductor



Figure 74 - Enclosure view



Figure 75 - Solar panel view



Figure 76 - Monitoring system successful installation (1/2)



Figure 77 - Monitoring system successful installation (2/2)